

Association of common polymorphisms with gestational diabetes mellitus in Japanese women: A case-control study

Yoshifumi Kasuga^{1), 2)}, Kenichiro Hata²⁾, Atsushi Tajima³⁾, Daigo Ochiai¹⁾, Yoshifumi Saisho⁴⁾, Tadashi Matsumoto¹⁾, Naoko Arata⁵⁾, Kei Miyakoshi¹⁾ and Mamoru Tanaka¹⁾

¹⁾ Department of Obstetrics and Gynecology, Keio University School of Medicine, Tokyo 160-8582, Japan

²⁾ Department of Maternal-Fetal Biology, National Research Institute for Child Health and Development, Tokyo 157-8583, Japan

³⁾ Department of Bioinformatics and Genomics, Graduate School of Advanced Preventive Medical Sciences, Kanazawa University, Kanazawa 920-8640, Japan

⁴⁾ Department of Internal Medicine, Keio University School of Medicine, Tokyo 160-8582, Japan

⁵⁾ Department of Women's Health, National Center for Child Health and Development, Tokyo 157-8583, Japan

Abstract. Gestational diabetes (GDM) and type 2 diabetes (T2DM) share part of pathomechanism and several T2DM susceptibility genes are demonstrated to be associated with GDM. No information on the genetics of GDM, however, was available in Japanese women. In this study, T2DM risk variants (45 single nucleotide polymorphisms [SNPs] from 36 genes) identified in previous studies were genotyped using matrix-assisted laser desorption/ionization time-of-flight mass spectrometry in a cohort of 171 Japanese women with GDM and 128 normal glucose tolerance (NGT) diagnosed by the new International Association of Diabetes in Pregnancy Study Group criteria. Of 45 SNPs, three genetic variants were nominally associated with the development of GDM: rs266729 ($p = 0.013$, odds ratio [OR]: 1.56, 95% confidence interval [CI]: 1.10–2.23) in *ADIPOQ*, rs10811661 ($p = 0.035$, OR: 1.46, 95% CI: 1.03–2.08) in *CDKN2A/2B*, and rs9505118 ($p = 0.046$, OR: 1.41, 95% CI: 1.01–1.97) in *SSRI-RREB1*. There was a significant difference in the number of risk alleles of three variants between women with GDM and NGT (3.79 ± 1.33 vs. 3.05 ± 1.41 , $p = 6.0 \times 10^{-6}$). In combined analysis of three genetic variants, women with five or more risk alleles had a 7.32-fold increased risk of GDM ($p = 5.6 \times 10^{-5}$, 95% CI: 4.54–11.96), compared with those having no more than one risk allele. Our results suggest several risk variants of T2DM had cumulative effects on the development of GDM in Japanese women.

Key words: Gestational diabetes mellitus, Single nucleotide polymorphism, Japanese women

GESTATIONAL DIABETES MELLITUS (GDM), defined as glucose intolerance with onset or first recognition during pregnancy, is a multifactorial disease that is similar to type 2 diabetes mellitus (T2DM): glucose intolerance is likely to be caused by the combination of environmental and genetic effects [1, 2]. With the recent advances in high-throughput genotyping technologies, the genetics of GDM as well as T2DM has been investigated over the past decade. For instance, genetic variants associated with insulin sensitivity and

beta cell function have been related to T2DM in various racial or ethnic groups including Japanese population by the linkage analysis, the candidate gene approach, and the genome-wide association studies (GWAS) [3-6]. In particular, several T2DM susceptibility genes were related to the development of GDM in Caucasians [7-11]. Since the susceptibility to glucose intolerance depends on racial or ethnic groups, the effect of T2DM risk genetic variants on GDM might be different between Caucasian and Japanese women. To date, however, no information on risk variants of GDM was available in Japanese women.

Women with GDM are at a high risk of developing future T2DM as well as perinatal complications (i.e. pregnancy-induced hypertension and macrosomia) [2, 12]. Offspring born to mother with GDM carries a risk of early onset obesity and glucose intolerance [12, 13]. Therefore, the optimal management of GDM is important not only to perinatal care, but also to maternal and

Submitted Sep. 14, 2016; Accepted Dec. 6, 2016 as EJ16-0431

Released online in J-STAGE as advance publication Feb. 16, 2017

Correspondence to: Kenichiro Hata, M.D., Ph.D., Department of Maternal-Fetal Biology, National Research Institute for Child Health and Development, 2-10-1 Okura, Setagaya-ku, Tokyo 157-8583, Japan. E-mail: hata-k@ncchd.go.jp

Co-correspondence to: Kei Miyakoshi, M.D., Department of Obstetrics and Gynecology, Keio University School of Medicine, 35 Shinanomachi, Shinjuku-ku, Tokyo 160-8582, Japan.

E-mail: kei.z7@keio.jp

©The Japan Endocrine Society

children's healthcare. In general, Asians are classified as a highly susceptible to glucose intolerance [14-16]. This means that genetic information would contribute to the identification of women at highest risk of T2DM as well as the understanding of the pathophysiology of GDM in Japanese women.

With this background, the current study was designed to examine the association between T2DM or GDM susceptibility genes previously reported and the development of GDM in Japanese women. Especially, in the present study, glucose tolerance status was evaluated by a single criterion (i.e. the new criteria proposed by International Association of Diabetes in Pregnancy Study Group [IADPSG]) and pregnant women with normal glucose tolerance (NGT) were considered as control to account for the environmental influence (i.e. pregnancy).

Materials and Methods

Subjects

We recruited a total of 299 Japanese women with singleton pregnancies who underwent the diagnostic 75g oral glucose tolerance test (75g-OGTT) at 24–32 gestational weeks at Keio University Hospital or at the National Center for Child Health and Development from April 2011 until December 2014. Gestational age was confirmed by crown-rump length measurements in the first trimester. Women with multi-fetal pregnancies, fetal congenital anomalies, overt diabetes in pregnancy, pre-gestational diabetes mellitus (i.e. type 1 diabetes and T2DM), and hypertensive disorders in pregnancy, chronic hypertension, and the use of medications known to affect glucose metabolism were excluded. This research was performed in accordance with the Declaration of Helsinki and informed consent was obtained from patients, where appropriate. The study was approved by Keio University School of Medicine Ethics Committee (No. 20100154) and the institutional review board of National Research Institute for Child Health and Development (No. 406).

According to IADPSG criteria, GDM was diagnosed if one or more values reached or exceeded the following thresholds: fasting plasma glucose level (FPG), 92 mg/dL (5.1 mmol/L); 1h-plasma glucose level during 75g-OGTT (1h-PG), 180 mg/dL (10.0 mmol/L); and 2h-plasma glucose level during 75g-OGTT (2h-PG), 153 mg/dL (8.5 mmol/L). Overt diabetes in pregnancy was defined as HbA1c > 6.5%,

FPG \geq 126 mg/dL (7.0 mmol/L), or random plasma glucose level \geq 200 mg/dL (11.1 mmol/L): the latter needing to be confirmed by one of the former [17]. Women with normal OGTT results were considered as NGT (i.e. control) in this study. As a result, there were 171 women with GDM and 128 with NGT in this study cohort. Statistical power of the current analysis using 171 GDM and 128 NGT was calculated using Genetic Power Calculator in the GDM prevalence rate of 10% [18]. The current study had 57% or 85% power to detect a GDM-susceptible allele with a genotype relative risk (GRR) of 1.4 or 1.6 (under an additive model in log-odds scale), respectively, assuming that the type I error rate was 0.05 and the susceptible allele frequency was 0.3.

Assessment of insulin sensitivity, insulin secretion, and beta cell function

Insulin sensitivity and insulin secretion were evaluated by parameters calculated using the diagnostic 75g-OGTT. The insulin sensitivity was estimated by the whole-body insulin sensitivity index derived from the OGTT (IS_{OGTT}) and the homeostasis model assessment of insulin resistance (HOMA-IR), and Quantitative insulin sensitivity check index (QUICKI). The IS_{OGTT} was calculated by the following formula: $10,000 / \text{square root} \{PG_0 \times Ins_0 \times (PG_0 + PG_{60} \times 2 + PG_{120}) / 2 \times (Ins_0 + Ins_{60} \times 2 + Ins_{120}) / 2\}$, where PG_y and Ins_y represent plasma glucose (mg/dL) and insulin values (mU/L), respectively, at time y min during the OGTT [19]. The HOMA-IR was calculated as $(PG_0 \times Ins_0) / 405$ [20]. The QUICKI was estimated as follows: $1 / [\log(Ins_0) + \log(PG_0)]$ [21]. Insulin secretion was assessed by the Insulinogenic Index (IGI): $\{Ins_{30} - Ins_0\} / \{PG_{30} - PG_0\}$ during the OGTT [22]. To evaluate beta cell function, we calculated the OGTT-derived disposition index using the following measures: Insulin Secretion-Sensitivity Index-2 (ISSI-2: $IS_{OGTT} \times$ the ratio of the total area under the insulin curve to the total area under the glucose curve during the OGTT) [23].

SNP selection and genotyping

A PubMed search was performed in October 2014 and we retrieved 151 SNPs from 88 genes, previously reported to be associated with T2DM or GDM (Supplementary Table 1). It is well known that an impaired insulin secretion plays a critical role in the development of T2DM or GDM in east Asian

including Japanese [24, 25]. Therefore, most of SNPs analyzed were insulin secretion candidate SNPs. Several T2DM susceptibility genes were identified in Japanese as well as Caucasian. All GDM risk gene variants examined were found in subjects other than Japanese. We selected the SNPs based on the criterion of the minor allele frequency (MAF) > 30% in Japanese population because this selection could provide adequate statistical power to detect SNPs with $GRR \geq 1.4$ in our study cohort, as was described above. Additionally, gene-based tag SNPs (pairwise $r^2 < 0.8$) using HapMap-JPT in this study and several SNPs were excluded because of technical reasons (e.g. polymerase chain reaction failures). Finally, we investigated the association between 45 SNPs from 36 genes and the development of GDM. All polymorphisms analyzed in this study were in Hardy-Weinberg equilibrium.

Maternal peripheral blood samples were collected after delivery and genomic DNA was extracted using QIASymphony DNA Midi Kit (96) (Qiagen, Valencia, CA, USA). Genotyping was performed using high-throughput genotyping MassARRAY[®] platform (Sequenom, Inc, San Diego, CA, USA). The primers including amplification and extension were designed using Assay Design Suite[®] (Sequenom, <https://seqpws1.sequenom.com/AssayDesignerSuite.html>) (Supplementary Table 2). Negative controls, at least quadruplicate, were placed at all 384 plates as quality controls. SNP genotyping success rate was > 94% and the concordance rate for genotyping was > 99.8% in this study.

Statistical analysis

Per-allele odd ratios (ORs) and their 95% confidence intervals (CIs) for the association between SNPs and GDM were estimated by logistic regression analysis. The possibility of multiple testing was avoided by Bonferroni correction. Therefore, we examined the combined effects of genetic variants on Japanese GDM and the cumulative effects of risk alleles at GDM-associated SNPs having lower p -value (pre-Bonferroni correction) [26]. Data are presented as mean \pm SD or the number of cases (percent). Continuous data were compared between the GDM and NGT groups by Student's t -test. The frequencies of SNPs between the two groups were evaluated by logistic regression analysis. Categorical variables were analyzed by the Fisher's exact test.

Statistical analyses were performed using SPSS v.22 (IBM, Chicago, IL, USA). A p -value < 0.05 was considered statistically significant. The calculation of linkage disequilibrium (LD) among SNPs and construction of a forest plot of per-allele ORs were done with R (version 3.3.1).

Results

Maternal characteristics

Maternal characteristics and metabolic measurements of the GDM and NGT (i.e. control) groups are shown in Table 1. There were no notable differences in maternal age at delivery, pregravid BMI, and the rate of overweight or nulliparous between the GDM and NGT groups. A first-degree family history of T2DM was more prevalent women with GDM, compared with NGT. With regard to metabolic measurements, FPG, 1h-PG, 2h-PG, and HOMA-IR were significantly higher in the GDM group compared with those in the NGT group. Women with GDM showed significantly lower levels of IS_{OGTT} , QUICKI, IGI, and ISSI-2, compared with NGT ($p < 0.05$).

Table 1 Comparison of maternal characteristics between the gestational diabetes mellitus and normal glucose tolerance groups

	GDM (n = 171)	NGT (n = 128)	p -value
Maternal age at delivery (years)	36.1 \pm 4.6	36.6 \pm 4.3	0.36
Pre-pregnancy BMI (kg/m ²)	21.4 \pm 3.3	20.7 \pm 2.5	0.05
Pre-pregnancy overweight	24 (14.0)	10 (7.8)	0.18
Nulliparous	111 (64.9)	79 (61.7)	0.63
A first-degree family history of diabetes	33 (19.3)	9 (7.0)	0.002
Prior miscarriage	57 (33.3)	58 (45.3)	0.04
Gestational week at OGTT (weeks)	27.5 \pm 3.1	27.8 \pm 2.8	0.36
Plasma glucose of OGTT			
0 min (mg/dL)	85.9 \pm 7.5	82.3 \pm 4.8	2.0×10^{-6}
60 min (mg/dL)	174.1 \pm 25.0	141.4 \pm 21.0	4.1×10^{-28}
120 min (mg/dL)	154.7 \pm 25.6	121.0 \pm 17.1	2.2×10^{-30}
IS_{OGTT}	5.09 \pm 2.46	7.79 \pm 3.51	6.5×10^{-12}
HOMA-IR	1.88 \pm 1.68	1.14 \pm 0.62	6.0×10^{-6}
QUICKI	0.36 \pm 0.03	0.38 \pm 0.04	9.1×10^{-9}
Insulinogenic index	0.78 \pm 0.49	1.03 \pm 0.99	0.01
ISSI-2	1.75 \pm 0.54	2.46 \pm 0.70	1.3×10^{-13}

BMI, body mass index; overweight, BMI ≥ 25 kg/m²; OGTT, oral glucose tolerance test; IS_{OGTT} , Insulin sensitivity index from OGTT; HOMA-IR, homeostasis model assessment for insulin resistance; QUICKI, quantitative insulin sensitivity check index; ISSI-2, Insulin Secretion-Sensitivity Index-2; Data, mean \pm SD or N (%).

Case-control study

In this study, we evaluated the frequencies of 45 SNPs in the GDM and NGT groups using logistic regression analysis. The individual allele odds ratio (OR) is shown in Fig. 1 and Supplementary Table 3. Three genetic variants had nominal associations with GDM (rs266729 [$p = 0.013$, OR: 1.56, 95% CI: 1.10–

2.23], rs10811661 [$p = 0.035$, OR: 1.46, 95% CI: 1.03–2.08], and rs9505118 [$p = 0.046$, OR: 1.41, 95% CI: 1.01–1.97]). Therefore, we examined the combined effects of the risk alleles from these three genetic variants (rs266729, rs10811661, and rs9505118). Taking into account these three variants, each individual could harbor between 0 and 6 possible risk alleles.

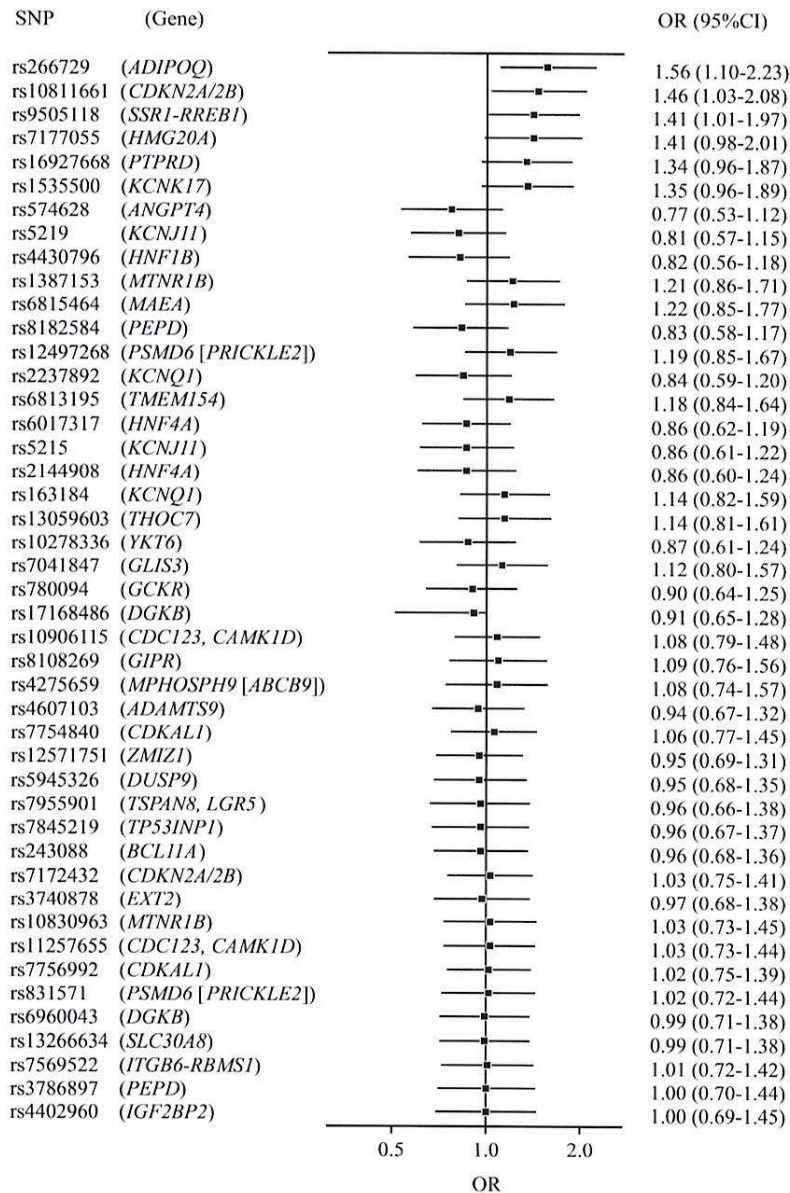


Fig. 1 A forest plot of per-allele odds ratio of 45 single nucleotide polymorphisms examined in this study
SNP, Single nucleotide polymorphism; OR, Odds ratio; CI, Confidence interval.

The distribution of risk alleles of the three genetic variants in the GDM and NGT groups are shown in Fig. 2A. The percentages of subjects with GDM increased in the subgroups with more risk alleles. Furthermore, there was a significant difference in the number of T2DM risk alleles between women with GDM and NGT (3.79 ± 1.33 vs. 3.05 ± 1.41 , $p = 6.0 \times 10^{-6}$). Especially, women with five or more risk alleles showed a 7.32-fold increased risk of GDM ($p = 5.6 \times 10^{-5}$, 95% CI: 4.54–11.97), compared with those having no more than one risk allele (Fig. 2B). The LD values among three SNPs calculated using r^2 were under 0.02 in both GDM and NGT groups.

Discussion

With the development of genetic association studies, information on T2DM susceptibility genes has been accumulated in Japanese population. To date, however, no studies on GDM risk variants in Japanese women have been reported, although GDM may share genetic backgrounds with T2DM to some extent. In addition, there is a paucity of information on genetics of GDM by the new IADPSG criteria because the number of healthcare associations adopting the criteria is still limited [27]. Therefore, we designed the current study to examine the association of previously reported T2DM or GDM susceptibility genes with having GDM by the new IADPSG criteria in Japanese women.

It is demonstrated that the prevalence of GDM by the IADPSG criteria is 10–15% [28, 29]. When analyzing statistical power of our cohort (i.e. GDM, 171 women; NGT, 128 women) using Genetic Power Calculator in the GDM prevalence of 10%, SNPs with MAF > 30% could provide adequate statistical power to detect risk variants with $GRR \geq 1.4$ in our study cohort. Of 45 SNPs examined, three genetic variants (rs266729, rs10811661, and rs9505118) were nominally associated with GDM in Japanese women. Since multiple genes would be involved in the development of GDM, we investigated the combined effects of three genetic variants on GDM. As a result, women with five or more risk alleles showed a 7.32-fold increased risk of GDM, compared with those having no more than one risk allele. Our results suggested the genetic background of GDM in a multi-genetic manner in Japanese women.

Of the three genetic variants, rs266729 (*ADIPOQ*) is a gene involved in insulin sensitivity, while rs10811661 (*CDKN2A/2B*) and rs9505118 (*SSR1-RREB1*) play an important role in insulin secretion. Several studies have shown that a single polymorphism rs266729 is associated with decreased levels of serum adiponectin in GDM as well as T2DM [30, 31]. *CDKN2A/2B* is cyclin-dependent kinases 4 suppressor gene that contributes to the proliferation and maintenance of pancreatic β -cells. Based on previous studies, *CDKN2A/2B* is considered as one of the T2DM susceptibility genes in

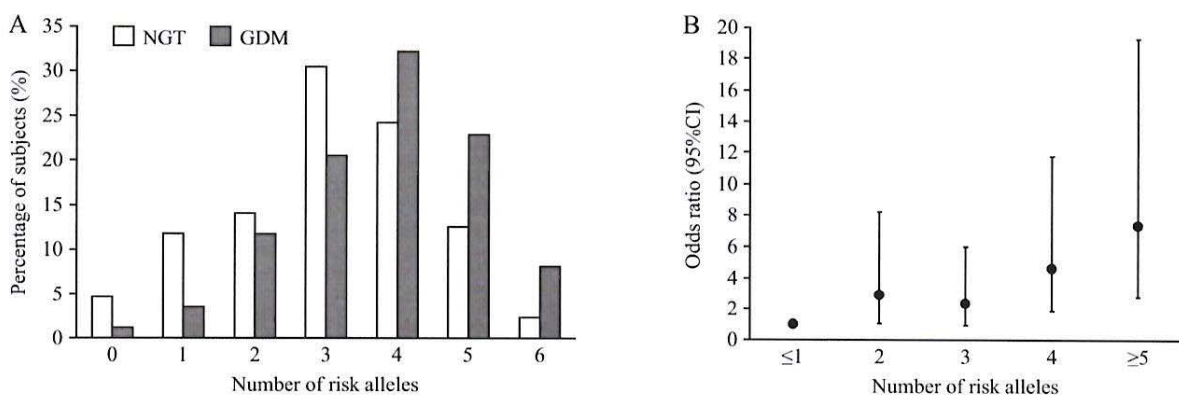


Fig. 2 Risk alleles of three genetic variants and the development of gestational diabetes mellitus

(A) Distribution of risk alleles of three genetic variants and in women with gestational diabetes mellitus (GDM) or normal glucose tolerance (NGT). Women with GDM presented significantly more T2DM risk alleles, compared with those with NGT. Black bars represent GDM ($n = 171$), while white bars represent NGT ($n = 128$). (B) Odds ratio for the risk of GDM according to the number of type 2 diabetes mellitus risk alleles carried. Women with five or more risk alleles showed a 7.32-fold increased risk of GDM ($p = 5.6 \times 10^{-5}$, 95% CI: 4.54–11.96), compared with those having no more than one risk allele.

Japanese as well as Europeans [3, 32]. With regard to *SSRI-RREB1*, it is demonstrated that the depletion of RAS-responsive element binding protein 1 (RREB1) encoded by *SSRI* reduces β -cell development and insulin secretion [33]. The meta-analysis of GWAS indicated that rs9505118 in *SSRI-RREB1* was associated with T2DM [34]. Therefore, the risk allele in *SSRI-RREB1* could be related to pancreatic β -cell dysfunction in T2DM. To the best of our knowledge, however, no association between *SSRI-RREB1* variants and risk of GDM has been demonstrated in previous reports. Our findings suggest that *SSRI-RREB1* might be one of risk variants associated with GDM in Japanese women.

It is demonstrated that a potential etiology for GDM is a limitation in beta cell reserves that manifests as maternal hyperglycemia when insulin secretion does not increase to match the escalated insulin needs during pregnancy. With regard to maternal characteristics, Asian women with GDM are less obese than Caucasian and Hispanic women [14, 16]. Thus, decreased insulin secretion in GDM might be more evident in Asians, compared with Caucasians and Hispanics [35]. Our previous investigation has shown that women with Japanese GDM have beta cell dysfunction irrespective of presence or absence of overweight [25]. Regarding the genetic background, several studies revealed risk variants related to insulin secretion in Korean and Chinese population [36-41]. Of the three genetic variants found in this study, two are related to the regulation of insulin secretion (i.e. beta cell function). Taken together, beta cell dysfunction might be the core pathophysiology of GDM in Japanese women.

The strength of the present study is that we performed the association analysis using SNPs more than ever before. Most previous studies on GDM risk variants were candidate gene approach using no more than ten variants [42], whereas we used 45 SNPs from 36 genes for analysis. In addition, women with GDM were diagnosed by a single criterion, and those with NGT were fully evaluated for the glucose tolerance status. All women in our cohort were taken care, based on the clinical recommendation by the Japan Society of Obstetrics and Gynecology [17]. The findings that maternal age at delivery, pre-pregnancy BMI and the rate of overweight were comparable between the GDM and NGT groups are important. Therefore, our study cohort is suitable to investigate GDM risk genes, as were suggested in previous reports [8, 40].

There are several limitations in this study. One of the limitations is that we focused on only SNPs with $MAF > 30\%$ since our study cohort was a relatively small panel. Therefore, we may have missed SNPs with $MAF \leq 30\%$ that are associated with GDM in Japanese women because more than 80 susceptibility genes for T2DM have been identified so far [43]. It is also important to replicate and evaluate the present findings in another independent case-control set. In this regard, the results of our study should be interpreted cautiously. In the future, we would conduct the multi-institutional collaborative genetic association study to investigate candidate gene variants for GDM. Ideally, GWAS should be performed to identify all candidate gene variants for GDM in Japanese women.

In conclusion, we performed the association analysis in the context of GDM in Japanese women for the first time and found that genetic variants in *ADIPOQ*, *CDKN2A/2B*, and *SSRI-RREB1* are nominally associated with the development of GDM in Japanese. Since women with GDM are at a high risk of future T2DM, genetic information on GDM would be useful for the T2DM risk classification [38, 41]. Further research using a larger cohort is warranted for better understanding the genetics of GDM in Japanese women.

Disclosure

The authors have no conflict of interest to declare in this study.

Funding

This study was supported by Japan Agency for Medical Research and Development Diseases (AMED, 16gm0510011h0205, 16ek0109067h0003, 16gk0110013s0801, 16gk0110018s0601), KAKENHI (26293365 and 26462500), Grants from the NCCHD of Japan (26-13), and a CREST Program of JST (Epigenomic analysis of the human placenta and endometrium constituting the fetal-maternal interface).

Acknowledgements

The authors are grateful to all medical staffs at Keio University Hospital for excellent patient care. We also appreciate medical staff in the perinatal unit of National Center for Child Health and Development.

Supplementary Table 1 Genotype information previously reported to be associated with type 2 diabetes or gestational diabetes mellitus

Chr	SNP	Nearby gene	Minor allele	MAF	Risk allele	Candidate gene for GDM	References on GDM	Candidate gene for T2DM	References on T2DM	Reasons for exclusion from our analysis
16	rs3785233	<i>A2BP1(RBFOX1)</i>	G	0.18	C			Yes	Miyake <i>et al.</i> J Hum Genet, 2009	
3	rs4607103	<i>ADAMTS9</i>	T	0.41	C			Yes	Zeggini <i>et al.</i> Nat Genet, 2008	
3	rs6795735	<i>ADAMTS9</i>	C	0.21	C			Yes	Voight <i>et al.</i> Nat Genet, 2010	
3	rs11717195	<i>ADCY5</i>	C	0	C			Yes	Saxena <i>et al.</i> Nat Genet, 2010	No variation in Japanese
3	rs11708067	<i>ADCY5</i>	G	0	A			Yes	Andersson <i>et al.</i> Diabetologia, 2010	No variation in Japanese
3	rs2241766	<i>ADIPOQ</i>	G	0.22	T	Yes	Belcheva <i>et al.</i> Arch Gynecol Obstet, 2014			
3	rs266729	<i>ADIPOQ</i>	G	0.31	C	Yes	Belcheva <i>et al.</i> Arch Gynecol Obstet, 2014	Yes	Han <i>et al.</i> Diabetologia, 2011	
8	rs4994	<i>ADRB3</i>	G	0.19	G			Yes	Jing <i>et al.</i> Endocrine, 2012	
20	rs574628	<i>ANGPT4</i>	A	0.37	G			Yes	Miyake <i>et al.</i> J Hum Genet, 2009	
8	rs515071	<i>ANK1</i>	A	0.22	C			Yes	Imamura <i>et al.</i> Hum Mol Genet, 2012	
8	rs516946	<i>ANK1</i>	T	0.16	C			Yes	Morris <i>et al.</i> Nat Genet, 2012	
15	rs2028299	<i>AP3S2</i>	C	0.20	C			Yes	Kooner <i>et al.</i> Nat Genet, 2011	
11	rs1552224	<i>ARAP1</i>	C	0.04	A	Yes	Huerta-Chagoya A <i>et al.</i> PLoS One, 2015	Yes	Voight <i>et al.</i> Nat Genet, 2010	
5	rs702634	<i>ARL15</i>	C	0.12	A			Yes	DIAGRAM Nat Genet, 2014	
16	rs7202877	<i>BCAR1</i>	G	0.21	G			Yes	Morris <i>et al.</i> Nat Genet, 2012	
2	rs243019	<i>BCL11A</i>	T	0.27	C			Yes	MetaboChip®	
2	rs243021	<i>BCL11A</i>	G	0.27	A			Yes	Voight <i>et al.</i> Nat Genet, 2010	
2	rs243088	<i>BCL11A</i>	T	0.44	T			Yes	Voight <i>et al.</i> Nat Genet, 2010	
15	rs7163757	<i>C2CD4A</i>	T	0.38	C			Yes	Yamauchi <i>et al.</i> Nat Genet, 2010	Gene-based genetic redundancy (pairwise $r^2 > 0.8$)
15	rs7172432	<i>C2CD4A, C2CD4B</i>	G	0.45	A			Yes	Yamauchi <i>et al.</i> Nat Genet, 2010	
10	rs10906115	<i>CDC123, CAMK1D</i>	G	0.49	A			Yes	Shu <i>et al.</i> PLoS Genet, 2010	
10	rs11257655	<i>CDC123, CAMK1D</i>	T	0.41	T			Yes	Voight <i>et al.</i> Nat Genet, 2010	
10	rs12779790	<i>CDC123, CAMK1D</i>	G	0.12	G			Yes	Zeggini <i>et al.</i> Nat Genet, 2008	
6	rs10440833	<i>CDKALI</i>	A	0.40	A			Yes	Voight <i>et al.</i> Nat Genet, 2010	Gene-based genetic redundancy (pairwise $r^2 > 0.8$)
6	rs7754840	<i>CDKALI</i>	C	0.41	C	Yes	Zhang <i>et al.</i> Hum Reprod Update, 2013	Yes	Scott <i>et al.</i> Science, 2007	
6	rs7756992	<i>CDKALI</i>	G	0.46	G	Yes	Cho YM <i>et al.</i> Diabetologia, 2009	Yes	Voight <i>et al.</i> Nat Genet, 2010	
6	rs4712523	<i>CDKALI</i>	G	0.41	G			Yes	Takeuchi <i>et al.</i> Diabetes, 2009	Gene-based genetic redundancy (pairwise $r^2 > 0.8$)
9	rs10811661	<i>CDKN2A, CDKN2B</i>	C	0.48	T	Yes	Cho YM <i>et al.</i> Diabetologia, 2009	Yes	Scott <i>et al.</i> Science, 2007	
9	rs10965250	<i>CDKN2A, CDKN2B</i>	A	0.43	G			Yes	Voight <i>et al.</i> Nat Genet, 2010	Gene-based genetic redundancy (pairwise $r^2 > 0.8$)
9	rs2383208	<i>CDKN2A, CDKN2B</i>	G	0.45	A	Yes	Wang Y <i>et al.</i> PLoS One, 2011	Yes	Takeuchi <i>et al.</i> Diabetes, 2009	Gene-based genetic redundancy (pairwise $r^2 > 0.8$)
9	rs13292136	<i>CHCHD9</i>	T	0.13	C			Yes	Voight <i>et al.</i> Nat Genet, 2010	
19	rs10401969	<i>CHLP2(SUGP1)</i>	C	0.09	C			Yes	Morris <i>et al.</i> Nat Genet, 2012	
7	rs17168486	<i>DGKB</i>	T	0.41	T			Yes	Dupuis <i>et al.</i> Nat Genet, 2010	
7	rs2191349	<i>DGKB</i>	G	0.27	T			Yes	Dupuis <i>et al.</i> Nat Genet, 2010	
7	rs6960043	<i>DGKB</i>	C/T	0.50	C			Yes	Dupuis <i>et al.</i> Nat Genet, 2010	
X	rs5945326	<i>DUSP9</i>	G	0.38	A			Yes	Voight <i>et al.</i> Nat Genet, 2010	
11	rs3740878	<i>EXT2</i>	C	0.36	A			Yes	Takeuchi <i>et al.</i> Diabetes, 2009	
1	rs17106184	<i>EAF1</i>	A	0.06	G			Yes	DIAGRAM Nat Genet, 2014	
12	rs3741872	<i>FAM60A</i>	C	0.27	C			Yes	Miyake <i>et al.</i> J Hum Genet, 2009	
16	rs8050136	<i>FTO</i>	A	0.18	A			Yes	Scott <i>et al.</i> Science, 2007	
16	rs11642841	<i>FTO</i>	A	0.06	A			Yes	Voight <i>et al.</i> Nat Genet, 2010	
16	rs9936385	<i>FTO</i>	C	0.12	C			Yes	Voight <i>et al.</i> Nat Genet, 2010	
7	rs17867832	<i>GCC1</i>	G	0.05	T			Yes	Cho <i>et al.</i> Nat Genet, 2012	
7	rs6467136	<i>GCC1</i>	A	0.18	G			Yes	Cho <i>et al.</i> Nat Genet, 2012	
7	rs1799884	<i>GCK</i>	T	0.17	T	Yes	Zhang <i>et al.</i> Hum Reprod Update, 2013			
7	rs4607517	<i>GCK</i>	A	0.20	A	Yes	Mao <i>et al.</i> PLoS One, 2012	Yes	Dupuis <i>et al.</i> Nat Genet, 2010	
2	rs780094	<i>GCKR</i>	C	0.44	C	Yes	Huopio H <i>et al.</i> Eur J Endocrinol, 2013	Yes	Dupuis <i>et al.</i> Nat Genet, 2010	
19	rs8108269	<i>GIPR</i>	T	0.39	G			Yes	Morris <i>et al.</i> Nat Genet, 2012	
9	rs7041847	<i>GLIS3</i>	G	0.47	A			Yes	Cho <i>et al.</i> Nat Genet, 2012	
9	rs11787792	<i>GPSM1</i>	G	0.05	A			Yes	Hara <i>et al.</i> Hum Mol Genet, 2014	

Supplementary Table 1 Cont.

Chr	SNP	Nearby gene	Minor allele	MAF	Risk allele	Candidate gene for GDM	References on GDM	Candidate gene for T2DM	References on T2DM	Reasons for exclusion from our analysis
2	rs13389219	<i>GRB14</i>	T	0.08	C			Yes	Kooner <i>et al.</i> Nat Genet, 2011	
2	rs3923113	<i>GRB14</i>	C	0.09	A			Yes	Kooner <i>et al.</i> Nat Genet, 2011	
10	rs5015480	<i>HHEX</i>	C	0.20	C	Yes	Cho YM <i>et al.</i> Diabetologia, 2009	Yes	Voight <i>et al.</i> Nat Genet, 2010	
10	rs7923837	<i>HHEX</i>	G	0.20	G	Yes	Cho YM <i>et al.</i> Diabetologia, 2009	Yes	Qian <i>et al.</i> PLoS One, 2012	
15	rs7177055	<i>HMG20A</i>	A	0.41	A			Yes	Kooner <i>et al.</i> Nat Genet, 2011	
15	rs7178572	<i>HMG20A</i>	G	0.46	G			Yes	Fukuda <i>et al.</i> PLoS One, 2012	Polymerase chain reaction failures
12	rs2261181	<i>HMG22(RPSAP52)</i>	T	0.15	T			Yes	Voight <i>et al.</i> Nat Genet, 2010	
12	rs1531343	<i>HMG22(RPSAP52)</i>	C	0.13	C			Yes	Voight <i>et al.</i> Nat Genet, 2010	
12	rs2612035	<i>HMG22(RPSAP52)</i>	G	0.13	G			Yes	Voight <i>et al.</i> Nat Genet, 2011	
12	rs12427353	<i>HNF1A</i>	C	0	G			Yes	Langenberg <i>et al.</i> PLoS Med, 2014	No variation in Japanese
17	rs11651755	<i>HNF1B</i>	C	0.29	C			Yes	MetaboChip®	
17	rs11651052	<i>HNF1B</i>	A	0.30	A			Yes	Voight <i>et al.</i> Nat Genet, 2010	
17	rs4430796	<i>HNF1B</i>	G	0.36	G			Yes	Voight <i>et al.</i> Nat Genet, 2010	
20	rs2144908	<i>HNF4A</i>	A	0.42	A	Yes	Shaar N <i>et al.</i> Diabetologia, 2006	Yes	Chavali <i>et al.</i> J Hum Genet, 2011	
20	rs4812829	<i>HNF4A</i>	A	0.40	A			Yes	Kooner <i>et al.</i> Nat Genet, 2011	Gene-based genetic redundancy (pairwise $r^2 > 0.8$)
20	rs6017317	<i>HNF4A</i>	T	0.46	G			Yes	Cho <i>et al.</i> Nat Genet, 2012	
3	rs4402960	<i>IGF2BP2</i>	T	0.30	T	Yes	Mao <i>et al.</i> PLoS One, 2012	Yes	Voight <i>et al.</i> Nat Genet, 2010	
3	rs1470579	<i>IGF2BP2</i>	C	0.33	C			Yes	Saxena <i>et al.</i> Science, 2007	Gene-based genetic redundancy (pairwise $r^2 > 0.8$)
3	rs6769511	<i>IGF2BP2</i>	C	0.33	C			Yes	Long <i>et al.</i> Am J Epidemiol, 2012	Polymerase chain reaction failures
2	rs7578326	<i>IRS1</i>	G	0.18	A			Yes	Voight <i>et al.</i> Nat Genet, 2010	
2	rs1801278	<i>IRS1</i>	T	0.08	T	Yes	Zhang <i>et al.</i> Hum Reprod Update, 2013	Yes	Alharbi <i>et al.</i> Endocrine, 2014	
2	rs2943640	<i>IRS1</i>	A	0.07	C			Yes	Voight <i>et al.</i> Nat Genet, 2010	
2	rs2943641	<i>IRS1</i>	T	0.07	C			Yes	Rung <i>et al.</i> Nat Genet, 2009	
2	rs7593730	<i>ITGB6-RBMS1</i>	T	0.12	C			Yes	Qi <i>et al.</i> Hum Mol Genet, 2010	
2	rs7569522	<i>ITGB6-RBMS1</i>	A	0.38	A			Yes	Qi <i>et al.</i> Hum Mol Genet, 2010	
7	rs849134	<i>JAZF1</i>	G	0.21	A			Yes	Voight <i>et al.</i> Nat Genet, 2010	
7	rs864745	<i>JAZF1</i>	C	0.21	T	Yes	Stuebe AM <i>et al.</i> Am J Perinatol, 2014	Yes	Zeggini <i>et al.</i> Nat Genet, 2008	
7	rs849135	<i>JAZF1</i>	A	0	G			Yes	Langenberg <i>et al.</i> PLoS Med, 2014	No variation in Japanese
11	rs5215	<i>KCNJ11</i>	C	0.34	C			Yes	Scott <i>et al.</i> Science, 2007	
11	rs5219	<i>KCNJ11</i>	T	0.35	T	Yes	Mao <i>et al.</i> PLoS One, 2012	Yes	Sokolova <i>et al.</i> PLoS One, 2014	
6	rs1535500	<i>KCNK17</i>	T	0.40	T			Yes	Cho <i>et al.</i> Nat Genet, 2012	
11	rs231362	<i>KCNQ1</i>	T	0.13	G			Yes	Voight <i>et al.</i> Nat Genet, 2010	
11	rs163184	<i>KCNQ1</i>	G	0.42	G	Yes	Huerta-Chagoya A <i>et al.</i> PLoS One, 2015	Yes	Voight <i>et al.</i> Nat Genet, 2010	
11	rs2237892	<i>KCNQ1</i>	T	0.36	C	Yes	Mao <i>et al.</i> PLoS One, 2012	Yes	Yasuda <i>et al.</i> Nat Genet, 2008	
11	rs231361	<i>KCNQ1</i>	C	0.17	A			Yes	Voight <i>et al.</i> Nat Genet, 2010	
11	rs2237895	<i>KCNQ1</i>	C	0.3	C	Yes	Mao <i>et al.</i> PLoS One, 2012	Yes	Unoki <i>et al.</i> Nat Genet, 2008	Unique primer design failure
7	rs13233731	<i>KLF14</i>	A	0.29	G			Yes	Voight <i>et al.</i> Nat Genet, 2010	
7	rs972283	<i>KLF14</i>	A	0.29	G			Yes	Voight <i>et al.</i> Nat Genet, 2010	
12	rs10842994	<i>KLHDC5</i>	T	0.21	T			Yes	Morris <i>et al.</i> Nat Genet, 2012	
12	rs2307027	<i>KRT4</i>	C	0.17	C			Yes	Miyake <i>et al.</i> J Hum Genet, 2009	
4	rs6819243	<i>MAEA</i>	C	0.36	T			Yes	Cho <i>et al.</i> Nat Genet, 2012	Gene-based genetic redundancy (pairwise $r^2 > 0.8$)
4	rs6815464	<i>MAEA</i>	G	0.36	C			Yes	Cho <i>et al.</i> Nat Genet, 2012	
18	rs12970134	<i>MC4R</i>	A	0.19	A			Yes	Morris <i>et al.</i> Nat Genet, 2012	
7	rs791595	<i>MIR129-LEP</i>	A	0.10	A			Yes	Hara <i>et al.</i> Hum Mol Genet, 2014	
12	rs4275659	<i>MPHOSPH9(ABC9)</i>	T	0.33	C			Yes	DIAGRAM Nat Genet, 2014	
11	rs10830963	<i>MTNR1B</i>	G	0.47	G	Yes	Mao <i>et al.</i> PLoS One, 2012	Yes	Dupuis <i>et al.</i> Nat Genet, 2010	
11	rs1387153	<i>MTNR1B</i>	T	0.48	T	Yes	Zhang <i>et al.</i> Hum Reprod Update, 2013	Yes	Voight <i>et al.</i> Nat Genet, 2010	
1	rs10923931	<i>NOTCH2</i>	T	0.02	T			Yes	Zeggini <i>et al.</i> Nat Genet, 2008	
19	rs8182584	<i>PEPD</i>	G	0.36	T			Yes	Cho <i>et al.</i> Nat Genet, 2012	
19	rs3786897	<i>PEPD</i>	G	0.45	A			Yes	Cho <i>et al.</i> Nat Genet, 2012	

Supplementary Table 1 Cont.

Chr	SNP	Nearby gene	Minor allele	MAF	Risk allele	Candidate gene for GDM	References on GDM	Candidate gene for T2DM	References on T2DM	Reasons for exclusion from our analysis
19	rs10425678	PEPD	C	0.27	C			Yes	Cho <i>et al.</i> Nat Genet, 2012	Polymerase chain reaction failures
6	rs3130501	POU5F1	A	0.45	G			Yes	Nair <i>et al.</i> Diabetologia, 2014	Unique primer design failure
3	rs1801282	PPARG	G	0.06	C	Yes	Wu L <i>et al.</i> Sci Rep, 2016	Yes	Saxena <i>et al.</i> Science, 2007	
3	rs13081389	PPARG	G	0.04	A			Yes	Voight <i>et al.</i> Nat Genet, 2010	
15	rs12899811	PRCI	A	0.01	G			Yes	Voight <i>et al.</i> Nat Genet, 2010	
15	rs8042680	PRCI-ASI	C	0	A			Yes	DIAGRAM Nat Genet, 2014	No variation in Japanese
1	rs2075423	PROX1	T	0.14	G			Yes	Dupuis <i>et al.</i> Nat Genet, 2010	
1	rs340874	PROX1-ASI	C	0.33	C			Yes	Hu <i>et al.</i> PLoS One, 2010	Polymerase chain reaction failures
3	rs12497268	PSMD6(PRICKLE2)	C	0.39	G			Yes	Cho <i>et al.</i> Nat Genet, 2012	
3	rs831571	PSMD6(PRICKLE2)	T	0.31	C			Yes	Cho <i>et al.</i> Nat Genet, 2012	
3	rs13059603	PSMD6(THOC7)	G	0.32	A			Yes	Cho <i>et al.</i> Nat Genet, 2012	
9	rs16927668	PTPRD	T	0.43	T			Yes	Tsai <i>et al.</i> PLoS One, 2010	
9	rs17584499	PTPRD	T	0.15	T			Yes	Tsai <i>et al.</i> PLoS One, 2010	
2	rs7560163	RBM43, RND3	G	0.19	C			Yes	Palmer <i>et al.</i> PLoS One, 2012	
2	rs4410242	RBMS1	A	0.17	G			Yes	MetaboChip®	
17	rs312457	SLC16A13	C	0.07	G			Yes	Hara <i>et al.</i> Hum Mol Genet, 2014	Unique primer design failure
8	rs13266634	SLC30A8	T	0.44	C	Yes	Cho YM <i>et al.</i> Diabetologia, 2009	Yes	Sladek <i>et al.</i> Science, 2007	
8	rs3802177	SLC30A8	A	0.45	G	Yes	Liang Z <i>et al.</i> Diabetes Res Clin Pract, 2010	Yes	Voight <i>et al.</i> Nat Genet, 2010	Gene-based genetic redundancy (pairwise $r^2 > 0.8$)
17	rs391300	SRR	T	0.22	G	Yes	Wang Y <i>et al.</i> PLoS One, 2011	Yes	Tsai <i>et al.</i> PLoS One, 2010	
6	rs9505118	SSRI-RREB1	G	0.41	A			Yes	DIAGRAM Nat Genet, 2014	
3	rs16861329	ST6GAL1	T	0.24	G			Yes	Kooner <i>et al.</i> Nat Genet, 2011	
3	rs17301514	ST6GAL1	A	0.04	A			Yes	Kooner <i>et al.</i> Nat Genet, 2011	
10	rs12255372	TCF7L2	T	0.02	T	Yes	Zhang <i>et al.</i> Hum Reprod Update, 2013	Yes	Tabara <i>et al.</i> Diabetes, 2009	
10	rs7901695	TCF7L2	C	0.04	C	Yes	Huerta-Chagoya A <i>et al.</i> PLoS One, 2015	Yes	Yamauchi <i>et al.</i> Nat Genet, 2010	
2	rs10203174	THADA	T	0.02	C			Yes	Voight <i>et al.</i> Nat Genet, 2010	
2	rs7578597	THADA	C	0.01	T			Yes	Zeggini <i>et al.</i> Nat Genet, 2008	
2	rs11899863	THADA	C	0	C			Yes	Mercader <i>et al.</i> PLoS Genet, 2012	No variation in Japanese
9	rs17791513	TLE4	G	0.08	A			Yes	Voight <i>et al.</i> Nat Genet, 2010	
4	rs6813195	TMEM154	T	0.46	C			Yes	DIAGRAM Nat Genet, 2014	
6	rs1800629	TNF	A	0.02	G	Yes	Wu L <i>et al.</i> Sci Rep, 2016	Yes	Boraska <i>et al.</i> BMC Med Genet, 2010	Unique primer design failure
8	rs7845219	TP53INP1	T	0.46	T			Yes	Voight <i>et al.</i> Nat Genet, 2010	
12	rs4760790	TSPAN8, LGR5	A	0.24	A			Yes	Voight <i>et al.</i> Nat Genet, 2010	
12	rs7961581	TSPAN8, LGR5	C	0.23	C	Yes	Stuebe AM <i>et al.</i> Am J Perinatol, 2014	Yes	Zeggini <i>et al.</i> Nat Genet, 2008	
12	rs4760915	TSPAN8, LGR5	T	0.27	T			Yes	MetaboChip®	
12	rs7955901	TSPAN8, LGR5	T	0.30	C			Yes	Voight <i>et al.</i> Nat Genet, 2010	
3	rs7612463	UBE2E2	A	0.15	C	Yes	Kim JY <i>et al.</i> Gynecol Endocrinol, 2013	Yes	Yamauchi <i>et al.</i> Nat Genet, 2010	
3	rs1496653	UBE2E2	G	0.15	A			Yes	Yamauchi <i>et al.</i> Nat Genet, 2010	
3	rs6780569	UBE2E2	A	0.15	G			Yes	Yamauchi <i>et al.</i> Nat Genet, 2010	
10	rs1802295	VPS26A	T	0.12	A			Yes	Kooner <i>et al.</i> Nat Genet, 2011	
10	rs12242953	VPS26A	A	0.05	G			Yes	Kooner <i>et al.</i> Nat Genet, 2011	
4	rs4458523	WFS1	T	0.02	G			Yes	Voight <i>et al.</i> Nat Genet, 2010	
4	rs4689388	WFS1	G	0.02	T			Yes	Rung <i>et al.</i> Nat Genet, 2009	
4	rs1801214	WFS1	C	0	T			Yes	Long <i>et al.</i> Am J Epidemiol, 2013	No variation in Japanese
16	rs17797882	WWOX	T	0.21	C			Yes	Sakai <i>et al.</i> PLoS One, 2013	
7	rs10278336	YKT6	G	0.43	A			Yes	Dupuis <i>et al.</i> Nat Genet, 2010	
5	rs4457053	ZBED3	G	0.03	G			Yes	Voight <i>et al.</i> Nat Genet, 2010	
5	rs6878122	ZBED3	G	0.02	G			Yes	Voight <i>et al.</i> Nat Genet, 2010	
6	rs9470794	ZFAND3	C	0.20	C			Yes	Cho <i>et al.</i> Nat Genet, 2012	
6	rs4299828	ZFAND3(BTBD9)	G	0.06	A			Yes	Cho <i>et al.</i> Nat Genet, 2012	
15	rs11634397	ZFAND6	G	0.09	G			Yes	Voight <i>et al.</i> Nat Genet, 2010	
10	rs12571751	ZMIZI	G	0.42	G			Yes	Morris <i>et al.</i> Nat Genet, 2012	

The information was retrieved from HapMap JPT as well as previous studies. Chr, Chromosome; SNP, Single nucleotide polymorphism; MAF, Minor allele frequency; T2DM, Type 2 diabetes mellitus; GDM, Gestational diabetes mellitus.

Supplementary Table 2 Primers designed by Assay Design Suite in this study

SNP	Forward primer sequence	Reverse primer sequence	Extension primer sequence
rs10278336	ACGTTGGATGGAACAATCCTGTGGATTGTG	ACGTTGGATGGCACTGTGCTAAAATCCTC	AATCCTCATATGATTGAAAGG
rs10811661	ACGTTGGATGGTCAATAAGCGTCTTGCCC	ACGTTGGATGGATCAGGAGGGTAATAGAC	cccgtAGGGTAATAGACTTACTGTCATG
rs10830963	ACGTTGGATGAGGTCACCTCTGTCTATGCTG	ACGTTGGATGCCAGGCAGTTACTGGTTCT	gggcGGCAGTTACTGGTCTTGATAG
rs10906115	ACGTTGGATGATTGAGGACTCCGTTTTGGC	ACGTTGGATGGTTACGTGTATGCGATCCC	cgggACGTGTATGCGATCCCAAGTTTG
rs11257655	ACGTTGGATGTGCAAAGCACCTACTGCTTC	ACGTTGGATGCCACGGAGATGGTTTCATGC	ttaaGGTTTTCATGCCAGTA
rs12497268	ACGTTGGATGAGGCACCCCTTGAAAAACA	ACGTTGGATGGAAACTGATAGTAGATGCTG	GCITGATCAGAGCAGGA
rs12571751	ACGTTGGATGGGTGTGTGCATGGTACGTAT	ACGTTGGATGAAACACCTACAGACCCGAG	ttgGGAGGAGGAAAACAGTG
rs13059603	ACGTTGGATGTGACAGACTGCTCAAGCTAC	ACGTTGGATGGTCTCAGTCTCTTCAGATAA	cTTTAAAAATACAAACTAATGCTTTC
rs13266634	ACGTTGGATGGCAATCAGTGTAAATCTCCC	ACGTTGGATGTTCTCTCCGAACCACCTTG	tctccCACTTGGCTGTCCC
rs1387153	ACGTTGGATGCTCTCTCTAGAGCTCACAAC	ACGTTGGATGTGTCTGTGGAATGCTAGCAA	CTTTTACAGATAAGAAAATTGAGTT
rs1535500	ACGTTGGATGAGAGATGGGGATCTTCTGAG	ACGTTGGATGAGCTCTGGCTGCTCAGTAGG	aGGCTCAAGGATGGGG
rs163184	ACGTTGGATGTTTGTCTCAGTAACGGACTGG	ACGTTGGATGGGTAAAGTGTCTGTGAAAAG	ccGGGCAAGGGTGGAG
rs16927668	ACGTTGGATGCCATTTTAGTGGCTGTTGG	ACGTTGGATGCACCTTCAGAACTGGAAGG	gaagaTTCAGAACTGGAAGGAATAGG
rs17168486	ACGTTGGATGGCACCCGTGAGGGATAATTAAG	ACGTTGGATGTCTGTGATCTGGTTGATCTT	cttgcTCTCTGCCAATTGACACC
rs2144908	ACGTTGGATGACCACGTGCATTGCAAAGAC	ACGTTGGATGCCCTGACTAGAGTCAGGAGAT	TCTGTCAATCCCTGGC
rs2237892	ACGTTGGATGCAGATGATGGAGCTGTAC	ACGTTGGATGTAAGGCATCTGGTGGAGAGG	CTAGGCCCTCACCCC
rs243088	ACGTTGGATGTGAGAGTAGGGTAGGAACAC	ACGTTGGATGTGTGAAAAGGGTAGCTCCG	tgGTAGCTCCGAGAAGA
rs266729	ACGTTGGATGATGTGTGGCTTGCAAGAACC	ACGTTGGATGTGGACTTCTTGGCACGCTC	CGTCAATGTTTTGTTTTGAAG
rs3740878	ACGTTGGATGCAAAAACATACCTGGCTGTC	ACGTTGGATGCACAAAAGAATGCAGTGTGG	ccggCACAGCATGATTTTATGTCTCT
rs3786897	ACGTTGGATGAAGCCATCTGGAAGACCTG	ACGTTGGATGATCTGCATAGGACAGCCCA	ggagGCCGTTGGCTGAGCCCTGAG
rs4275659	ACGTTGGATGAGAGGTGATAAGACTGCTG	ACGTTGGATGTCTGACGCATGTAAGTGCC	AGACTGTCTGAGGCTAA
rs4402960	ACGTTGGATGAGCAGTAAGGTAGGATGGAC	ACGTTGGATGTGGGGCATGTTTGCAAAACAC	ggggGCAAAACAATCAGTATCTT
rs4430796	ACGTTGGATGTGAATACAGAGAGGCAGCAC	ACGTTGGATGCAAAAGACCAACAACGCTTG	gggatAGGCAGCACAGACTGGA
rs4607103	ACGTTGGATGTCATAATCTCAGGCCAG	ACGTTGGATGGTGTGTACCAAGGACATCCA	AGGCCAGCAGGTTT
rs5215	ACGTTGGATGCTGTGGTCTCATCAAGCTG	ACGTTGGATGACGGACGTTACTCTGTGGAC	GTGTGGGCACCTTGA
rs5219	ACGTTGGATGTGTTCTTGTGGCCACGTTG	ACGTTGGATGGCATCCTCCCGAGGAATA	gagaCACGGTACCTGGGCT
rs574628	ACGTTGGATGCTCTTGACCCACATCAAAG	ACGTTGGATGTCTCAGTGCCTAATCCGGAG	CCACATCAAAGGTCAGG
rs5945326	ACGTTGGATGCAGGGATCTCAGGCTCTTIA	ACGTTGGATGTGTCTCCAGGGCTTTGCAC	GGGGCCGTAGCAATG
rs6017317	ACGTTGGATGAAGAAAAGGCAAAAGGATCTG	ACGTTGGATGTGGCCATTCTATGTTGTC	TCTATGTTGTCTTGTGTTTGGAG
rs6813195	ACGTTGGATGGGGAGAGGAAGCAAGTAAAC	ACGTTGGATGATGGCAACCACACTCCTGCT	gaggGTAATACTGGCCTTGC
rs6815464	ACGTTGGATGCTGCACACATCCTGCTTAG	ACGTTGGATGAGCTCTCAGGAAAGCAAT	cgggACCGATACCTGTACCCCGGGTTTTG
rs6960043	ACGTTGGATGCCCTTTTGGACTAATAGCTG	ACGTTGGATGGCCCTTGAATGTGAGGTTTA	AACCTGTCTGCTCA
rs7041847	ACGTTGGATGGATGCCGGGTGTAATCAC	ACGTTGGATGCCACCTCATCGCATACATTT	TCCTTCCCTTGACCA
rs7172432	ACGTTGGATGCTTTGGGAGATAGGTTCTGC	ACGTTGGATGGCTTAAAAGAGGGCTTGGG	AGACAGTTTCTTTGGGAA
rs7177055	ACGTTGGATGCACAGCTTCTACCTTACGTG	ACGTTGGATGCTAGGAGGACATCTTACCTG	ccccCCTTACGTGCTGAGAC
rs7569522	ACGTTGGATGCTGTCCAAATGCTTTTCAG	ACGTTGGATGGCCAGTGCATGTATGAAAT	GTAATAAGTTATGGGGATTGAAATA
rs7754840	ACGTTGGATGATCAACTGCTGTGTTGGG	ACGTTGGATGCAGAGACATCACTGTCCITT	AAATCCTCTATCAAGTCAAC
rs7756992	ACGTTGGATGGACAATTAATATCCCCCTG	ACGTTGGATGATGCAACCAAGAGAGGTCCTG	cattaCCCCCTGATTTTAGTTTT
rs780094	ACGTTGGATGAGGGCCCCAGTTTTTAGAC	ACGTTGGATGCCCGCCCTCAACAAATGAT	cttgTAGACCATGACTGACACAT
rs7845219	ACGTTGGATGTTCTTTGGGCTTCGTGTTCC	ACGTTGGATGACCCCTATTGTGGAGCTCTA	CTTCGTGTTCCATTATCTGAA
rs7955901	ACGTTGGATGATGCATTCATAGACACCACC	ACGTTGGATGTGTTGTGTACATGCATGGG	gggagGGGAGCCCAAGTGGTT
rs8108269	ACGTTGGATGGGGTCTGATTTCAACACCT	ACGTTGGATGCCCAATTTCTGGATAGGGA	ttAGACATGTCACCTTGA
rs8182584	ACGTTGGATGGCATGACGACAACACAGAC	ACGTTGGATGTTGCTCAFTTCAGGCACCTG	GCACTCGGAGCCTCAG
rs831571	ACGTTGGATGGACAAGGCTATTCATCCTC	ACGTTGGATGGTACCTAGAGATAGGGCTG	TCTTGACAACAAGATAGGCTTTA
rs9505118	ACGTTGGATGACTTGGTTATTGACTGCTG	ACGTTGGATGCAGCAGTTTTTAAGCGTTTAC	ACTGCTGAAGACACC

SNP, Single nucleotide polymorphism.

Supplementary Table 3 Association analysis results between single nucleotide polymorphisms and the risk of gestational diabetes mellitus

SNP	Chr	Nearby gene	Insulin sensitivity	Insulin secretion	Risk allele	Japanese major allele	Japanese minor allele	RAF in this study		The present study		
								GDM	NGT	p-value	OR (95%CI)	
1	rs266729	3	<i>ADIPOQ</i>	Yes	C	C	G	0.79	0.69	0.013	1.56 (1.10-2.23)	
2	rs10811661	9	<i>CDKN2A2B</i>		Yes	T	T	C	0.58	0.49	0.035	1.46 (1.03-2.08)
3	rs9505118	6	<i>SSRI-RREB1</i>		Yes	A	A	G	0.58	0.50	0.046	1.41 (1.01-1.97)
4	rs7177055	15	<i>HMG20A</i>		Yes	A	G	A	0.39	0.32	0.064	1.41 (0.98-2.01)
5	rs16927668	9	<i>PTPRD</i>	Yes		T	T	C	0.55	0.48	0.083	1.34 (0.96-1.87)
6	rs1535500	6	<i>KCNK17</i>			T	G	T	0.38	0.31	0.087	1.35 (0.96-1.89)
7	rs574628	20	<i>ANGPT4</i>	Yes		G	G	A	0.59	0.64	0.165	0.77 (0.53-1.12)
8	rs5219	11	<i>KCNJ11</i>		Yes	T	C	T	0.36	0.41	0.245	0.81 (0.57-1.15)
9	rs4430796	17	<i>HNF1B</i>		Yes	G	A	G	0.31	0.35	0.279	0.82 (0.56-1.18)
10	rs1387153	11	<i>MTNR1B</i>		Yes	T	C	T	0.49	0.45	0.280	1.21 (0.86-1.71)
11	rs6815464	4	<i>MAEA</i>	Yes		C	C	G	0.68	0.64	0.282	1.22 (0.85-1.77)
12	rs8182584	19	<i>PEPD</i>	Yes		T	T	G	0.62	0.67	0.284	0.83 (0.58-1.17)
13	rs12497268	3	<i>PSMD6(PRICKLE2)</i>			G	G	C	0.65	0.60	0.312	1.19 (0.85-1.67)
14	rs2237892	11	<i>KCNQ1</i>		Yes	C	C	T	0.63	0.67	0.326	0.84 (0.59-1.20)
15	rs6813195	4	<i>TMEM154</i>		Yes	C	T	C	0.48	0.44	0.341	1.18 (0.84-1.64)
16	rs6017317	20	<i>HNF4A</i>		Yes	G	G	T	0.52	0.56	0.357	0.86 (0.62-1.19)
17	rs5215	11	<i>KCNJ11</i>		Yes	C	T	C	0.38	0.42	0.393	0.86 (0.61-1.22)
18	rs2144908	20	<i>HNF4A</i>		Yes	A	G	A	0.46	0.48	0.425	0.86 (0.60-1.24)
19	rs163184	11	<i>KCNQ1</i>		Yes	G	T	G	0.48	0.45	0.430	1.14 (0.82-1.59)
20	rs13059603	3	<i>THOC7</i>			A	A	G	0.66	0.63	0.446	1.14 (0.81-1.61)
21	rs10278336	7	<i>YKT6</i>			A	A	G	0.67	0.70	0.446	0.87 (0.61-1.24)
22	rs7041847	9	<i>GLIS3</i>		Yes	A	G	A	0.47	0.44	0.506	1.12 (0.80-1.57)
23	rs780094	2	<i>GCKR</i>	Yes		G	A	G	0.44	0.47	0.512	0.90 (0.64-1.25)
24	rs17168486	7	<i>DGKB</i>		Yes	T	C	T	0.39	0.41	0.598	0.91 (0.65-1.28)
25	rs10906115	10	<i>CDC123, CAMK1D</i>		Yes	A	A	G	0.58	0.56	0.642	1.08 (0.79-1.48)
26	rs8108269	19	<i>GIPR</i>	Yes		G	G	T	0.68	0.66	0.645	1.09 (0.76-1.56)
27	rs4275659	12	<i>MPHOSPH9(ABC9)</i>			C	C	T	0.71	0.70	0.687	1.08 (0.74-1.57)
28	rs4607103	3	<i>ADAMTS9</i>	Yes		C	C	T	0.61	0.62	0.716	0.94 (0.67-1.32)
29	rs7754840	6	<i>CDKAL1</i>		Yes	C	G	C	0.45	0.44	0.737	1.06 (0.77-1.45)
30	rs12571751	10	<i>ZMIZ1</i>			G	A	G	0.45	0.46	0.738	0.95 (0.69-1.31)
31	rs5945326	X	<i>DUSP9</i>	Yes		A	A	G	0.65	0.66	0.769	0.95 (0.68-1.35)
32	rs7955901	12	<i>TSPAN8, LGR5</i>		Yes	C	C	T	0.68	0.69	0.807	0.96 (0.66-1.38)
33	rs7845219	8	<i>TP53INP1</i>		Yes	T	C	T	0.31	0.32	0.814	0.96 (0.67-1.37)
34	rs243088	2	<i>BCL11A</i>	Yes		T	A	T	0.32	0.33	0.830	0.96 (0.68-1.36)
35	rs7172432	15	<i>C2CD4A-4B</i>		Yes	A	A	G	0.59	0.58	0.852	1.03 (0.75-1.41)
36	rs3740878	11	<i>EXT2</i>		Yes	A	A	G	0.63	0.64	0.876	0.97 (0.68-1.38)
37	rs10830963	11	<i>MTNR1B</i>		Yes	G	C	G	0.48	0.47	0.880	1.03 (0.73-1.45)
38	rs11257655	10	<i>CDC123, CAMK1D</i>		Yes	T	C	T	0.47	0.46	0.882	1.03 (0.73-1.44)
39	rs7756992	6	<i>CDKAL1</i>		Yes	G	A	G	0.49	0.48	0.893	1.02 (0.75-1.39)
40	rs831571	3	<i>PSMD6(PRICKLE2)</i>			C	C	T	0.67	0.32	0.918	1.02 (0.72-1.44)
41	rs6960043	7	<i>DGKB</i>		Yes	C	C	T	0.51	0.51	0.931	0.99 (0.71-1.38)
42	rs13266634	8	<i>SLC30A8</i>		Yes	C	C	T	0.61	0.61	0.961	0.99 (0.71-1.38)
43	rs7569522	2	<i>ITGB6-RBMS1</i>	Yes		A	G	A	0.34	0.34	0.963	1.01 (0.72-1.42)
44	rs3786897	19	<i>PEPD</i>	Yes		A	A	G	0.58	0.58	0.982	1.00 (0.70-1.44)
45	rs4402960	3	<i>IGF2BP2</i>		Yes	T	G	T	0.32	0.31	0.987	1.00 (0.69-1.45)

SNP, Single nucleotide polymorphism; Chr, Chromosome; GDM, Gestational diabetes mellitus; RAF, Risk allele frequency; OR, Odds ratio; CI, confidence interval.

References

1. Reece EA, Leguizamón G, Wiznitzer A (2009) Gestational diabetes: the need for a common ground. *Lancet* 373: 1789-1797.
2. Buchanan TA, Xiang AH, Page KA (2012) Gestational diabetes mellitus: risks and management during and after pregnancy. *Nat Rev Endocrinol* 8: 639-649.
3. Imamura M, Maeda S (2011) Genetics of type 2 diabetes: the GWAS era and future perspectives [Review]. *Endocr J* 58: 723-739.
4. Imamura M, Maeda S, Yamauchi T, Hara K, Yasuda K, *et al.* (2012) A single-nucleotide polymorphism in ANK1 is associated with susceptibility to type 2 diabetes in Japanese populations. *Hum Mol Genet* 21: 3042-3049.
5. Fukuda H, Imamura M, Tanaka Y, Iwata M, Hirose H, *et al.* (2012) A single nucleotide polymorphism within DUSP9 is associated with susceptibility to type 2 diabetes in a Japanese population. *PLoS One* 7: e46263.
6. Imamura M, Iwata M, Maegawa H, Watada H, Hirose H, *et al.* (2011) Genetic variants at CDC123/CAMK1D and SPRY2 are associated with susceptibility to type 2 diabetes in the Japanese population. *Diabetologia* 54: 3071-3077.
7. Lauenborg J, Grarup N, Damm P, Borch-Johnsen K, Jorgensen T, *et al.* (2009) Common type 2 diabetes risk gene variants associate with gestational diabetes. *J Clin Endocrinol Metab* 94: 145-150.
8. Zhang C, Bao W, Rong Y, Yang H, Bowers K, *et al.* (2013) Genetic variants and the risk of gestational diabetes mellitus: a systematic review. *Hum Reprod Update* 19: 376-390.
9. Zhang Y, Sun CM, Hu XQ, Zhao Y (2014) Relationship between melatonin receptor 1B and insulin receptor substrate 1 polymorphisms with gestational diabetes mellitus: a systematic review and meta-analysis. *Sci Rep* 4: 6113.
10. Watanabe RM, Black MH, Xiang AH, Allayee H, Lawrence JM, *et al.* (2007) Genetics of gestational diabetes mellitus and type 2 diabetes. *Diabetes Care* 30: S134-140.
11. Robitaille J, Grant AM (2008) The genetics of gestational diabetes mellitus: evidence for relationship with type 2 diabetes mellitus. *Genet Med* 10: 240-250.
12. Hillier TA, Pedula KL, Schmidt MM, Mullen JA, Charles MA, *et al.* (2007) Childhood obesity and metabolic imprinting: the ongoing effects of maternal hyperglycemia. *Diabetes Care* 30: 2287-2292.
13. Clausen TD, Mathiesen ER, Hansen T, Pedersen O, Jensen DM, *et al.* (2008) High prevalence of type 2 diabetes and pre-diabetes in adult offspring of women with gestational diabetes mellitus or type 1 diabetes: the role of intrauterine hyperglycemia. *Diabetes Care* 31: 340-346.
14. Ramachandran A, Ma RC, Snehalatha C (2010) Diabetes in Asia. *Lancet* 375: 408-418.
15. Tutino GE, Tam WH, Yang X, Chan JC, Lao TT, *et al.* (2014) Diabetes and pregnancy: perspectives from Asia. *Diabet Med* 31: 302-318.
16. Hedderson M, Ehrlich S, Sridhar S, Darbinian J, Moore S, *et al.* (2012) Racial/ethnic disparities in the prevalence of gestational diabetes mellitus by BMI. *Diabetes Care* 35: 1492-1498.
17. Minakami H, Maeda T, Fujii T, Hamada H, Iitsuka Y, *et al.* (2014) Guidelines for obstetrical practice in Japan: Japan Society of Obstetrics and Gynecology (JSOG) and Japan Association of Obstetricians and Gynecologists (JAOG) 2014 edition. *J Obstet Gynaecol Res* 40: 1469-1499.
18. Purcell S, Cherny SS, Sham PC (2003) Genetic Power Calculator: design of linkage and association genetic mapping studies of complex traits. *Bioinformatics* 19: 149-150.
19. Matsuda M, DeFronzo RA (1999) Insulin sensitivity indices obtained from oral glucose tolerance testing: comparison with the euglycemic insulin clamp. *Diabetes Care* 22: 1462-1470.
20. Matthews DR, Hosker JP, Rudenski AS, Naylor BA, Treacher DF, *et al.* (1985) Homeostasis model assessment: insulin resistance and beta-cell function from fasting plasma glucose and insulin concentrations in man. *Diabetologia* 28: 412-419.
21. Katz A, Nambi SS, Mather K, Baron AD, Follmann DA, *et al.* (2000) Quantitative insulin sensitivity check index: a simple, accurate method for assessing insulin sensitivity in humans. *J Clin Endocrinol Metab* 85: 2402-2410.
22. Kosaka K, Hagura R, Kuzuya T, Kuzuya N (1974) Insulin secretory response of diabetics during the period of improvement of glucose tolerance to normal range. *Diabetologia* 10: 775-782.
23. Retnakaran R, Qi Y, Goran MI, Hamilton JK (2009) Evaluation of proposed oral disposition index measures in relation to the actual disposition index. *Diabet Med* 26: 1198-1203.
24. Yabe D, Seino Y (2016) Type 2 diabetes via beta-cell dysfunction in east Asian people. *Lancet Diabetes Endocrinol* 4: 2-3.
25. Saisho Y, Miyakoshi K, Tanaka M, Shimada A, Ikenoue S, *et al.* (2010) Beta cell dysfunction and its clinical significance in gestational diabetes. *Endocr J* 57: 973-980.
26. Qian Y, Lu F, Dong M, Lin Y, Li H, *et al.* (2015) Cumulative effect and predictive value of genetic variants associated with type 2 diabetes in Han Chinese: a case-control study. *PLoS One* 10: e0116537.
27. Freathy RM, Hayes MG, Urbanek M, Lowe LP, Lee H, *et al.* (2010) Hyperglycemia and Adverse Pregnancy Outcome (HAPO) study: common genetic variants

- in GCK and TCF7L2 are associated with fasting and postchallenge glucose levels in pregnancy and with the new consensus definition of gestational diabetes mellitus from the International Association of Diabetes and Pregnancy Study Groups. *Diabetes* 59: 2682-2689.
28. Laafira A, White SW, Griffin CJ, Graham D (2016) Impact of the new IADPSG gestational diabetes diagnostic criteria on pregnancy outcomes in Western Australia. *Aust N Z J Obstet Gynaecol* 56: 36-41.
 29. Mayo K, Melamed N, Vandenberghe H, Berger H (2015) The impact of adoption of the international association of diabetes in pregnancy study group criteria for the screening and diagnosis of gestational diabetes. *Am J Obstet Gynecol* 212: 224.e1-e9.
 30. Hivert MF, Manning AK, McAteer JB, Florez JC, Dupuis J, *et al.* (2008) Common variants in the adiponectin gene (ADIPOQ) associated with plasma adiponectin levels, type 2 diabetes, and diabetes-related quantitative traits: the Framingham Offspring Study. *Diabetes* 57: 3353-3359.
 31. Beltcheva O, Boyadzhieva M, Angelova O, Mitev V, Kaneva R, *et al.* (2014) The rs266729 single-nucleotide polymorphism in the adiponectin gene shows association with gestational diabetes. *Arch Gynecol Obstet* 289: 743-748.
 32. Zeggini E, Weedon MN, Lindgren CM, Frayling TM, Elliott KS, *et al.* (2007) Replication of genome-wide association signals in UK samples reveals risk loci for type 2 diabetes. *Science* 316: 1336-1341.
 33. Ray SK, Li HJ, Metzger E, Schule R, Leiter AB (2014) CtBP and associated LSD1 are required for transcriptional activation by NeuroD1 in gastrointestinal endocrine cells. *Mol Cell Biol* 34: 2308-2317.
 34. DIAbetes Genetics Replication And Meta-analysis (DIAGRAM) Consortium, Asian Genetic Epidemiology Network Type 2 Diabetes (AGEN-T2D) Consortium, South Asian Type 2 Diabetes (SAT2D) Consortium, Mexican American Type 2 Diabetes (MAT2D) Consortium, Type 2 Diabetes Genetic Exploration by Next-generation sequencing in multi-Ethnic Samples (T2D-GENES) Consortium, *et al.* (2014) Genome-wide trans-ancestry meta-analysis provides insight into the genetic architecture of type 2 diabetes susceptibility. *Nat Genet* 46: 234-244.
 35. Morkrid K, Jenum AK, Sletner L, Vardal MH, Waage CW, *et al.* (2012) Failure to increase insulin secretory capacity during pregnancy-induced insulin resistance is associated with ethnicity and gestational diabetes. *Eur J Endocrinol* 167: 579-588.
 36. Wu Y, Li H, Loos RJ, Yu Z, Ye X, *et al.* (2008) Common variants in CDKAL1, CDKN2A/B, IGF2BP2, SLC30A8, and HHEX/IDE genes are associated with type 2 diabetes and impaired fasting glucose in a Chinese Han population. *Diabetes* 57: 2834-2842.
 37. Cho YS, Chen CH, Hu C, Long J, Ong RT, *et al.* (2012) Meta-analysis of genome-wide association studies identifies eight new loci for type 2 diabetes in east Asians. *Nat Genet* 44: 67-72.
 38. Kwak SH, Choi SH, Jung HS, Cho YM, Lim S, *et al.* (2013) Clinical and genetic risk factors for type 2 diabetes at early or late post partum after gestational diabetes mellitus. *J Clin Endocrinol Metab* 98: E744-752.
 39. Ao D, Wang HJ, Wang LF, Song JY, Yang HX, *et al.* (2015) The rs2237892 Polymorphism in KCNQ1 Influences Gestational Diabetes Mellitus and Glucose Levels: A Case-Control Study and Meta-Analysis. *PLoS One* 10: e0128901.
 40. Kwak SH, Kim SH, Cho YM, Go MJ, Cho YS, *et al.* (2012) A genome-wide association study of gestational diabetes mellitus in Korean women. *Diabetes* 61: 531-541.
 41. Kwak SH, Choi SH, Kim K, Jung HS, Cho YM, *et al.* (2013) Prediction of type 2 diabetes in women with a history of gestational diabetes using a genetic risk score. *Diabetologia* 56: 2556-2563.
 42. Wang Y, Nie M, Li W, Ping F, Hu Y, *et al.* (2011) Association of six single nucleotide polymorphisms with gestational diabetes mellitus in a Chinese population. *PLoS One* 6: e26953.
 43. Imamura M, Takahashi A, Yamauchi T, Hara K, Yasuda K, *et al.* (2016) Genome-wide association studies in the Japanese population identify seven novel loci for type 2 diabetes. *Nat Commun* 7: 10531.

RESEARCH ARTICLE

Potential roles of DNA methylation in the initiation and establishment of replicative senescence revealed by array-based methylome and transcriptome analyses

Mizuho Sakaki^{1,2*}, Yukiko Ebihara¹, Kohji Okamura³, Kazuhiko Nakabayashi¹, Arisa Igarashi⁴, Kenji Matsumoto⁴, Kenichiro Hata¹, Yoshiro Kobayashi^{2*}, Kayoko Maehara^{5*}

1 Department of Maternal-Fetal Biology, National Research Institute for Child Health and Development, Setagaya, Tokyo, Japan, **2** Department of Biomolecular Science, Graduate School of Science, Toho University, Funabashi, Chiba, Japan, **3** Department of Systems BioMedicine, National Research Institute for Child Health and Development, Setagaya, Tokyo, Japan, **4** Department of Allergy and Clinical Immunology, National Research Institute for Child Health and Development, Setagaya, Tokyo, Japan, **5** Department of Nutrition, Graduate School of Health Science, Kio University, Kitakatsuragi, Nara, Japan

* sakaki-m@ncchd.go.jp (MS); yoshiro@biomol.sci.toho-u.ac.jp (YK); k.maehara@kio.ac.jp (K. Maehara)



OPEN ACCESS

Citation: Sakaki M, Ebihara Y, Okamura K, Nakabayashi K, Igarashi A, Matsumoto K, et al. (2017) Potential roles of DNA methylation in the initiation and establishment of replicative senescence revealed by array-based methylome and transcriptome analyses. PLoS ONE 12(2): e0171431. doi:10.1371/journal.pone.0171431

Editor: Robert Dante, Centre de Recherche en Cancerologie de Lyon, FRANCE

Received: August 29, 2016

Accepted: January 20, 2017

Published: February 3, 2017

Copyright: © 2017 Sakaki et al. This is an open access article distributed under the terms of the [Creative Commons Attribution License](https://creativecommons.org/licenses/by/4.0/), which permits unrestricted use, distribution, and reproduction in any medium, provided the original author and source are credited.

Data Availability Statement: Most relevant data are within the paper and its Supporting Information files. The microarray data for gene expression have been deposited in GEO (GSE81798). The microarray data for methylation have been deposited in GEO (GSE81788 and GSE81797). The microarray data for miRNA expression have been deposited in the GEO (GSE90942).

Funding: This work was supported by the Takeda Science Foundation (<http://www.takeda-sci.or.jp/>)

Abstract

Cellular senescence is classified into two groups: replicative and premature senescence. Gene expression and epigenetic changes are reported to differ between these two groups and cell types. Normal human diploid fibroblast TIG-3 cells have often been used in cellular senescence research; however, their epigenetic profiles are still not fully understood. To elucidate how cellular senescence is epigenetically regulated in TIG-3 cells, we analyzed the gene expression and DNA methylation profiles of three types of senescent cells, namely, replicatively senescent, *ras*-induced senescent (RIS), and non-permissive temperature-induced senescent SVTs8 cells, using gene expression and DNA methylation microarrays. The expression of genes involved in the cell cycle and immune response was commonly either down- or up-regulated in the three types of senescent cells, respectively. The altered DNA methylation patterns were observed in replicatively senescent cells, but not in prematurely senescent cells. Interestingly, hypomethylated CpG sites detected on non-CpG island regions (“open sea”) were enriched in immune response-related genes that had non-CpG island promoters. The integrated analysis of gene expression and methylation in replicatively senescent cells demonstrated that differentially expressed 867 genes, including cell cycle- and immune response-related genes, were associated with DNA methylation changes in CpG sites close to the transcription start sites (TSSs). Furthermore, several miRNAs regulated in part through DNA methylation were found to affect the expression of their targeted genes. Taken together, these results indicate that the epigenetic changes of DNA methylation regulate the expression of a certain portion of genes and partly contribute to the introduction and establishment of replicative senescence.

to KMae, a grant from Kio University (<http://www.kio.ac.jp/>) to KMae, grant 24-3 from the National Research Institute for Child Health and Development to KN and KMat, and Grant-in-Aid for Young Scientists (B 15K19439) from JSPS KAKENHI to AI. The funders had no role in study design, data collection and analysis, decision to publish, or preparation of the manuscript.

Competing Interests: The authors have declared that no competing interests exist.

Introduction

Cellular senescence is the irreversible cessation of cell proliferation [1] and is classified into two groups: replicative senescence and premature senescence [2]. Replicative senescence is caused by telomere shortening due to repeated DNA replication [3], while premature senescence is caused by stress, such as oncogene activation [4] and reactive oxygen species (ROS) [5], without apparent loss of telomere length and function. Although cellular senescence has been shown to be associated with tumor suppression in several cancers [2, 6, 7], it has been reportedly involved in cancer progression through the induction of epithelial-mesenchymal transitions and tumor invasion [8]. In addition, senescent cells secrete several factors associated with inflammation such as interleukin (IL)-6 and IL-8 [9], which are referred to as senescence-associated secretory phenotypes (SASP). Recently, SASP has been implicated in the pathogenesis of age-related diseases such as rheumatoid arthritis, periodontitis and Alzheimer's disease [8, 10]. Therefore, elucidation of the mechanism contributing to induction and establishment of the senescent state will help overcome such age-related diseases.

Epigenetic regulation such as histone modification, DNA methylation and interference with micro RNA (miRNA) is one of the mechanisms that modulate gene expression. Alteration of the chromatin structure occurs in human senescent fibroblasts, where epigenetic regulation contributes to the establishment of the senescent state partly through the p16^{INK4A} / retinoblastoma (RB) protein pathway [11]. Modification of histones, trimethylated histone H3 at lysine9 (H3K9me3) and trimethylated histone H3 at lysine 27 (H3K27me3) is enriched in the senescent-associated heterochromatic foci (SAHF), although the spreading of repressive histone marks is not necessary for SAHF formation [12]. So far as known, histone modification is reportedly involved in expression of key molecules of senescence, such as p16^{INK4A}, p14^{ARF} and p53. Loss of H3K27me3 is involved in expression of p16^{INK4A} and p14^{ARF}, whereas H4 acetylation and trimethylation of histone H3 at lysine 4 (H3K4me3) are involved in expression of p53 [13–16]. Furthermore, Takahashi, A. *et al.* [17] showed that the expression levels of SASP factors, IL-6 and IL-8, are regulated by demethylation of H3K9 through the APC/C^{Cdh1}-G9a/GLP pathway.

DNA methylation changes have also been observed during cellular senescence and individual aging. Many studies have elucidated the role of epigenetics in senescence using various approaches such as pyrosequencing, array-based methylome and combined bisulfite restriction analysis (COBRA), as well as using various types of cells and different tissues derived from genetically different individuals [18–21]. These studies have shown that DNA methylation profiles are tissue- and cell-type specific, and the epigenetic control of gene expression seems to promote in part tissue- and cell-type specific differentiation in addition to cellular senescence. For instance, the DNA methylation profile of fibroblast cells is different to that of mesenchymal stromal cells [22]. Moreover, principal component analysis showed that the methylation pattern of fibroblast cells from one dermal region is different to that from other dermal regions [23]. Christensen *et al.* also showed interindividual variation in methylation profiles among 11 tissues, including blood and brain [24]. In contrast to the studies using genetically different tissues and cells derived from individuals, age-related changes in DNA methylation between monozygotic twins were reported to arise with chronological time, indicating that the differences in genetically identical individuals are driven by different cellular responses to environmental changes [25]. Therefore, we hypothesized that a specific type of cultured cell leading to senescent states induced by different methods and demonstrating differences in methylation profiles will allow us to characterize in detail the role of epigenetic regulation in response to cellular senescence.

The effects of DNA methylation on gene transcription have been extensively studied in relation to the states of CpG islands (CGIs) near the transcription start sites (TSS). According to recent studies examining the relationship between gene body methylation and gene expression, hypermethylation correlated to not only high gene expression but also low gene expression [26], suggesting a more complex regulation. Varley *et al.* also reported that the relationship between methylation and gene expression is context-dependent, although the current models reported by several groups indicate that methylation in the promoter regions is associated with gene silencing, and gene body methylation is associated with expression [20].

Furthermore, some senescence-associated genes are regulated in part by miRNA [27–31]. MiR-34 has been well known as a tumor suppressor and its targeted genes encode the cell cycle regulators including E2F, c-Myc, cyclin D1, cyclin E2, cdk4, and cdk6 [32–34]. Recent studies on cancers have revealed that the expression of some tumor suppressive miRNAs is regulated by DNA methylation in the miRNA promoter regions [35–37]. Despite these recent advances, much of the relationship between DNA methylation and miRNA expression and how this relates to senescence genes remains unclear.

In this study, we examined characteristic features of DNA methylation during cellular senescence using TIG-3 cells established from fetal lung fibroblasts. Although such TIG-3 cells have been a common focus in senescence research, much of the epigenetics remains unexplored. To test the hypothesis that the differences in genetically identical cells are driven by different cellular responses to senescence, we examined array-based gene expression and DNA methylation profiles using genetically identical TIG-3 cells which had been induced to a senescent state by three different methods, namely, replicatively senescent, *ras*-induced senescent (RIS), and senescent SVts8 cells. Originally derived from TIG-3 cells, SVts8 cells can induce senescence under non-permissive temperature by inactivation of the temperature-sensitive SV40 large T antigen. We then searched for the positional trend of methylation changes and the possible effects of DNA methylation changes on gene expression using integrated analysis.

Materials and methods

Cells and cell culture

Normal human diploid fibroblast TIG-3 cells (obtained from the Health Science Research Resources Bank, Japan) were cultured in DMEM+GlutaMAX-I (GIBCO) supplemented with 10% fetal bovine serum (FBS) (HyClone) and 1% penicillin/streptomycin (Nacalai Tesque) at 37°C under a 5% CO₂ atmosphere. TIG-3 cells were cultured until they senesced at population doubling level (PDL) 85. The TIG-3 cells were harvested for DNA extraction at PDL 36, 49, 69 and 85, for RNA extraction to analyze gene expression at PDL 36 and 84, and for RNA extraction to analyze miRNA expression at PDL 44, 60, 78 and 80.

To prepare RIS cells, retroviral infection was performed as reported previously [38]. Briefly, Phoenix-Eco cells (obtained from Dr. G. P. Nolan, Stanford University, CA, USA) were transfected with the pBabe-puro-H-Ras-V12 or pBabe-puro plasmid by the Chen-Okayama method [39]. Viral supernatants were prepared from the cells after transfection, passed through a 0.45- μ m-pore-size syringe filter, and pooled. The supernatant and 8 μ g/mL hexadimethrine bromide (Sigma-Aldrich) were added to TIG-3 cells expressing an ecotropic receptor at a proliferating phase. After infection, the cells were selected with growth medium containing 300 μ g/mL G418 and 2 μ g/mL puromycin for 9 days before being harvested.

SVts8 cells (obtained from the Health Science Research Resources Bank, Japan) [40] continued to proliferate at a permissive temperature (33.5°C), because of suppression of RB and p53 through induction of a temperature-sensitive mutant of the simian virus (SV) 40 large T

antigen to TIG-3 cells and the high ability of telomere maintenance. Senescent SVts8 cells were obtained by culturing SVts8 cells at a non-permissive temperature (38°C) for 6 days.

Microarray assays

Gene expression. Total RNA was isolated with a ReliaPrep RNA Cell MiniPrep System (Promega) according to the manufacturer's instructions. Starting with 200 ng of the isolated RNA for each sample, double stranded cDNA and cyanine 3 labeled cRNA were synthesized using a low input quick amp labeling kit (one-color) and RNA spike-in kit (Agilent). The labeled cRNA was purified with an RNeasy mini kit (Qiagen), and hybridized to a SurePrint G3 Human GE microarray 8×60K Ver. 2.0 (Agilent). After washing the microarray to remove unhybridized cRNA, the microarray was scanned with an Agilent DNA microarray scanner G2505B, and then feature extraction was performed using the GE1_QCMT_Sep09 protocol.

DNA methylation. Genomic DNA was isolated using DNeasy Blood & Tissue (Qiagen) according to the manufacturer's instructions. Genomic DNA (1.5 µg) was bisulfite-converted using the EpiTec Plus DNA Bisulfite Kit (Qiagen). From each sample, 300 ng of bisulfite-treated DNA was subjected to DNA methylation profiling using an Infinium HumanMethylation27 or HumanMethylation450 BeadChip array (Illumina) according to the manufacturer's standard protocol. The array slides were scanned with an iScan system (Illumina).

MicroRNA (miRNA) expression. Total RNA including miRNA was isolated with a ReliaPrep miRNA Cell and Tissue MiniPrep System (Promega) according to the manufacturer's instructions. Approximately 100 ng of the isolated RNA for each sample was labeled with cyanine 3 using miRNA Complete Labelling and Hyb Kit (Agilent) according to the manufacturer's protocols. The labeled RNA was hybridized to a SurePrint G3 Human miRNA Microarray (Release 21.0) (Agilent). After washing, the microarray was immediately scanned using one color scan setting for 8×60k array slides with an Agilent DNA microarray scanner G2505C. The images were extracted with Feature Extraction Software 10.7.3.1 (Agilent) using default parameters.

Data analysis

Gene expression. The SurePrint G3 Human GE microarray data were analyzed using the Subio Platform (Ver. 1.18.4625). The data were normalized as to low signal cutoff (cutoff 1.0 and replace), log transformation (base 2), and global normalization (percentile 75), and then the ratios to those of the control sample (mean) were obtained. In this study, ≥ 2 -fold and < 0.5 -fold changes were regarded as up- and down-regulated gene expression, respectively. In order to calculate fold-change differences and construct a heatmap, each gene expression level in the senescent cells was compared with that in the control cells, namely replicative senescent cells versus proliferating cells, RIS cells versus cells infected with the empty vector, and senescent SVts8 cells versus proliferating SVts8 cells. The heatmap with sample clustering was drawn using Subio Platform with Uncentered Correlation. The microarray data for gene expression have been deposited in the GEO (GSE81798).

DNA methylation. The Infinium HumanMethylation27 BeadChip includes probes for 27,578 CpG sites [41]. The Infinium HumanMethylation450 BeadChip includes probes for 485,577 CpG sites covering 21,231 RefSeq genes (99%), and 26,658 CGIs (96%), and 3,091 probes for non-CpG loci [42]. The image data obtained by the iScan system were subjected to background subtraction and control normalization using GenomeStudio V2011.1 (Illumina). Methylation levels were calculated as β values (= intensity of the methylation allele / [intensity of the unmethylated allele + intensity of the methylated allele + 100]), which ranged from 0 (0% methylation) to 1 (100% methylation). Probes for CpG sites with a detection p-value

of > 0.05 or a blank β value were eliminated from further analysis. The β values of control cells were subtracted from those of senescent cells ($\Delta\beta$). $\Delta\beta > 0.2$ and $\Delta\beta < -0.2$ were regarded as hyper- and hypomethylation in this study. TIG-3 cells at PDL 36 were regarded as control cells for those at higher PDLs (49, 69, and 85). An Infinium HumanMethylation27 BeadChip was used to obtain methylation profiles for all samples (TIG-3, RIS, and SVts8 cells). An Infinium HumanMethylation450 BeadChip was used to obtain more comprehensive methylation profiles of TIG-3 cells at PDL 36 and PDL 85, and RIS cells. The BeadChip data have been deposited in the GEO (GSE81788 and GSE81797). Scatter plots for β values were drawn using Genome Studio. Hyper- and hypo-methylated CpG sites were classified into six CpG subcategories depending on the location relative to the CpG island (CpG island, N_Shore, S_Shore, N_Shelf, S_Shelf, and the open sea) and into seven gene feature subcategories (-1500 to -200 bp upstream of the TSS (TSS1500), -200 bp to 0 bp upstream of TSS (TSS200), 5' untranslated region (5'UTR), first exon (1st exon), gene body, 3' untranslated region (3'UTR), and intergenic region), according to the probe annotation (HumanMethylation450_15017482_v.1.1.csv) provided by Illumina [43].

Integrated analysis of DNA methylation and gene expression. Normalized gene expression and DNA methylation array data were integrated based on the genomic locations of the RefSeq genes' TSS composed in the expression array and the genomic location of the CpG sites placed in the BeadChip array using custom perl scripts. RefSeq information was retrieved from <http://hgdownload.cse.ucsc.edu/goldenPath/hg19/database/refGene.txt.gz>. We assessed $\Delta\beta$ values for the CpG sites located within 8 kb distance from the closest TSS of the RefSeq genes and the fold-change value of the corresponding gene expression. The gene expression data were obtained from probes annotated by the RefSeq ID for mRNA. When multiple expression probes existed in the same RefSeq ID, the mean of multiple intensities was calculated for the RefSeq ID. The distance from the methylation site to the TSS was calculated with a computer using the location information on the methylation probes and RefSeq (as described above). Promoters registered in RefSeq were classified into two classes, CGI and non-CGI promoters, using the following criteria: $> = 50\%$ GC content and observed-to-expected ratio of CpG $> = 0.6$.

Gene ontology (GO) analysis. GO analysis was performed using the Database for Annotation, Visualization and Integrated Discovery (DAVID) v6.7 (<http://david.abcc.ncifcrf.gov/>) [15–17] with GOTERM_BP_ALL and functional annotation clustering. The genes for GO analysis were extracted according to each cut-off value given in the methylation and integrated analysis section. For GO analysis using only gene expression data, genes exhibiting a more than 3-fold change of expression were used due to the limited gene numbers loaded onto the annotation tool. The top 10 represented GO terms are shown in some tables. Enrichment scores of more than 1.3 gave p-values of less than 0.05.

To conduct GO analysis on gene feature- and CpG site-categories, the genes related to differentially methylated CpG sites on the gene-coding region based on the probe annotation were analyzed with GOTERM_BP_ALL and a functional annotation chart due to the small numbers of extracted genes. The ratios of the number of genes with similar functions were calculated for all gene feature- and CpG site-subcategories.

miRNA expression regulated by DNA methylation and its targeted genes. To measure the expression level of miRNAs during replicative senescence, the Human miRNA microarray data were analyzed using GeneSpring (Ver. 12.5). The data were normalized by a 90-percentile shift, and then the ratios to those of the control sample (PDL 44) were obtained. The cut-off for miRNA expression change used in this study was a ± 1.5 -fold change. The microarray data for miRNA expression have been deposited in the GEO (GSE90942). miRNAs exhibiting methylation changes were obtained from HumanMethylation450 BeadChip data using the

“MIR” keyword in the “UCSC_REFGENE_NAME” column provided by Illumina. We searched for miRNAs with hypermethylated promoter regions and down-regulated expression, and vice versa, by comparing methylation changes ($\Delta\beta$ cut-off was ± 0.2) with expression changes (fold-change cut-off, ± 1.5). Genes targeted by those miRNAs for which expression seemed to be regulated by DNA methylation were picked up by TargetScanHuman Release 7.0. The resulting genes were then further filtered by more than two miRNAs and the gene expression levels based on our microarray data.

Results

Similar biological outcomes, but different gene expression patterns were detected in three types of senescent cells

We prepared three types of senescent cells, namely, replicatively senescent, RIS and senescent SVts8 cells. The senescence state in SVts8 cells was rapidly induced by the inactivation of the temperature-sensitive mutant of the SV40 large T antigen under non-permissive temperature. Senescence was confirmed by the growth arrest, appearance (a large flat morphology), senescence-associated beta-galactosidase (SA- β -Gal) activity, and protein and mRNA levels of p16^{INK4A} and p21^{Cip1/Waf1} (S1 Fig). Gene expression data for senescent cells obtained with SurePrint G3 Human GE microarrays (Agilent) showed that less than 10% of the probes tended to show similar changes in the three types of senescent cells (up-regulated: 358 of 4,355 probes in replicatively senescent cells, 3,927 probes in RIS cells and 5,124 probes in senescent SVts8 cells; down-regulated: 278 of 4,679 probes in replicatively senescent cells, 4,557 probes in RIS cells and 3,823 probes in senescent SVts8 cells), whereas more than 50% of the probes showed changes specific to each type of senescent cell (up-regulated: 2,396 of 4,355 probes in replicatively senescent cells, 2,384 of 3,927 probes in RIS cells, and 3,408 of 5,124 probes in senescent SVts8 cells; down-regulated: 2,561 of 4,679 probes in replicatively senescent cells, 2,750 of 4,557 probes in RIS cells, and 2,840 of 3,823 probes in senescent SVts8 cells) (Fig 1). A heatmap also showed different patterns of gene expression among the three types of senescent cells, even though sample clustering indicated that replicatively senescent cells and RIS cells were closer than senescent SVts8 cells (Fig 2).

According to the GO analysis of more than 3-fold changed genes, the down-regulated genes in the replicatively senescent, RIS and senescent SVts8 cells were mostly related to the “cell cycle” (S1 Table). On the other hand, the up-regulated genes were related to “immune response”, “locomotion”, and “cell migration” in all three types of senescent cells that we examined. Both up-regulated and down-regulated genes included “developmental process” genes. The results suggest that different genes with similar functions contributed to the senescent process, although the biological outcomes were similar among the three types of senescent cells.

Replicatively senescent cells showed DNA methylation changes

The DNA methylation profiles of senescent and proliferating cells were obtained using the Infinium HumanMethylation27 BeadChip. Among the three types of senescent cells examined, only the replicatively senescent cells (TIG-3 at PDL 85) were notably differentially methylated compared to the proliferating control cells (TIG-3 at PDL 36), whereas prematurely senescent cells (RIS and SVts8) were not (Fig 3, upper panels). Among the 629 and 366 CpG sites that were hyper- and hypo-methylated, respectively, in TIG-3 at PDL 85 (Fig 3, lower table), 565 (89.8%) and 310 (84.7%) sites showed a stepwise increase and decrease, respectively, of DNA methylation along with the progression of PDLs (36, 49, 69, and 85) (Table 1). Genes

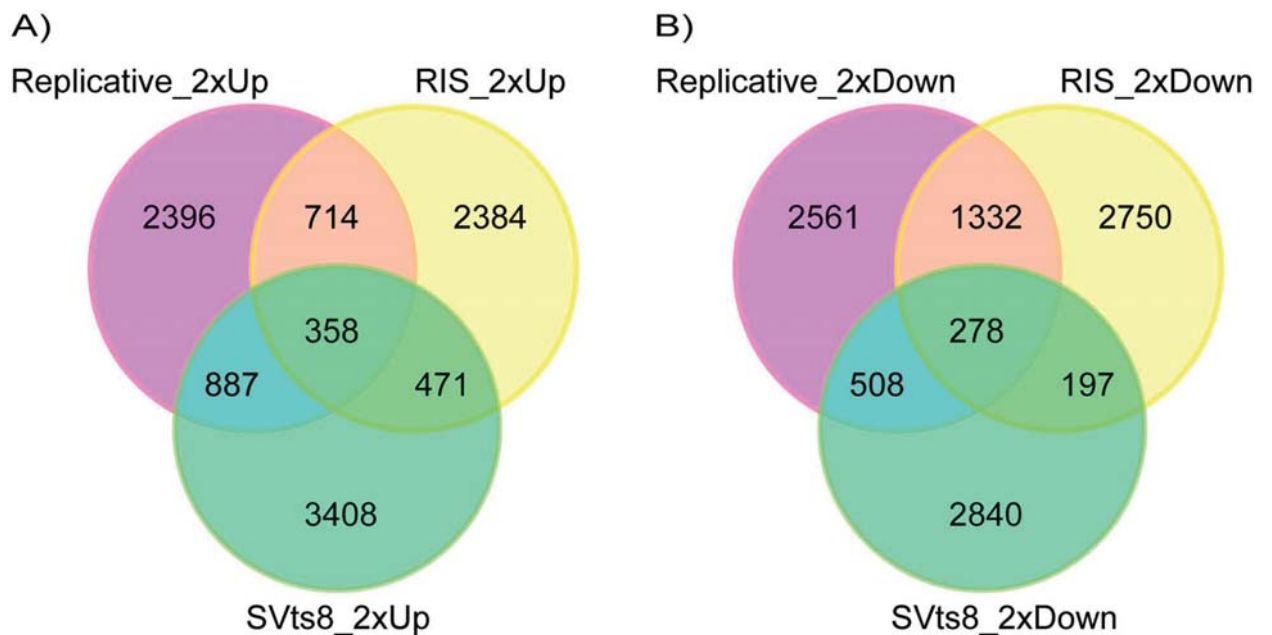


Fig 1. The number of probes indicating up- or down-regulated genes in three types of senescent cells. The number of up-regulated (A) or down-regulated probes (B) are shown in three types of senescent cells. The probes exhibiting a more than 2-fold change were counted. Purple circles, replicatively senescent cells; yellow circles, RIS cells; green circles, senescent SVts8 cells.

doi:10.1371/journal.pone.0171431.g001

hosting the differentially methylated CpG sites detected in TIG-3 at PDL 85 were subjected to GO analysis using DAVID. Genes associated with hypomethylated CpG sites were found to be most enriched in the term “immune response” (enrichment score 7.86) and its related terms (S2 Table). On the other hand, genes associated with hypermethylated CpG sites were enriched in a wider variety of terms such as regulation of biological and developmental processes with lower enrichment scores (4.24 or lower).

To more comprehensively examine the alteration of DNA methylation upon senescence, we obtained the DNA methylation profiles of TIG-3 cells at PDL 36 and PDL 85, and RIS cells using the Infinium HumanMethylation450 BeadChip. Again, replicatively senescent TIG-3 cells were differentially methylated compared to the proliferating control cells, whereas RIS cells were not (Fig 3D and 3E). Among 484,662 probes that passed quality control procedures, 14,214 and 12,727 probes were hyper- and hypo-methylated, respectively, in TIG-3 cells at PDL 85 as compared with TIG-3 cells at PDL 36 (Fig 3F). The ratios of differentially methylated probes were determined for each of the seven gene features and six CpG subcategories (Fig 4). The frequency of hypermethylated CpG sites was higher than that of hypomethylated CpG sites in TSS1500 (1.6 fold), TSS200 (2.1 fold), 5’UTR (1.5 fold), 1st exon (2.0 fold) and gene body (1.2 fold) subcategories (Fig 4A). As shown in Fig 4B, the frequency of hypermethylated CpG sites was higher in CGI (16.0 fold), N_Shore (2.2 fold), and S_shore (2.4 fold) subcategories, but was lower in N_Shelf (0.44 fold), S_Shelf (0.39 fold), and the open sea (0.51 fold) subcategories. We applied GO analyses to genes hosting the differentially methylated CpG sites to characterize the features of the genes that were supposed to be regulated in part by DNA methylation in each gene feature- and CpG site-subcategories. A total of 8,114 genes hosting the differentially methylated CpG sites were classified by GO terms into the subcategories. The GO terms obtained from functional annotation charts using DAVID were further categorized into seven groups: “immune response”, “metabolic process”, “transport”, “cell

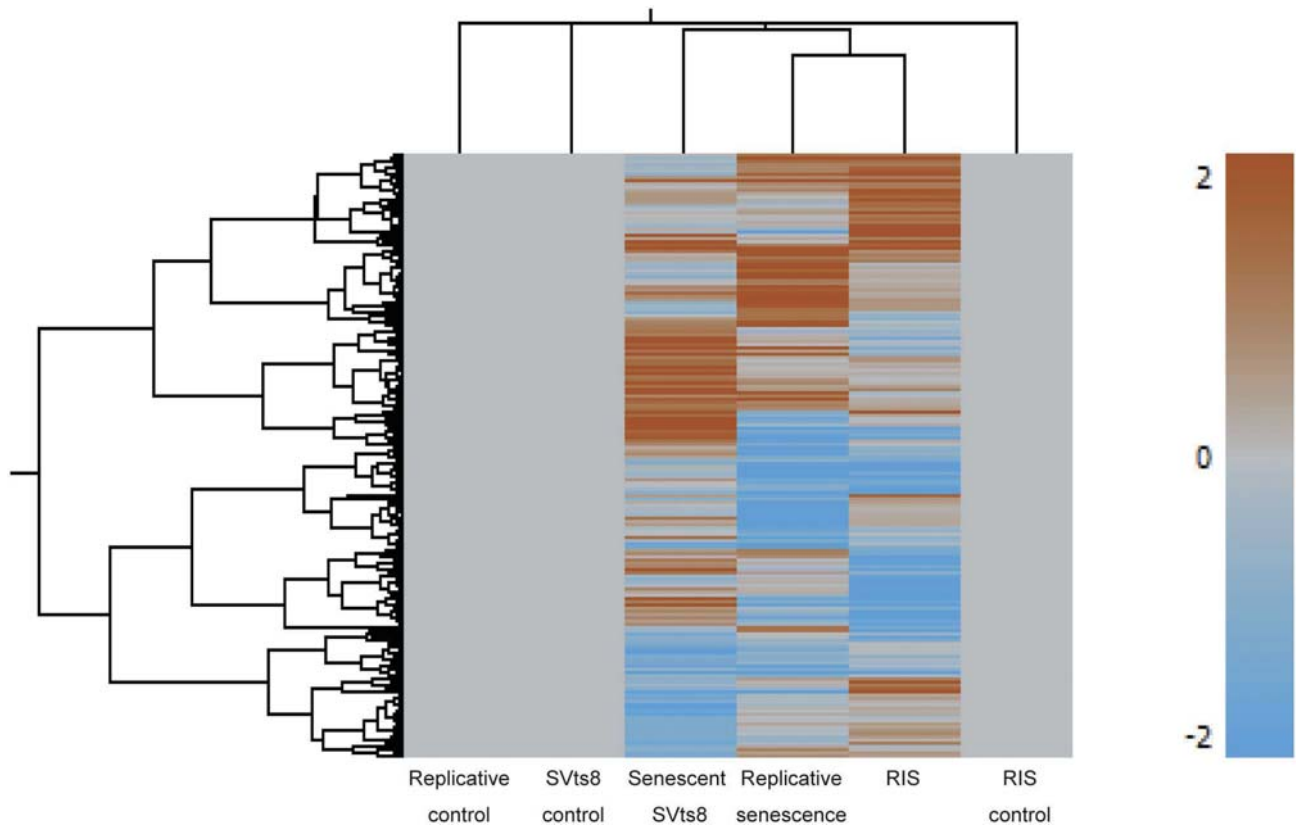


Fig 2. Heatmap of gene expression in three types of senescent cells. Gene expression patterns in three types of senescent cells are shown as a heatmap with sample clustering using uncentered correlation.

doi:10.1371/journal.pone.0171431.g002

adhesion”, “development”, “signal transduction”, and “transcription”, plus an additional group, others (Figs 5A–5H and 6A–6H and S3 Table). The “immune response”-related genes hosting hypomethylated CpG sites were enriched in all of the gene feature subcategories, whereas a small portion of those hosting hypermethylated sites were located in the TSS1500, 5’UTR, 1st exon and gene body subcategories (Fig 5A). Interestingly, in the region from – 200 bp to 0 bp upstream of TSS (TSS200), all of the classified 63 genes related to “immune response” consisted of the hypomethylated CpG sites. Consistent with the results of GO analyses using HumanMethylation27 data (S2 Table), the genes hosting hypomethylated CpG sites were found to be markedly enriched with the genes involved in “immune response”. In sharp contrast, the “transcription”-related genes hosting hypermethylated CpG sites were enriched in all of the gene feature subcategories except for “1st exon”, whereas no “transcription”-related genes hosting the hypomethylated ones were located in the gene feature subcategories except “gene body” (Fig 5G). The results of the GO analyses conducted on the CpG site subcategories are shown in Fig 6. Genes related to “immune response” were enriched only in the genes hosting hypomethylated CpG sites in the “open sea”, but not those in other subcategories (islands, shores, and shelves) (Fig 6A). In addition, genes related to “transcript” were enriched in the genes hosting hypomethylated CpG sites in the “CpG islands” (Fig 6G). However, genes related to the other six groups of GO terms were enriched in the genes hosting hypomethylated CpGs in several CpG subcategories (Fig 6B–6F and 6H). When we focused on the genes hosting hypermethylated CpG sites, genes related to “immune response” were enriched in

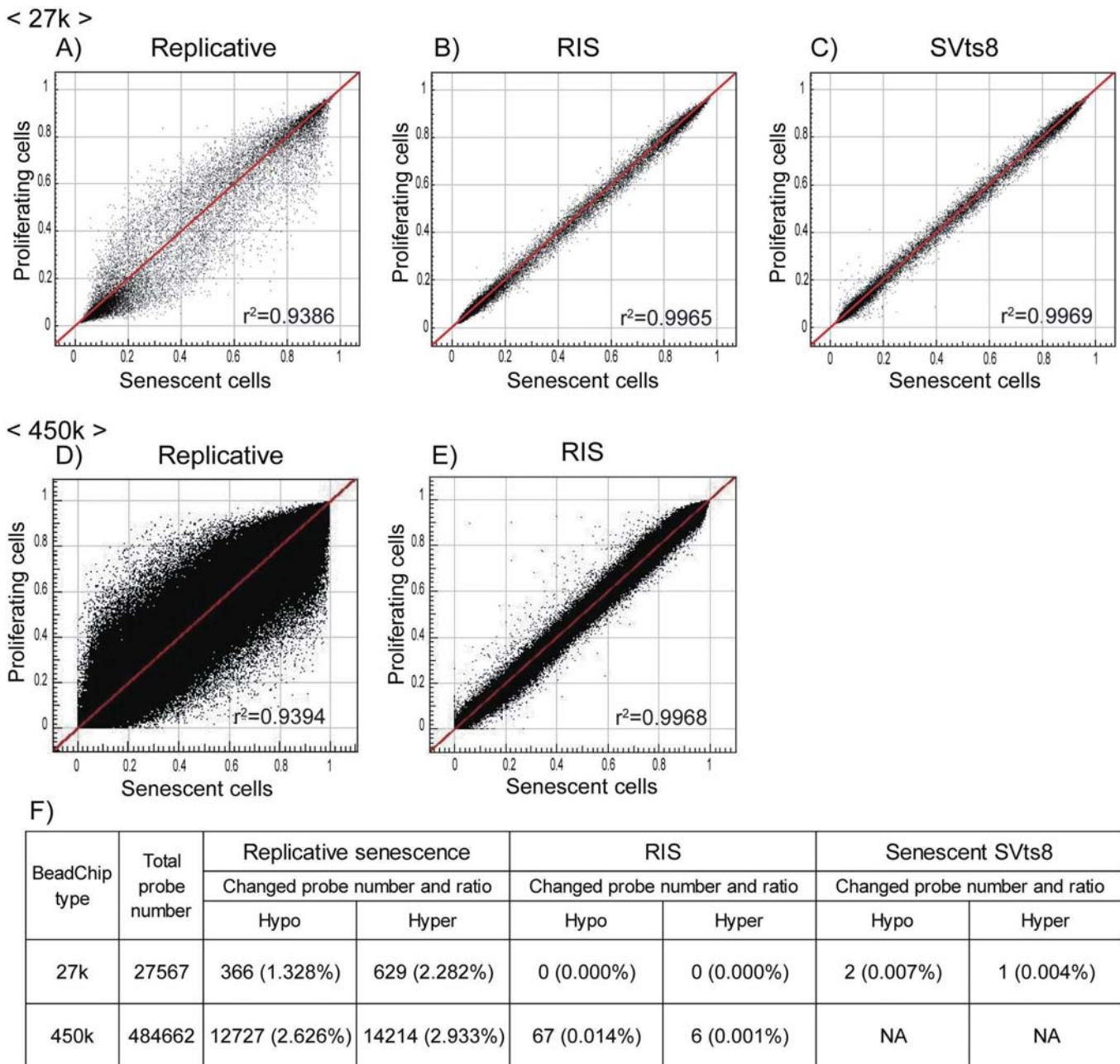


Fig 3. Comparison of DNA methylation profiles in three types of senescent cells. DNA methylation β values of senescent (x-axis) and proliferating control (y-axis) cells in the three types of senescent models are shown in scatter plots. The data were obtained by Infinium HumanMethylation27 (upper panels, A–C) and HumanMethylation450 BeadChip (middle panels, D–E). The correlation coefficient (r^2) is shown in each plot. The lower table (F) shows the numbers of CpG sites that were hyper- ($\Delta\beta > 0.2$) and hypo-methylated ($\Delta\beta < -0.2$) upon senescence.

doi:10.1371/journal.pone.0171431.g003

“N_shore” rather than in the “open sea”. In addition, genes related to other groups were enriched in the genes hosting hypermethylated CpG sites regardless of the CpG site locations (islands, shores, shelves, and the open sea) (Fig 6B–6G). Thus, a certain portion of “immune response”-related genes might be regulated in part by DNA methylation via CpG sites being outside of the CpG islands.

Table 1. Sequential changes of DNA methylation during replicative senescence.

		PDL 49 vs PDL 36	PDL 69 vs PDL 36	PDL 85 vs PDL36
Hypomethylated CpG sites	Total number	64	165	366
	Number of sites with sequential change	–	156 (94.5%)	310(84.7%)
Hypermethylated CpG sites	Total number	76	277	629
	Number of sites with sequential change	–	273 (98.6%)	565 (89.8%)

doi:10.1371/journal.pone.0171431.t001

Hypomethylation observed in the open sea was frequently associated with the up-regulation of genes related to immune response

Next, we performed an integrated analysis of HumanMethylation450 BeadChip and gene expression profiles to investigate potential functional effects of DNA methylation on gene expression in replicative senescence. Most methylation changes were unlikely to have a significant impact on gene expression (S2 Fig). Out of 212,885 probes located within 8 kb distance from a TSS of RefSeq genes, 1,596 CpG sites were differentially methylated along with the altered expression of the nearest genes to these CpG sites: 1,101 hyper- and 495 hypo-methylated CpG sites for which the nearest genes were down- and up-regulated, respectively, upon senescence (S4 Table). The genes nearest to these 1,596 differentially methylated CpG sites were subjected to GO analysis using DAVID. Those genes with up-regulated expression that were in a hypomethylated state in close proximity (within 8 kb) to their TSS were involved in “immune response” and “cell death” as ranked in the top 10 terms (Table 2). The immune response-related genes included *MHC II*, and the cell death-related genes included *FAS* and *oxidized low density lipoprotein receptor 1 (OLR1)*. In contrast, those genes with down-regulated expression that were in a hypermethylated state in close proximity to their TSS were categorized into several categories such as “development” and “cell cycle”.

We also assessed the distribution of the distances between each of the 1,596 differentially methylated CpG sites and the nearest TSS. In this analysis, we classified genes into two subcategories based on promoter types, CGI and non-CGI promoters. The number of probes for all CpG sites within CGI and non-CGI promoters on the array were 204,829 and 94,432 respectively (Fig 7A). The number of probes located within 1 kb distance to the TSS was 186,998 (62%). The 1,101 hypermethylated CpG sites for which the nearest gene was down-regulated upon replicative senescence consisted of 744 and 357 CpG sites within CGI and non-CGI promoters, respectively. The hypermethylated CpG sites tended to be located more frequently in CGI promoters than in non-CGI promoters, and located close to the TSS: 630 out of 1,101 (57%) within 1 kb distance (Fig 7B). The distribution patterns were similar between all CpG sites (Fig 7A) and 1,101 hypermethylated CpG sites (Fig 7B). In sharp contrast, 495 hypomethylated CpG sites for which the nearest gene was up-regulated were mainly located in non-CGI promoters (Fig 7C). Within 1 kb distance of the TSS, 202 hypomethylated CpG sites, for which the nearest gene was up-regulated upon replicative senescence, consisted of 36 and 166 CpG sites within CGI and non-CGI promoters, respectively (Fig 7C). This distribution pattern was similar to that of a subset of hypomethylated CpG sites, for which the nearest gene was up-regulated and related to “immune response” (Fig 7D). This result suggests the possibility that DNA methylation on the promoter modulates the expression of a subset of “immune response” genes in replicative senescence.

DNA methylation affected the expression of miRNAs and the target genes during replicative senescence

A HumanMethylation450 BeadChip includes 3,436 probes related to miRNA. In replicatively senescent TIG-3 cells, 98 CpG sites corresponding to 66 miRNAs were hypomethylated,

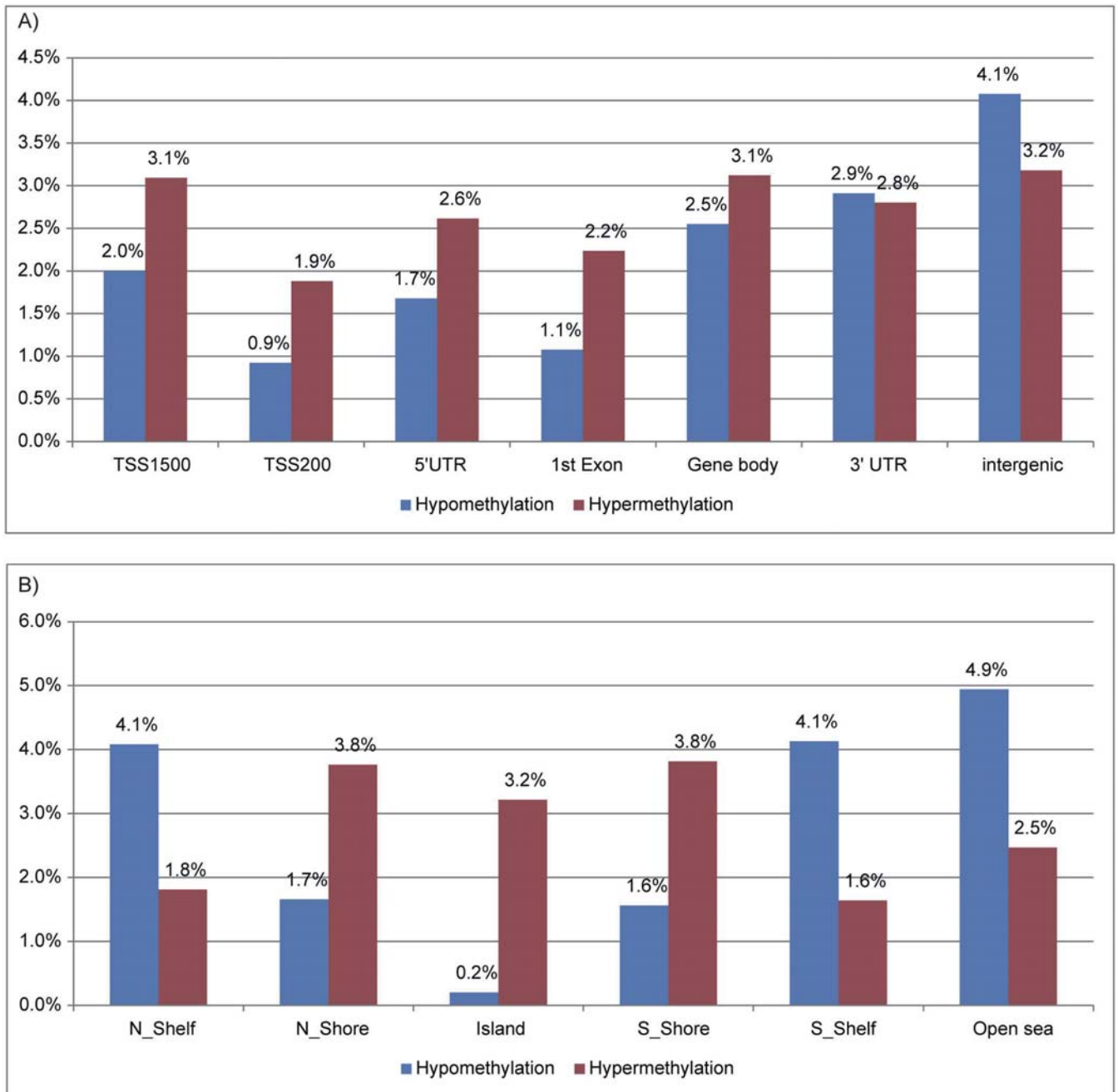


Fig 4. Rates of differentially methylated CpG sites in replicatively senescent TIG-3 cells in seven gene- feature (A) and six CpG- site (B) subcategories. CpG sites showing $\Delta\beta > 0.2$ and $\Delta\beta < -0.2$ in senescent TIG-3 cells (at PDL 85) compared to those at PDL 36 were regarded as hyper- and hypo-methylated, respectively. Seven gene-feature subcategories: TSS1500, TSS200, 5'UTR, 1st exon, gene body, 3'UTR, and intergenic region. Six CpG subcategories: CpG island, N_Shore, S_Shore, N_Shelf, S_Shelf, and the open sea.

doi:10.1371/journal.pone.0171431.g004

whereas 102 CpG sites corresponding to 62 miRNAs were hypermethylated (S5 Table). The expression levels of miRNAs were examined using Human miRNA microarray (Release 21.0), where 2,549 human miRNAs were represented. During replicative senescence, 178 miRNAs (fold-change $\geq \pm 1.5$) showed up- or down-regulated (data not shown). To select miRNAs

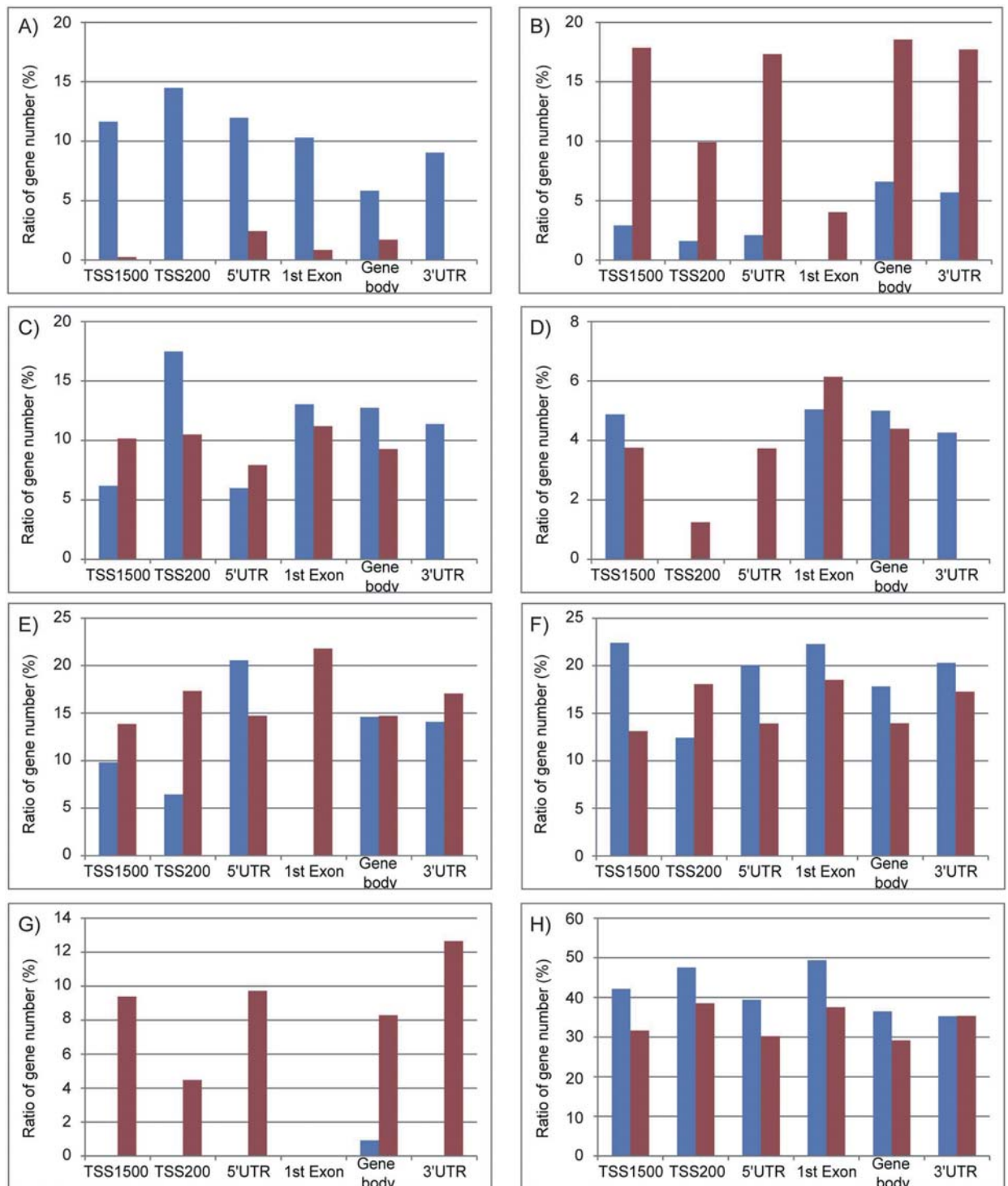


Fig 5. The characterization of genes hosting differentially methylated CpG sites in the gene feature subcategories. GO analyses for gene hosting differentially methylated CpG sites were performed using DAVID (functional annotation chart and GOTERM_BP_ALL). The genes hosting hypermethylated (red) or hypomethylated (blue) CpG sites were classified into six gene feature categories (TSS1500, TSS200, 5'UTR, 1st exon, gene body and 3'UTR). Using the GO terms detected to be enriched (p-value = < 0.05) by DAVID, genes with similar functions were classified into seven groups: immune response (A), metabolic process (B), transport (C), cell adhesion (D), development (E), signal transduction (F), and transcription (G), plus an additional group, others (H). Histograms (A–H) show the ratio of the number of genes classified by GO terms in gene features subcategories (S3 Table shows the number of genes analyzed and classified).

doi:10.1371/journal.pone.0171431.g005

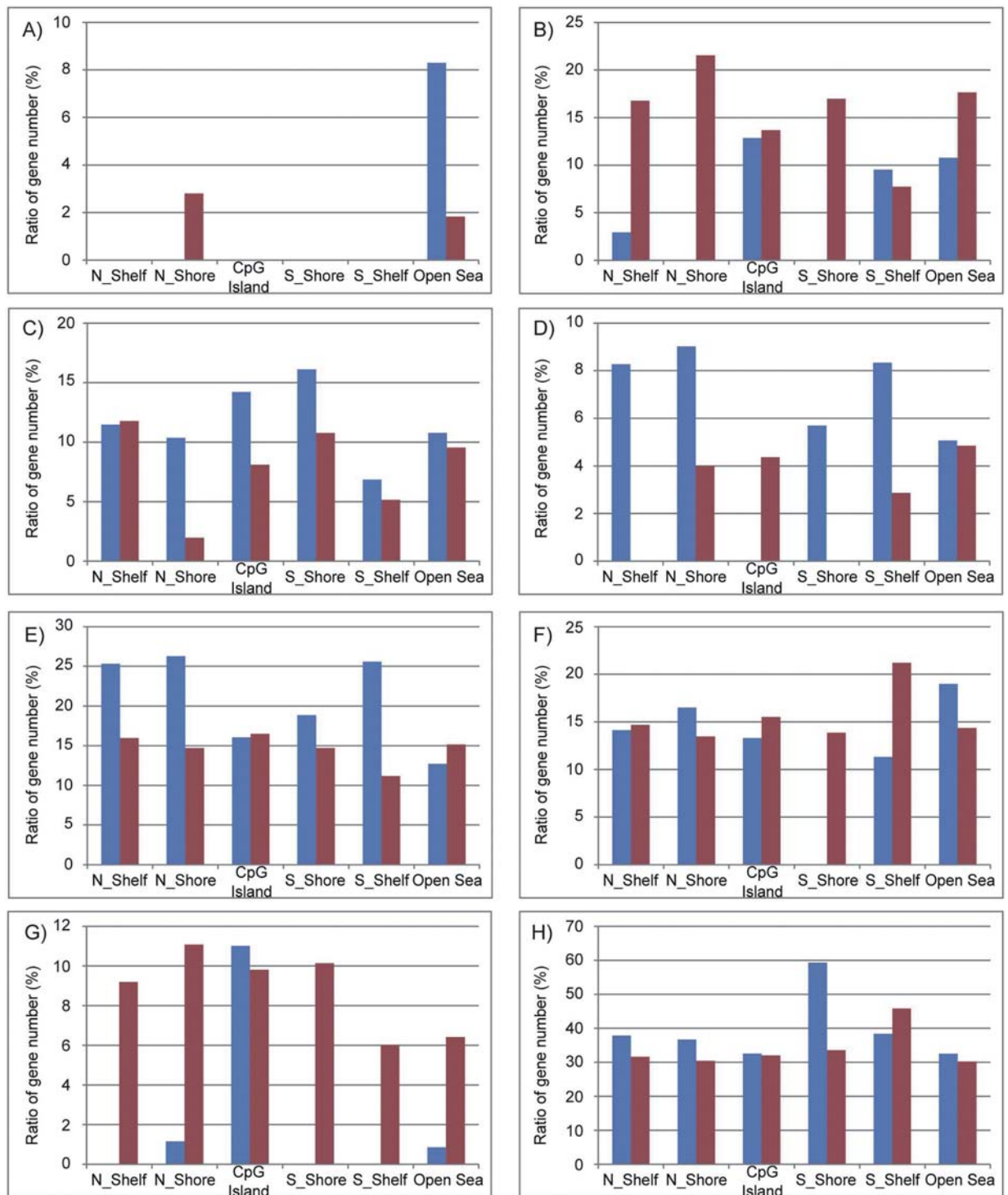


Fig 6. The characterization of genes hosting differentially methylated CpG sites in the CpG site subcategories. The same type of GO analyses shown in Fig 5 was applied to six CpG subcategories (N_Shelf, N_Shore, CpG island, S_Shore, S_Shelf, and the open sea). S3 Table shows the number of genes analyzed and classified.

doi:10.1371/journal.pone.0171431.g006

Table 2. GO analysis of genes showing the relationship between methylation and gene expression level in replicative senescence.

Rank	Hypomethylation & up-regulated gene expression (n = 351)		Hypermethylation & down-regulated gene expression (n = 516)	
	GO term categories	Enrichment Score	GO term categories	Enrichment Score
1	Response to stimulus	3.20	Developmental process	7.08
2	Immune response	3.19	Organ development	5.14
3	Inflammatory response	2.73	Lung alveolus development	3.69
4	Response to hormone stimulus, Response to corticosteroid stimulus	2.50	Embryonic development	3.64
5	Response to nutrient levels, Response to extracellular stimulus	2.30	Cell cycle	3.16
6	Regulation of transport	1.69	Negative regulation of transcription	3.11
7	Developmental process	1.62	Epithelial tube morphogenesis	2.70
8	Cell death	1.37	Mesenchymal cell development	2.47
9	Actin cytoskeleton organization	1.26	Ear development	2.46
10	Negative/positive regulation of kinase activity	1.25	Positive regulation of transcription, DNA-dependent, positive regulation of metabolic process	2.34

* More than 1.3 of enrichment scores gave less than 0.05 p-value.

doi:10.1371/journal.pone.0171431.t002

for which expression seemed to be regulated by DNA methylation, we compared the methylation changes of CpG sites related to miRNA with the miRNA expression changes. Among 18 miRNAs selected, seven miRNAs showed a decrease in expression accompanied with a hypermethylated CpG site in the promoters (S6 Table). This result was consistent with a previous report using IMR 90 cells, where the expression levels of six of the seven miRNAs were down-regulated during replicative senescence [27]. In contrast, no miRNAs showed an increase in expression along with a hypomethylated CpG site in the promoters. We next searched for candidate genes targeted by the seven miRNAs using TargetScan Human Release 7.0, and these genes were further selected by more than two miRNAs and the targeted gene expression levels based on our microarray data. As a result, we identified 27 genes for which expression seemed to be indirectly regulated by DNA methylation on the promoters of targeting miRNAs (Table 3). The genes encoding IL-6 signal transducer (*IL6ST*) and Zinc finger matrin-type 3 (*ZMAT3*) were included in the targeted genes.

Discussion

In this study, we examined DNA methylation levels in three types of senescent cells and found that only replicatively senescent cells were differentially methylated, whereas prematurely senescent ones (RIS and SVts8) were not (Fig 3 and Table 1). These results were in good agreement with previous studies showing DNA methylation changes in aged tissues and cells [16, 21, 24, 44]. There are several reasons why the DNA methylation profile is strongly modified during replicative senescence and not during premature senescence. Firstly, errors may accumulate due to repeated cell division. Laird *et al.* evaluated the fidelity of transmission of the DNA methylation state in the CpG island of the *FMRI* gene in normal human lymphocytes using hairpin-bisulfite PCR [45]. Although the high fidelity of inheritance of the methylated state of cytosine was estimated, the results clearly showed that errors in maintaining DNA methylation occurred to some extent in every DNA replication. When culturing TIG-3 cells from PDL 36 to PDL 85, the cells would be divided approximately 2⁵⁰ times. In contrast, as RIS and senescent SVts8 cells were rapidly induced to a senescent state, prematurely senescent

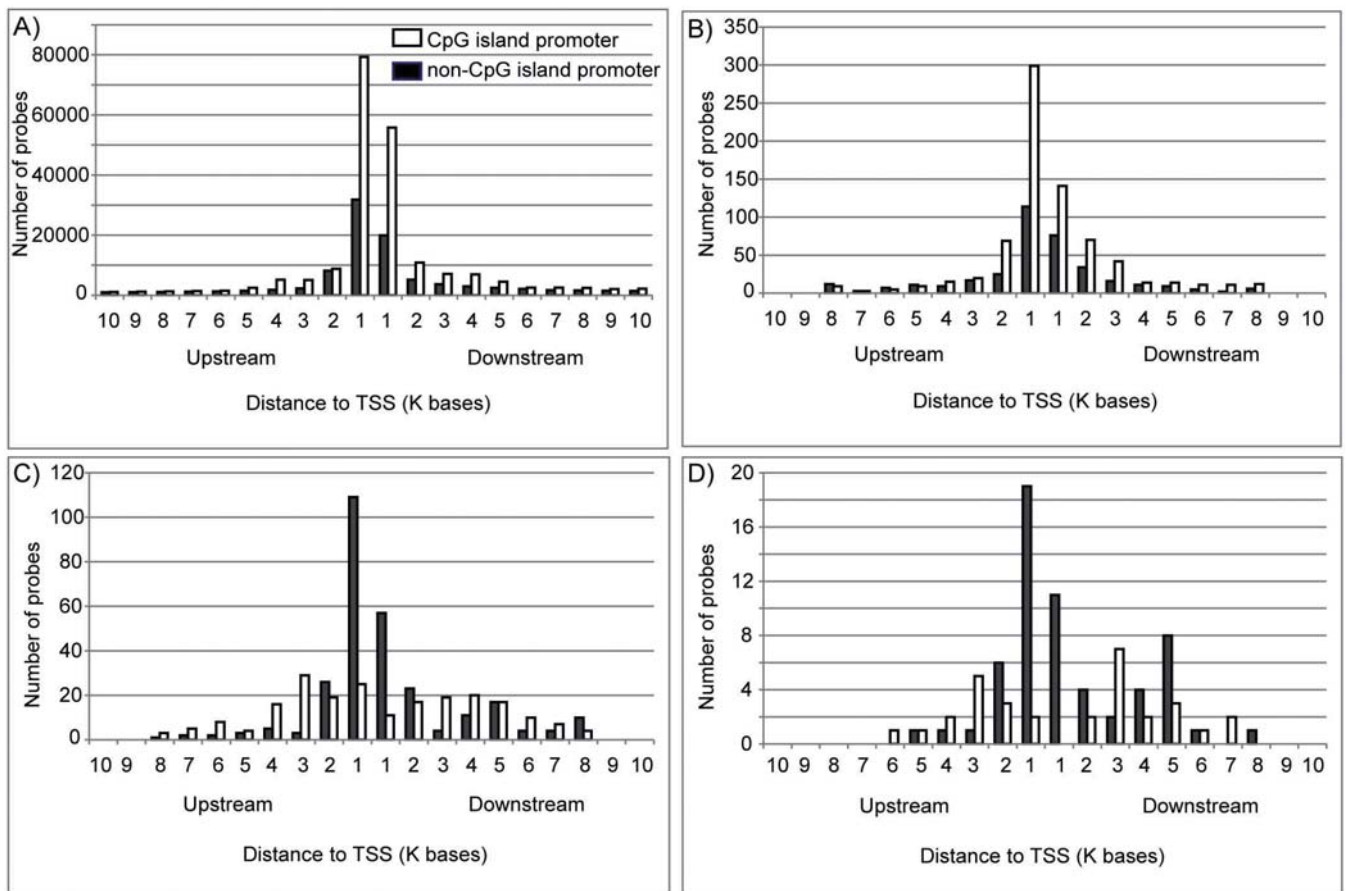


Fig 7. Distribution patterns of the distances between CpG sites and the nearest TSS. Distribution patterns for all 299,261 CpG probes on the HumanMethylation450 BeadChip (A), 1,101 hypermethylated CpG sites for which the nearest gene was down-regulated upon replicative senescence (B), 495 hypomethylated CpG sites for which the nearest gene was up-regulated upon replicative senescence (C), and 90 hypomethylated CpG sites for which the nearest gene was up-regulated upon replicative senescence and related to immune response (D) are shown.

doi:10.1371/journal.pone.0171431.g007

cells would not have enough rounds of cell division to accumulate any errors. Secondly, reduced activity of DNA methyltransferase 1 (DNMT1), which primarily maintains DNA methylation patterns during replication, may increase the incidence of errors. The expression profiles in this study exhibited a marked decrease in *DNMT1* in replicatively senescent cells (0.23-fold reduction, data not shown), whereas the expression levels of *DNMT1* in RIS (0.70-fold reduction, data not shown) and senescent SVts8 (0.80-fold reduction, data not shown) were slightly reduced. This is consistent with the results reported by Kaneda *et al.*, who reported that DNA methylation was not altered in RIS using methylated DNA immunoprecipitation (MeDIP) sequencing and bisulfite sequencing, and the *Dnmt1* expression level was not altered in RIS, or during 3 passages (passage 2 to 5) using mouse embryonic fibroblasts [16]. Thirdly, a marked decrease in Ten-eleven translocation 1 (*TET1*) expression could alter DNA methylation patterns. Recent studies have suggested active DNA demethylation is mediated by *TET*, the enzyme that converts 5-methylcytosine (5mC) to 5-hydroxymethylcytosine (5hmC), 5-formylcytosine (5fc), and 5-carboxylcytosine (5caC) [46–49]. There are three *TET* proteins: *TET1*, *TET2* and *TET3*. The expression levels of *TET1* and *TET3* genes, but not *TET2*, reportedly decrease along with aging, and *TET3* expression is important for decreasing genomic

Table 3. Targeted genes mediated in part by miRNAs, with miRNA expression regulated via methylation in the promoter regions.

Targeted gene symbol	Gene expression (fold-change)	miRNAs of regulating targeted gene		
EIF4EBP2	3.0	hsa-miR-7-5p	hsa-miR-193a-5p	hsa-miR-335-5p
HECW2	4.2	hsa-miR-7-5p	hsa-miR-25-3p	hsa-miR-505-3p
CADM1	8.2	hsa-miR-7-5p	hsa-miR-505-3p	
CNNM2	2.9	hsa-miR-335-5p	hsa-miR-505-3p	
CPEB2	2.6	hsa-miR-7-5p	hsa-miR-505-3p	
CRY2	2.2	hsa-miR-7-5p	hsa-miR-17-5p	
DAAM1	2.5	hsa-miR-130b-3p	hsa-miR-335-5p	
DGKH	2.5	hsa-miR-130b-3p	hsa-miR-505-3p	
DOK6	2.2	hsa-miR-17-5p	hsa-miR-335-5p	
EGR2	2.8	hsa-miR-17-5p	hsa-miR-25-3p	
FAM134C	2.2	hsa-miR-17-5p	hsa-miR-335-5p	
GRIN2A	2.0	hsa-miR-7-5p	hsa-miR-130b-3p	
HPCAL4	7.6	hsa-miR-7-5p	hsa-miR-335-5p	
IL6ST	2.2	hsa-miR-130b-3p	hsa-miR-505-3p	
KLHL28	2.4	hsa-miR-7-5p	hsa-miR-335-5p	
MEF2D	2.7	hsa-miR-335-5p	hsa-miR-505-3p	
MYO1D	5.9	hsa-miR-193a-5p	hsa-miR-335-5p	
NR4A3	2.1	hsa-miR-7-5p	hsa-miR-335-5p	
OXR1	2.9	hsa-miR-7-5p	hsa-miR-17-5p	
PGM2L1	4.8	hsa-miR-17-5p	hsa-miR-130b-3p	
PIP4K2C	2.1	hsa-miR-25-3p	hsa-miR-505-3p	
PPARGC1B	2.6	hsa-miR-7-5p	hsa-miR-505-3p	
RAB11FIP5	2.8	hsa-miR-7-5p	hsa-miR-17-5p	
RNF141	2.4	hsa-miR-7-5p	hsa-miR-335-5p	
SEMA6D	5.9	hsa-miR-7-5p	hsa-miR-193a-5p	
ZDHHC8	5.2	hsa-miR-17-5p	hsa-miR-335-5p	
ZMAT3	3.4	hsa-miR-7-5p	hsa-miR-130b-3p	

doi:10.1371/journal.pone.0171431.t003

5hmC during aging in human T cells [50]. In replicatively senescent TIG-3 cells, the expression levels of the *TET1* gene were drastically decreased, although we have no expression data for the *TET3* gene due to a lack of *TET3* probes in the expression array. A recent study showed that *Tet1/Tet2* double-knockout mouse embryonic fibroblasts (MEFs) had defects in maintaining hypomethylation and resulted in hypermethylation of DNA methylation canyons where developmental genes are associated [51]. Taken together, methylation changes during senescence would be required for many rounds of cell division and the decreased activities of DNA methyltransferase and methylcytosine deoxygenase, such as DNMT1 and TET1, might produce the altered methylation patterns within long-term culture.

We found that hypomethylation observed in the open sea was frequently associated with the up-regulation of genes related to immune response. When the genes hosting hypomethylated CpG sites were classified into six CpG subcategories using annotated GO terms, genes related to “immune response” were enriched only in the genes hosting hypomethylated CpG sites in the “open sea” (Fig 6A). Consistent with the results, the promoter types of genes categorized as “immune response” were mainly non-CGI promoters (Fig 7D). Nevertheless, the probes in the HumanMethylation450 BeadChip covered much more CpG island promoter genes than non-CpG island promoter genes (Fig 7A). In contrast, genes categorized into other groups, namely “metabolic process”, “transport”, “cell adhesion”, “development”, “signal

transduction”, and “transcription”, exhibited hypermethylation rather than hypomethylation in the CpG sites close to the TSS (S3 Table). Furthermore, integrated analyses showed that “immune response” was ranked in GO terms of genes up-regulated and concomitantly hypomethylated in close proximity to their TSS (Table 2). These results suggest that hypomethylation in the open sea may increase the expression of the “immune response”-related genes during replicative senescence. For example, *MHC II* has non-CGI promoters exhibiting hypomethylated CpG sites and its expression was up-regulated during replicative senescence. Several studies also indicated the effects of DNA methylation in the promoter regions on the expression of inflammatory genes [52–54].

Currently we cannot explain the mechanism by which hypomethylation in the non-CpG promoter increases the expression of a certain portion of the “immune response”-related genes during replicative senescence. We speculate that TET2 may play a role in this regulation. As mentioned above, TET proteins contribute to active DNA demethylation. In our data, the expression levels of one of the *TET2* probes showed a 2-fold increase in replicatively senescent cells and senescent SVts8 cells, whereas no increase in *TET2* expression was detected in the RIS cells. Unlike TET1 and TET3, TET2 does not have a CXXC domain, which is required for binding to the CpG site [55, 56]. These results suggest that collaboration between TET2 and its associated factor(s) may be required for DNA binding and demethylation. In fact, TET2 was reported to need a cofactor for binding to DNA [49]. During differentiation of helper T (Th) cells, TET2 induced DNA demethylation at the loci of key cytokine genes in a lineage-specific transcription factor-dependent manner and promoted signature cytokine expression in Th1 and Th17 cells [57]. Depending on the cofactor, TET2 may bind to non-CGI promoters in senescence-associated genes, and increase gene expression. Further studies are needed to investigate the effects of TET2 on hypomethylation at the specific CpG sites and its interacting factor(s) during senescence.

Recently, senescence-associated miRNAs (SA-miRNAs) have been reported to regulate genes associated with senescence [27–31]. We examined the effects of DNA methylation in the promoter regions of miRNAs on miRNA expression using human miRNA expression microarray and further selected miRNAs that likely affected the predicted gene expression. As a result, we identified seven miRNAs and 27 targeted genes (Table 3). These genes included eukaryotic translation initiation factor 4E binding protein 2 (*EIF4EBP2*), which inhibits translation initiation [58], and cryptochrome circadian clock 2 (*CRY2*), which is a key component in regulating circadian rhythm [59]. Among the 27 genes, the IL-6 signal transducer (*IL6ST*) and zinc finger matrin-type 3 (*ZMAT3*) are involved in immune response. *IL6ST*, which is supposed to be up-regulated by decreased levels of has-miR-130b-3p and has-miR-505-3p, encodes glycoprotein 130 (gp130) [60]. The protein gp130 is a signal transducer shared by many cytokines including IL-6, one of the SASP factors [61], IL-11, IL-27, and oncostatin-M [62–64]. In addition, *ZMAT3*, a predicted gene regulated by has-miR-7-5p and has-miR-130b-3p, encodes a double-stranded-RNA-binding zinc finger protein Wig-1 (for wild-type p53-induced gene 1). Wig-1, a transcriptional target of p53, stabilizes p53 by binding to the 3' UTR of p53 mRNA and protecting it from deadenylation [65]. A high level of p53 triggers cell cycle arrest, senescence and apoptosis, and efficiently inhibits tumor development [7, 66, 67]. In addition to the p53 transcription factor, miRNAs with expression regulated by DNA methylation via their promoter regions may also contribute to *ZMAT3* expression. MiR-34 is one of the SA-miRNAs and is up-regulated by p53 [27, 28, 32, 33, 68, 69]. Although increased levels of miRNA-34 were detected upon replicative senescence, the methylation changes ($\Delta\beta$ cut-off was ± 0.2) in the promoter regions of miRNA-34 were not included in our data (data not shown).

In this study, we investigated the possibility of regulation by DNA methylation during senescence. We found that hypomethylation in the open sea may contribute to the up-

regulation of genes related to immune response. Several miRNAs targeting genes associated with a senescent state seem to regulate expression by DNA methylation in the promoter regions. However, we have to consider the possibility that DNA methylation results from alteration of gene expression. To investigate this possibility, we need to collect more data and explore the mechanism of methylation and demethylation change. Moreover, in order to reveal the whole mechanism of DNA methylation, we also need to focus on the methylation profile in hypomethylation and outside of the TSS and CpG islands.

Conclusion

Three types of senescent TIG-3 cells showed similar biological outcomes, but the regulatory mechanisms were different. Replicatively senescent cells showed sequential DNA methylation changes, but prematurely senescent RIS and SVts8 cells did not. In replicative senescence, hypomethylation with up-regulated gene expression often occurred in the open sea. Moreover, hypomethylation was observed in non-CGI promoters of genes related to the immune response. These results suggested that hypomethylation in the open sea regulates the expression of a certain portion of immune-related genes in replicative senescence. In addition, several miRNAs that seemed to have expression levels regulated in part by DNA methylation may also contribute to the expression of senescence-associated genes.

Supporting information

S1 Fig. Confirmation of senescence. Senescent cells were subjected to senescence-associated beta-galactosidase (SA- β -Gal) staining, qRT-PCR and immunoblotting. SA- β -Gal staining of the control A), C), E), replicatively senescent B), RIS D), and senescent SVts8 cells F). The percentages of SA- β -Gal-positive cells are shown at the bottom of each picture. Bar, 200 μ m. Objective, $\times 10$. G) The expression levels of p16^{INK4A} and p21^{Cip1/Waf1} obtained with SurePrint G3 Human GE microarrays and qRT-PCR. H) Representative western blotting of p16^{INK4A} and p21^{Cip1/Waf1}, Ras, and loading control (actin). Images of p16^{INK4A} are shown separately shown due to different exposure time.
(TIF)

S2 Fig. Integrated analysis of methylation and gene expression in replicative senescence. Each plot represents the values obtained from a single gene using integrated analyses. DNA methylation β values and gene expression levels are plotted along the abscissa and the ordinate, respectively. Red lines show the cut-off border. For methylation, $\Delta\beta$ for hypermethylation is ≥ 0.2 , $\Delta\beta$ for hypomethylation is ≤ -0.2 . For gene expression, the cut-off for increased/decreased expression was a ± 2 -fold change.
(TIF)

S1 Table. GO terms for up- or down-regulated genes in three types of senescent cells.
(XLSX)

S2 Table. GO terms for hypo- or hyper-methylated genes in replicatively senescent cells.
(XLSX)

S3 Table. The number of genes hosting differentially methylated CpG sites in the gene feature- and the CpG site- subcategories.
(XLSX)

S4 Table. Integrated analysis of gene expression and methylation changes in replicatively senescent cells.
(ZIP)

S5 Table. Hypo- or hyper-methylated miRNAs in the promoter regions of replicatively senescent cells.

(XLSX)

S6 Table. miRNA expression regulated by DNA methylation in the promoter region.

(XLSX)

Acknowledgments

We thank Dr. Takao Yokoyama for assisting with the data analysis and Ms. Emma L. Barber (National Research Institute for Child Health and Development, Japan) for editing the manuscript.

Author contributions

Conceptualization: MS KH K. Maehara.

Data curation: MS KO KN.

Formal analysis: MS AI KN KO.

Funding acquisition: AI KN K. Matsumoto K. Maehara.

Investigation: MS YE AI K. Matsumoto K. Maehara.

Methodology: KO KN.

Project administration: K. Maehara.

Resources: K. Matsumoto KH K. Maehara.

Software: KO.

Supervision: KH YK K. Maehara.

Validation: MS KN KO AI K. Maehara.

Visualization: MS.

Writing – original draft: MS.

Writing – review & editing: KN YK K. Maehara.

References


1. Hayflick L. The limited in vitro lifetime of human diploid cell strains. *Exp Cell Res.* 1965; 37:614–636. PMID: [14315085](#)
2. Kuilman T, Michaloglou C, Mooi WJ, Peeper DS. The essence of senescence. *Genes Dev.* 2010; 24(22):2463–2479. doi: [10.1101/gad.1971610](#) PMID: [21078816](#)
3. Harley CB, Futcher AB, Greider CW. Telomeres shorten during ageing of human fibroblasts. *Nature.* 1990; 345(6274):458–460. doi: [10.1038/345458a0](#) PMID: [2342578](#)
4. Serrano M, Lin AW, McCurrach ME, Beach D, Lowe SW. Oncogenic ras provokes premature cell senescence associated with accumulation of p53 and p16INK4a. *Cell.* 1997; 88(5):593–602. PMID: [9054499](#)
5. Takahashi A, Ohtani N, Yamakoshi K, Iida S, Tahara H, Nakayama K, et al. Mitogenic signalling and the p16INK4a-Rb pathway cooperate to enforce irreversible cellular senescence. *Nat Cell Biol.* 2006; 8(11):1291–1297. doi: [10.1038/ncb1491](#) PMID: [17028578](#)
6. Collado M, Blasco MA, Serrano M. Cellular senescence in cancer and aging. *Cell.* 2007; 130(2):223–233. doi: [10.1016/j.cell.2007.07.003](#) PMID: [17662938](#)

7. Campisi J. Cellular senescence as a tumor-suppressor mechanism. *Trends Cell Biol.* 2001; 11(11): S27–31. PMID: [11684439](#)
8. Campisi J. Aging, cellular senescence, and cancer. *Annu Rev Physiol.* 2013; 75:685–705. doi: [10.1146/annurev-physiol-030212-183653](#) PMID: [23140366](#)
9. Coppe JP, Patil CK, Rodier F, Sun Y, Munoz DP, Goldstein J, et al. Senescence-associated secretory phenotypes reveal cell-nonautonomous functions of oncogenic RAS and the p53 tumor suppressor. *PLoS Biol.* 2008; 6(12):2853–2868. doi: [10.1371/journal.pbio.0060301](#) PMID: [19053174](#)
10. Wu Z, Nakanishi H. Lessons from Microglia Aging for the Link between Inflammatory Bone Disorders and Alzheimer's Disease. *J Immunol Res.* 2015; 2015:1–9.
11. Narita M, Nunez S, Heard E, Narita M, Lin AW, Hearn SA, et al. Rb-mediated heterochromatin formation and silencing of E2F target genes during cellular senescence. *Cell.* 2003; 113(6):703–716. PMID: [12809602](#)
12. Narita M, Narita M, Krizhanovsky V, Nunez S, Chicas A, Hearn SA, et al. A novel role for high-mobility group a proteins in cellular senescence and heterochromatin formation. *Cell.* 2006; 126(3):503–514. doi: [10.1016/j.cell.2006.05.052](#) PMID: [16901784](#)
13. Zhang W, Hu D, Ji W, Yang L, Yang J, Yuan J, et al. Histone modifications contribute to cellular replicative and hydrogen peroxide-induced premature senescence in human embryonic lung fibroblasts. *Free Radic Res.* 2014; 48(5):550–559. doi: [10.3109/10715762.2014.893580](#) PMID: [24528089](#)
14. Shah PP, Donahue G, Otte GL, Capell BC, Nelson DM, Cao K, et al. Lamin B1 depletion in senescent cells triggers large-scale changes in gene expression and the chromatin landscape. *Genes Dev.* 2013; 27(16):1787–1799. doi: [10.1101/gad.223834.113](#) PMID: [23934658](#)
15. Bracken AP, Kleine-Kohlbrecher D, Dietrich N, Pasini D, Gargiulo G, Beekman C, et al. The Polycomb group proteins bind throughout the INK4A-ARF locus and are disassociated in senescent cells. *Genes Dev.* 2007; 21(5):525–530. doi: [10.1101/gad.415507](#) PMID: [17344414](#)
16. Kaneda A, Fujita T, Anai M, Yamamoto S, Nagae G, Morikawa M, et al. Activation of Bmp2-Smad1 signal and its regulation by coordinated alteration of H3K27 trimethylation in Ras-induced senescence. *PLoS Genet.* 2011; 7(11):e1002359. doi: [10.1371/journal.pgen.1002359](#) PMID: [22072987](#)
17. Takahashi A, Imai Y, Yamakoshi K, Kuninaka S, Ohtani N, Yoshimoto S, et al. DNA damage signaling triggers degradation of histone methyltransferases through APC/C(Cdh1) in senescent cells. *Mol Cell.* 2012; 45(1):123–131. doi: [10.1016/j.molcel.2011.10.018](#) PMID: [22178396](#)
18. Zhang Y, Elgizouli M, Schotker B, Holleccek B, Nieters A, Brenner H. Smoking-associated DNA methylation markers predict lung cancer incidence. *Clin Epigenetics.* 2016; 8(127):1–12.
19. Asada K, Kotake Y, Asada R, Saunders D, Broyles RH, Towner RA, et al. LINE-1 hypomethylation in a choline-deficiency-induced liver cancer in rats: dependence on feeding period. *J Biomed Biotechnol.* 2006; 2006(1):1–6.
20. Varley KE, Gertz J, Bowling KM, Parker SL, Reddy TE, Pauli-Behn F, et al. Dynamic DNA methylation across diverse human cell lines and tissues. *Genome Res.* 2013; 23(3):555–567. doi: [10.1101/gr.147942.112](#) PMID: [23325432](#)
21. Horvath S, Zhang Y, Langfelder P, Kahn RS, Boks MP, van Eijk K, et al. Aging effects on DNA methylation modules in human brain and blood tissue. *Genome Biol.* 2012; 13(10):1–18.
22. Koch CM, Wagner W. Epigenetic biomarker to determine replicative senescence of cultured cells. *Methods Mol Biol.* 2013; 1048:309–321. doi: [10.1007/978-1-62703-556-9_20](#) PMID: [23929112](#)
23. Koch CM, Suschek CV, Lin Q, Bork S, Goergens M, Jousen S, et al. Specific age-associated DNA methylation changes in human dermal fibroblasts. *PLoS One.* 2011; 6(2):e16679. doi: [10.1371/journal.pone.0016679](#) PMID: [21347436](#)
24. Christensen BC, Houseman EA, Marsit CJ, Zheng S, Wrensch MR, Wiemels JL, et al. Aging and environmental exposures alter tissue-specific DNA methylation dependent upon CpG island context. *PLoS Genet.* 2009; 5(8):e1000602. doi: [10.1371/journal.pgen.1000602](#) PMID: [19680444](#)
25. Fraga MF, Ballestar E, Paz MF, Ropero S, Setien F, Ballestar ML, et al. Epigenetic differences arise during the lifetime of monozygotic twins. *Proc Natl Acad Sci U S A.* 2005; 102(30):10604–10609. doi: [10.1073/pnas.0500398102](#) PMID: [16009939](#)
26. Jjingo D, Conley AB, Yi SV, Lunyak VV, Jordan IK. On the presence and role of human gene-body DNA methylation. *Oncotarget.* 2012; 3(4):462–474. doi: [10.18632/oncotarget.497](#) PMID: [22577155](#)
27. Dhahbi JM, Atamna H, Boffelli D, Magis W, Spindler SR, Martin DI. Deep sequencing reveals novel microRNAs and regulation of microRNA expression during cell senescence. *PLoS One.* 2011; 6(5): e20509. doi: [10.1371/journal.pone.0020509](#) PMID: [21637828](#)
28. Lafferty-Whyte K, Cairney CJ, Jamieson NB, Oien KA, Keith WN. Pathway analysis of senescence-associated miRNA targets reveals common processes to different senescence induction mechanisms. *Biochim Biophys Acta.* 2009; 1792(4):341–352. doi: [10.1016/j.bbadis.2009.02.003](#) PMID: [19419692](#)

29. Taguchi YH. Inference of Target Gene Regulation via miRNAs during Cell Senescence by Using the MiRaGE Server. *Aging Dis.* 2012; 3(4):301–306. PMID: [23185711](#)
30. Overhoff MG, Garbe JC, Koh J, Stampfer MR, Beach DH, Bishop CL. Cellular senescence mediated by p16INK4A-coupled miRNA pathways. *Nucleic Acids Res.* 2014; 42(3):1606–1618. doi: [10.1093/nar/gkt1096](#) PMID: [24217920](#)
31. Li CW, Wang WH, Chen BS. Investigating the specific core genetic-and-epigenetic networks of cellular mechanisms involved in human aging in peripheral blood mononuclear cells. *Oncotarget.* 2016; 7(8):8556–8579. doi: [10.18632/oncotarget.7388](#) PMID: [26895224](#)
32. Tazawa H, Tsuchiya N, Izumiya M, Nakagama H. Tumor-suppressive miR-34a induces senescence-like growth arrest through modulation of the E2F pathway in human colon cancer cells. *Proc Natl Acad Sci U S A.* 2007; 104(39):15472–15477. doi: [10.1073/pnas.0707351104](#) PMID: [17875987](#)
33. He X, He L, Hannon GJ. The guardian's little helper: microRNAs in the p53 tumor suppressor network. *Cancer Res.* 2007; 67(23):11099–11101. doi: [10.1158/0008-5472.CAN-07-2672](#) PMID: [18056431](#)
34. Christoffersen NR, Shalgi R, Frankel LB, Leucci E, Lees M, Klausen M, et al. p53-independent upregulation of miR-34a during oncogene-induced senescence represses MYC. *Cell Death Differ.* 2010; 17(2):236–245. doi: [10.1038/cdd.2009.109](#) PMID: [19696787](#)
35. Ayala-Ortega E, Arzate-Mejia R, Perez-Molina R, Gonzalez-Buendia E, Meier K, Guerrero G, et al. Epigenetic silencing of miR-181c by DNA methylation in glioblastoma cell lines. *BMC Cancer.* 2016; 16(226):1–12.
36. Asuthkar S, Velpula KK, Chetty C, Gorantla B, Rao JS. Epigenetic regulation of miRNA-211 by MMP-9 governs glioma cell apoptosis, chemosensitivity and radiosensitivity. *Oncotarget.* 2012; 3(11):1439–1454. doi: [10.18632/oncotarget.683](#) PMID: [23183822](#)
37. Yin H, Song P, Su R, Yang G, Dong L, Luo M, et al. DNA Methylation mediated down-regulating of MicroRNA-33b and its role in gastric cancer. *Sci Rep.* 2016; 6(18824):1–12.
38. Maehara K, Takahashi K, Saitoh S. CENP-A reduction induces a p53-dependent cellular senescence response to protect cells from executing defective mitoses. *Mol Cell Biol.* 2010; 30(9):2090–2104. doi: [10.1128/MCB.01318-09](#) PMID: [20160010](#)
39. Chen C, Okayama H. High-efficiency transformation of mammalian cells by plasmid DNA. *Mol Cell Biol.* 1987; 7(8):2745–2752. PMID: [3670292](#)
40. Tsuyama N, Miura M, Kitahira M, Ishibashi S, Ide T. SV40 T-antigen is required for maintenance of immortal growth in SV40-transformed human fibroblasts. *Cell Struct Funct.* 1991; 16(1):55–62. PMID: [1851674](#)
41. Bibikova M, Le J, Barnes B, Saedinia-Melnyk S, Zhou L, Shen R, et al. Genome-wide DNA methylation profiling using Infinium(R) assay. *Epigenomics.* 2009; 1(1):177–200. doi: [10.2217/epi.09.14](#) PMID: [22122642](#)
42. Bibikova M, Barnes B, Tsan C, Ho V, Klotzle B, Le JM, et al. High density DNA methylation array with single CpG site resolution. *Genomics.* 2011; 98(4):288–295. doi: [10.1016/j.ygeno.2011.07.007](#) PMID: [21839163](#)
43. Price ME, Cotton AM, Lam LL, Farre P, Emberly E, Brown CJ, et al. Additional annotation enhances potential for biologically-relevant analysis of the Illumina Infinium HumanMethylation450 BeadChip array. *Epigenetics Chromatin.* 2013; 6(4):1–15.
44. Hannum G, Guinney J, Zhao L, Zhang L, Hughes G, Sada S, et al. Genome-wide methylation profiles reveal quantitative views of human aging rates. *Mol Cell.* 2013; 49(2):359–367. doi: [10.1016/j.molcel.2012.10.016](#) PMID: [23177740](#)
45. Laird CD, Pleasant ND, Clark AD, Sneed JL, Hassan KM, Manley NC, et al. Hairpin-bisulfite PCR: assessing epigenetic methylation patterns on complementary strands of individual DNA molecules. *Proc Natl Acad Sci U S A.* 2004; 101(1):204–209. doi: [10.1073/pnas.2536758100](#) PMID: [14673087](#)
46. Chen ZX, Riggs AD. DNA methylation and demethylation in mammals. *J Biol Chem.* 2011; 286(21):18347–18353. doi: [10.1074/jbc.R110.205286](#) PMID: [21454628](#)
47. Wu SC, Zhang Y. Active DNA demethylation: many roads lead to Rome. *Nat Rev Mol Cell Biol.* 2010; 11(9):607–620. doi: [10.1038/nrm2950](#) PMID: [20683471](#)
48. Weber AR, Krawczyk C, Robertson AB, Kusnierczyk A, Vagbo CB, Schuermann D, et al. Biochemical reconstitution of TET1-TDG-BER-dependent active DNA demethylation reveals a highly coordinated mechanism. *Nat Commun.* 2016; 7(10806):1–13.
49. Pastor WA, Aravind L, Rao A. TETonic shift: biological roles of TET proteins in DNA demethylation and transcription. *Nat Rev Mol Cell Biol.* 2013; 14(6):341–356. doi: [10.1038/nrm3589](#) PMID: [23698584](#)
50. Truong TP, Sakata-Yanagimoto M, Yamada M, Nagae G, Enami T, Nakamoto-Matsubara R, et al. Age-Dependent Decrease of DNA Hydroxymethylation in Human T Cells. *J Clin Exp Hematop.* 2015; 55(1):1–6. doi: [10.3960/jslrt.55.1](#) PMID: [26105999](#)

51. Wiehle L, Raddatz G, Musch T, Dawlaty MM, Jaenisch R, Lyko F, et al. Tet1 and Tet2 Protect DNA Methylation Canyons against Hypermethylation. *Mol Cell Biol*. 2015; 36(3):452–461. doi: [10.1128/MCB.00587-15](https://doi.org/10.1128/MCB.00587-15) PMID: [26598602](https://pubmed.ncbi.nlm.nih.gov/26598602/)
52. Oliveira NF, Damm GR, Andia DC, Salmon C, Nociti FH Jr., Line SR, et al. DNA methylation status of the IL8 gene promoter in oral cells of smokers and non-smokers with chronic periodontitis. *J Clin Periodontol*. 2009; 36(9):719–725. doi: [10.1111/j.1600-051X.2009.01446.x](https://doi.org/10.1111/j.1600-051X.2009.01446.x) PMID: [19659670](https://pubmed.ncbi.nlm.nih.gov/19659670/)
53. Rusiecki JA, Byrne C, Galdzicki Z, Srikantan V, Chen L, Poulin M, et al. PTSD and DNA Methylation in Select Immune Function Gene Promoter Regions: A Repeated Measures Case-Control Study of U.S. Military Service Members. *Front Psychiatry*. 2013; 4:1–12.
54. Ushijima T. Epigenetic field for cancerization. *J Biochem Mol Biol*. 2007; 40(2):142–150. PMID: [17394762](https://pubmed.ncbi.nlm.nih.gov/17394762/)
55. Lee JH, Voo KS, Skalnik DG. Identification and characterization of the DNA binding domain of CpG-binding protein. *J Biol Chem*. 2001; 276(48):44669–44676. doi: [10.1074/jbc.M107179200](https://doi.org/10.1074/jbc.M107179200) PMID: [11572867](https://pubmed.ncbi.nlm.nih.gov/11572867/)
56. Williams K, Christensen J, Helin K. DNA methylation: TET proteins-guardians of CpG islands? *EMBO Rep*. 2012; 13(1):28–35.
57. Ichiyama K, Chen T, Wang X, Yan X, Kim BS, Tanaka S, et al. The methylcytosine dioxygenase Tet2 promotes DNA demethylation and activation of cytokine gene expression in T cells. *Immunity*. 2015; 42(4):613–626. doi: [10.1016/j.immuni.2015.03.005](https://doi.org/10.1016/j.immuni.2015.03.005) PMID: [25862091](https://pubmed.ncbi.nlm.nih.gov/25862091/)
58. Banko JL, Poulin F, Hou L, DeMaria CT, Sonenberg N, Klann E. The translation repressor 4E-BP2 is critical for eIF4F complex formation, synaptic plasticity, and memory in the hippocampus. *J Neurosci*. 2005; 25(42):9581–9590. doi: [10.1523/JNEUROSCI.2423-05.2005](https://doi.org/10.1523/JNEUROSCI.2423-05.2005) PMID: [16237163](https://pubmed.ncbi.nlm.nih.gov/16237163/)
59. van der Horst GT, Muijtjens M, Kobayashi K, Takano R, Kanno S, Takao M, et al. Mammalian Cry1 and Cry2 are essential for maintenance of circadian rhythms. *Nature*. 1999; 398(6728):627–630. doi: [10.1038/19323](https://doi.org/10.1038/19323) PMID: [10217146](https://pubmed.ncbi.nlm.nih.gov/10217146/)
60. Rose-John S, Heinrich PC. Soluble receptors for cytokines and growth factors: generation and biological function. *Biochem J*. 1994; 300:281–290. PMID: [8002928](https://pubmed.ncbi.nlm.nih.gov/8002928/)
61. Freund A, Orjalo AV, Desprez PY, Campisi J. Inflammatory networks during cellular senescence: causes and consequences. *Trends Mol Med*. 2010; 16(5):238–246. doi: [10.1016/j.molmed.2010.03.003](https://doi.org/10.1016/j.molmed.2010.03.003) PMID: [20444648](https://pubmed.ncbi.nlm.nih.gov/20444648/)
62. Baumann H, Schendel P. Interleukin-11 regulates the hepatic expression of the same plasma protein genes as interleukin-6. *J Biol Chem*. 1991; 266(30):20424–20427. PMID: [1718962](https://pubmed.ncbi.nlm.nih.gov/1718962/)
63. Heinrich PC, Behrmann I, Haan S, Hermanns HM, Muller-Newen G, Schaper F. Principles of interleukin (IL)-6-type cytokine signalling and its regulation. *Biochem J*. 2003; 374(Pt 1):1–20. doi: [10.1042/BJ20030407](https://doi.org/10.1042/BJ20030407) PMID: [12773095](https://pubmed.ncbi.nlm.nih.gov/12773095/)
64. Pflanz S, Hibbert L, Mattson J, Rosales R, Vaisberg E, Bazan JF, et al. WSX-1 and glycoprotein 130 constitute a signal-transducing receptor for IL-27. *J Immunol*. 2004; 172(4):2225–2231. PMID: [14764690](https://pubmed.ncbi.nlm.nih.gov/14764690/)
65. Vilborg A, Glahder JA, Wilhelm MT, Bersani C, Corcoran M, Mahmoudi S, et al. The p53 target Wig-1 regulates p53 mRNA stability through an AU-rich element. *Proc Natl Acad Sci U S A*. 2009; 106(37):15756–15761. doi: [10.1073/pnas.0900862106](https://doi.org/10.1073/pnas.0900862106) PMID: [19805223](https://pubmed.ncbi.nlm.nih.gov/19805223/)
66. Beausejour CM, Krtolica A, Galimi F, Narita M, Lowe SW, Yaswen P, et al. Reversal of human cellular senescence: roles of the p53 and p16 pathways. *EMBO J*. 2003; 22(16):4212–4222. doi: [10.1093/emboj/cdg417](https://doi.org/10.1093/emboj/cdg417) PMID: [12912919](https://pubmed.ncbi.nlm.nih.gov/12912919/)
67. Vousden KH. Outcomes of p53 activation—spoilt for choice. *J Cell Sci*. 2006; 119(Pt 24):5015–5020. doi: [10.1242/jcs.03293](https://doi.org/10.1242/jcs.03293) PMID: [17158908](https://pubmed.ncbi.nlm.nih.gov/17158908/)
68. Disayabutr S, Kim EK, Cha SI, Green G, Naikawadi RP, Jones KD, et al. miR-34 miRNAs Regulate Cellular Senescence in Type II Alveolar Epithelial Cells of Patients with Idiopathic Pulmonary Fibrosis. *PLoS One*. 2016; 11(6):e0158367. doi: [10.1371/journal.pone.0158367](https://doi.org/10.1371/journal.pone.0158367) PMID: [27362652](https://pubmed.ncbi.nlm.nih.gov/27362652/)
69. Harries LW. MicroRNAs as Mediators of the Ageing Process. *Genes (Basel)*. 2014; 5(3):656–670.

Human cytomegalovirus downregulates *SLITRK6* expression through IE2

Huanan Liao¹ · Haruna Sato¹ · Ryosuke Chiba¹ · Tomoko Kawai² · Kazuhiko Nakabayashi² · Kenichiro Hata² · Hidenori Akutsu³ · Shigeyoshi Fujiwara¹ · Hiroyuki Nakamura¹ 

Received: 9 March 2016 / Revised: 7 June 2016 / Accepted: 1 August 2016 / Published online: 16 August 2016
© Journal of NeuroVirology, Inc. 2016

Abstract Congenital human cytomegalovirus (HCMV) infection causes sensorineural hearing loss (SNHL) and other neurological disorders, although the neuropathogenesis of HCMV infection is not well understood. Here, we show that the expression of *SLITRK6*, one of causative genes for hereditary SNHL, was robustly downregulated by HCMV infection in cultured neural cells. We also show that HCMV-encoded immediate-early 2 (IE2) proteins mediate this downregulation and their carboxy-terminal region, especially amino acid residue Gln⁵⁴⁸, has a critical role. These findings suggest that the downregulation of *SLITRK6* expression by IE2 may have a role in HCMV-induced SNHL and other neurological disorders.

Keywords Human cytomegalovirus · IE2 · *SLITRK6* · Hearing loss

Introduction

Congenital human cytomegalovirus (HCMV) infection is the most common congenital viral infection, affecting 0.2 to 2.5 % of all live-born neonates (Cheeran et al. 2009; Ornoy

and Diav-Citrin 2006). Approximately 10 % of neonates with congenital HCMV infection are estimated to be symptomatic at birth and often manifest severe damages in various organs including the central nervous system (CNS) and the inner ear. A recent large-scale screening in Japan demonstrated that approximately 30 % of congenitally HCMV-infected newborns had some clinical manifestations at birth if abnormal findings of brain MRI are included (Koyano et al. 2011). Although the vast majority of neonates with congenital HCMV infection are thus asymptomatic at birth, approximately 10 % of these asymptomatic children will develop delayed sequelae caused by HCMV-induced nervous system damages, such as sensorineural hearing loss (SNHL), vestibular symptoms, and behavioral abnormalities (Bernard et al. 2015; Karltorp et al. 2014). Congenital HCMV infection is the leading cause of nongenetic congenital SNHL; 22 to 65 % of children that were symptomatic at birth and 6 to 23 % of children that were asymptomatic at birth develop SNHL (Fowler and Boppana 2006; Morton and Nance 2006).

Although HCMV infection and gene expression in the inner ear as well as various parts of the CNS have been analyzed in a limited number of congenitally infected children, the exact nature of HCMV infection in the human nervous system has not been well characterized. The mechanism of HCMV-induced neuropathogenesis therefore remains largely unknown. To get a new insight into HCMV-induced neuropathogenesis, we have been analyzing the effect of HCMV infection on the expression of cellular genes involved in the development and function of the CNS and/or auditory system. In this report, we demonstrate that the expression of *SLITRK6*, an etiologic gene for a group of hereditary SNHL (Morlet et al. 2014; Tekin et al. 2013), is robustly downregulated by HCMV infection in cultured neural cells. Further, we demonstrate that HCMV-encoded immediate-early 2 (IE2) proteins are involved in this *SLITRK6* downregulation.

✉ Hiroyuki Nakamura
nakamura-hry@ncchd.go.jp

¹ Department of Allergy and Clinical Immunology, National Research Institute for Child Health and Development, 2-10-1 Okura, Setagaya-ku, Tokyo 157-8535, Japan

² Department of Maternal-Fetal Biology, National Research Institute for Child Health and Development, Tokyo, Japan

³ Department of Reproductive Biology, Center for Regenerative Medicine, National Research Institute for Child Health and Development, Tokyo, Japan

Materials and methods

Cells and viruses

The human glioblastoma-astrocytoma cell lines U373 MG and Hs 683 were grown in Dulbecco's modified Eagle's medium (DMEM; Nacalai Tesque, Kyoto, Japan) supplemented with 10 % fetal bovine serum (FBS; Biowest, France), penicillin (200 U/mL), and streptomycin (200 µg/mL) at 37 °C in 5 % CO₂ atmosphere. The human neuroblastoma cell line SH-SY5Y was grown in DMEM/F-12 (Nacalai Tesque) supplemented with 10 % FBS and the antibiotics. The human foreskin fibroblast cell line hTERT-BJ1 (Clontech, Palo Alto, CA) was grown in a medium consisting of DMEM/medium 199 (Sigma-Aldrich, St. Louis, MO) (4:1) supplemented with 10 % FBS, 1 mM sodium pyruvate (Nacalai Tesque), 2 mM glutamine (Thermo Fisher Scientific; Madison, WI), and the antibiotics. The HCMV laboratory strains Towne (ATCC VR-977) and AD169 (ATCC VR-538) were propagated in cultured hTERT-BJ1 cells. Heat-inactivated (HI) HCMV was prepared by heating HCMV-containing culture media at 63 °C for 60 min. The Gibco episomal human iPSC line (Thermo Fisher Scientific), an induced pluripotent stem cell (iPSC) line generated using cord blood-derived CD34+ progenitors, was grown under feeder-free conditions in complete Essential 8 medium (Thermo Fisher Scientific) on vessels coated with vitronectin (Thermo Fisher Scientific). The iPSCs were differentiated into neural stem/progenitor cells (NSPCs) using PSC Neural Induction Medium (Thermo Fisher Scientific) according to manufacturer's instructions.

Antibodies and reagents

The antibodies used were as follows: sheep anti-SLITRK6 (R&D Systems, Minneapolis, MN); mouse anti-CMV IE1/IE2 (8B1.2, Merck Millipore, Bedford, MA); mouse anti-IE2 (5A8.2, Merck Millipore); mouse anti-IE2 (12E2, Santa Cruz Biotechnology, Santa Cruz, CA); mouse anti-IE1 (6E1, Santa Cruz Biotechnology); mouse anti-CMV gB (2F12, Abcam, Cambridge, MA); mouse anti-pp65 (3A12, Abcam); mouse anti-nestin (10C2, Merck Millipore), horseradish peroxidase (HRP)-conjugated mouse anti-β-actin (Wako Chemical, Osaka, Japan); Alexa Fluor 488-conjugated goat anti-mouse immunoglobulin G (IgG) (Thermo Fisher Scientific); HRP-conjugated donkey anti-sheep IgG (R&D Systems); and HRP-conjugated sheep anti-mouse IgG (GE Healthcare, Little Chalfont, Buckinghamshire, UK). Cellstain-DAPI solution was obtained from Dojindo Molecular Technologies (Kumamoto, Japan).

Plasmid constructs and the Flp-In/TREx expression system

HCMV-encoded genes and deletion mutants were generated by PCR with primers shown in Table 1. The PCR products

were cloned into the pcDNA5/FRT/TO vector (Thermo Fisher Scientific) to construct pcDNA5/FRT/TO-IE1 72, pcDNA5/FRT/TO-IE2 86, pcDNA5/FRT/TO-IE2 60, pcDNA5/FRT/TO-IE2 40, and pcDNA5/FRT/TO-pp65. To construct pcDNA5/FRT/FRT-IE2 (Q548R), site-directed mutagenesis was performed using QuikChange II site-directed mutagenesis kit (Agilent Technologies, Santa Clara, CA) with the following primers: forward 5'-GGCCTACGCCGTCCGCCGGTTTGAGCAGCCC-3', reverse 5'-GGGC TGCTCAAACCGGCCGACGGCGTAGGCC-3' as described previously (Petrik et al. 2006). To establish U373 MG cells expressing HCMV-encoded genes in a tetracycline-inducible manner, pFRT/lacZeo (Thermo Fisher Scientific) containing a Flp recombination target site and a lacZ-Zeocin fusion gene and pcDNA6/TR (Thermo Fisher Scientific) containing tetracycline repressor gene were sequentially transduced into U373 MG cells, and transfected cells were selected with zeocin (InvivoGen, San Diego, CA) and blasticidin (InvivoGen), respectively, as described previously (Nakamura et al. 2003). The resultant cells were co-transfected with pOG44 (Thermo Fisher Scientific) expressing Flp recombinase combined with pcDNA5/FRT/TO-IE1, pcDNA5/FRT/TO-IE2, pcDNA5/FRT/TO-pp65, or pcDNA5/FRT/TO, and selected with 500 µg/mL of hygromycin B (Wako Chemical) for 6 weeks. These cells were designated as Flp-In/TREx U373 MG-IE1, Flp-In/TREx U373 MG-IE2, Flp-In/TREx U373 MG-pp65, and Flp-In/TREx U373 MG-pcDNA5/FRT/TO cells, respectively. To induce viral gene expression, cells were treated with 3 µg/mL of doxycycline (Takara Bio, Shiga, Japan).

Reverse transcription PCR, real-time quantitative RT-PCR

Total RNA was extracted from cells using ReliaPrep RNA Cell Miniprep System (Promega, Madison, WI). First-strand complementary DNAs (cDNAs) were synthesized using a PrimeScript II 1st strand cDNA Synthesis Kit (Takara Bio). The resultant cDNAs were analyzed by either reverse transcription (RT)-PCR or real-time quantitative RT-PCR (RT-qPCR). RT-PCR was performed in a total volume of 50 µL for 30 cycles using the GeneAmp PCR System 9700 thermocycler (Thermo Fisher Scientific), and then the PCR products were analyzed by 1–2 % agarose gel electrophoresis. RT-qPCR was performed with pre-designed TaqMan probe and primer sets specific for human *SLITRK6* (TaqMan Gene Expression Assay, assay identification Hs00536106_s1; Thermo Fisher Scientific) and human TATA box-binding protein (*TBP*) (assay identification Hs00427620_m1) in a StepOne Plus System (Thermo Fisher Scientific). The relative quantification of gene expression was calculated using the $\Delta\Delta C_t$ method and normalized to *TBP* messenger RNA (mRNA).

Table 1 Primers used for molecular cloning and RT-PCR analysis

Gene	Forward primer	Reverse primer
Cloning		
IE1 72	CGCAAGCTT <u>GCCGCC</u> ACCATGGAGTCCTCTGCCAAGAGAAAG	CGCGGATCCTTACTGGTCAGCCTTGCTTCTAG
IE2 86	CGCAAGCTT <u>GCCGCC</u> ACCATGGAGTCCTCTGCCAAGAGAAAG	CGCGGATCCTTACTGAGACTTGTCCTCAGG
pp65	CGCGGATCCAGCATGGAGTCGCGCGGTTCGC	CGCCTCGAGTCAACCTCGGTGCTTTTTGGGC
IE2 (1–550)	CGCAAGCTT <u>GCCGCC</u> ACCATGGAGTCCTCTGCCAAGAGAAAG	CGCGGATCCTTACTCAAACCTGCCCCACGGCGTAG
IE2 (1–547)	CGCAAGCTT <u>GCCGCC</u> ACCATGGAGTCCTCTGCCAAGAGAAAG	CGCGGATCCTTACCCACGGCGTAGGCCTTCGC
IE2 (1–543)	CGCAAGCTT <u>GCCGCC</u> ACCATGGAGTCCTCTGCCAAGAGAAAG	CGCGGATCCTTAGGCCTTCGCGGCCGTCTCGTAG
IE2 60	CGCAAGCTT <u>GCCGCC</u> ACCATGCTGCCCTCATCAAACAGG	CGCGGATCCTTACTGAGACTTGTCCTCAGG
IE2 40	CGCAAGCTT <u>GCCGCC</u> ACCATGAACCACCCTCTTCCCGA	CGCGGATCCTTACTGAGACTTGTCCTCAGG
RT-PCR		
SLITRK6	CAGCAGCTTGCAAATGGTTA	GAGCCTCTGGATGAGAGCAC
IE1	ATGGAGTCCTCTGCCAAGAG	ATTCTATGCCGCACCATGTCC
IE2	ATGGAGTCCTCTGCCAAGAG	CTGAGACTTGTTCCCTCAGGTCCTG
pp65	CGCAACCTGGTGCCCATGG	CGTTTGGGTTGCGCAGCGGG
β-actin	ACCATGGATGATGATATCGC	TCATTGTAGAAGGTGTGGTG
TBP	TTCGAGAGTTCTGGGATTGTA	TGGACTGTTCTTCACTCTTGGC

Underlined letters indicate restriction enzyme recognition sites

Immunoblot analysis

Cellular proteins extracted with a sodium dodecyl sulfate (SDS) sample buffer (50 mM Tris-HCl, pH 6.8, 2 % SDS, 10 % glycerol, 6 % 2-mercaptoethanol, 0.1 % bromophenol blue) were subjected to sodium dodecyl sulfate-polyacrylamide gel electrophoresis (SDS-PAGE). Proteins were transferred to Immobilon-P transfer membranes (Merck Millipore). Membranes were blocked with 5 % non-fat milk (Nacalai Tesque) and then incubated with a primary antibody overnight at 4 °C in TBS-T (20 mM Tris, pH 7.6, 137 mM NaCl, 0.1 % Tween-20). Membranes were then incubated with a HRP-conjugated secondary antibody, and antigen proteins were visualized with ImmunoStar Zeta (Wako Chemicals) and detected by the GE LAS4000 Phosphor Imager (GE Healthcare Life Sciences).

Results

HCMV infection robustly downregulates *SLITRK6* expression

A variety of cellular genes have been identified as the causes of hereditary neurodevelopmental diseases (Mitchell 2011), and we speculated that HCMV infection may affect the expression of such genes to induce neurodevelopmental diseases. Among those genes, we

focused on *SLITRK6*, since it has been recently demonstrated as a causative gene of hereditary SNHL and myopia in mice and humans (Katayama et al. 2009; Matsumoto et al. 2011; Morlet et al. 2014; Tekin et al. 2013). RT-PCR analysis showed that the *SLITRK6* mRNA expression was clearly and robustly downregulated in HCMV-infected SH-SY5Y cells compared to mock-infected cells (Fig. 1(a)). This downregulation of *SLITRK6* mRNA expression was not observed following infection with heat-inactivated HCMV, indicating that viable HCMV is required. The downregulation of *SLITRK6* mRNA was also detected in U373 MG cells (Fig. 1(d)) and Hs 683 cells (data not shown) following HCMV infection. To confirm the results and obtain more quantitative data, we performed real-time quantitative RT-PCR (RT-qPCR) and the results demonstrated that *SLITRK6* mRNA expression in HCMV-infected SH-SY5Y cells (Fig. 1(b)) and U373 MG cells (Fig. 1(e)) was decreased 21–183-fold and 41–46-fold, respectively, compared to those cells infected with heat-inactivated HCMV. Immunoblot analysis showed that the downregulation of *SLITRK6* mRNA levels was reflected at the protein level; the *SLITRK6* protein expression was apparently abolished in SH-SY5Y (Fig. 1(c)), U373 MG cells (Fig. 1(f)), and Hs 683 cells (data not shown) following HCMV infection.

We previously demonstrated that neural stem/progenitor cells (NSPCs) derived from human induced pluripotent stem cells (iPSCs) can be infected with HCMV (Nakamura et al. 2013). Therefore, we examined whether

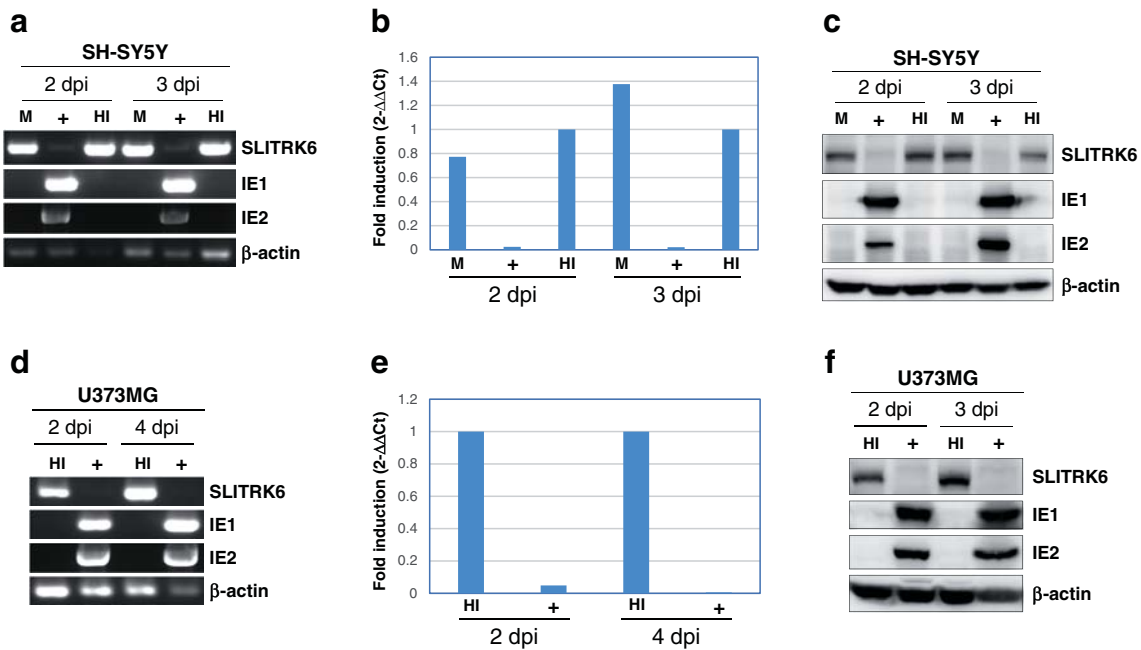


Fig. 1 HCMV infection robustly downregulates *SLITRK6* expression in neural cell lines. RT-PCR analysis of *SLITRK6* mRNA expression in the HCMV-infected cell lines SH-SY5Y (a) and U373 MG (d). Total RNAs isolated from cells infected with Towne HCMV (+), heat-inactivated Towne HCMV (HI), or mock-infected (M, culture media from HCMV-uninfected hTERT-BJ1 cells) at indicated days post-infection (dpi) were subjected to RT-PCR assays with *SLITRK6*-specific primers. RT-PCR assays with IE1- and IE2-specific primers were also performed. β -actin was used as an internal control. RT-qPCR analysis of *SLITRK6* mRNA expression in the HCMV-infected cell lines SH-SY5Y (b) and U373 MG

(e). RT-qPCR data was analyzed by the $2^{-\Delta\Delta C_t}$ method. The mRNA expression was normalized to that of TBP. The fold induction was calculated as the ratio of mRNA levels. Immunoblot analysis of *SLITRK6* protein expression in the HCMV-infected cell lines SH-SY5Y (c) and U373 MG (f). Whole-cell lysates of cells infected with Towne HCMV (+), heat-inactivated Towne HCMV (HI), or mock-infected (M) were extracted at indicated dpi and separated by SDS-PAGE and analyzed by immunoblotting with antibodies against *SLITRK6*, IE1, or IE2. Equal protein loading was established with anti- β -actin antibody

the expression of *SLITRK6* is downregulated by HCMV infection also in NSPCs derived from human iPSCs. RT-PCR (Fig. 2(a)), RT-qPCR (Fig. 2(b)), and immunoblot analyses (Fig. 2(c)) showed that *SLITRK6* was highly expressed in iPSC-derived NSPCs compared to parental iPSCs, suggesting that differentiation of iPSCs into NSPCs induced *SLITRK6* expression. In NSPCs derived from human iPSCs, the expression of *SLITRK6* was robustly downregulated by HCMV infection (Fig. 2(d–f)). These results indicated that the *SLITRK6* downregulation by HCMV is commonly observed in a variety of human neural cell lines.

IE2 mediates the downregulation of *SLITRK6* expression by HCMV

To clarify the mechanism of the *SLITRK6* downregulation by HCMV, we explored which viral gene is responsible for this downregulation. We initially examined whether HCMV-encoded immediate-early proteins IE1 72 and IE2 86 and viral tegument protein pp65 can affect *SLITRK6* expression. Using U373 MG cells, we established cell lines in which these individual viral genes were expressed in a tetracycline-inducible manner. The

cell lines were designated Flp-In/TREx U373 MG-IE1 72, Flp-In/TREx U373 MG-IE2 86, and Flp-In/TREx U373 MG-pp65, respectively. Flp-In/TREx U373 MG-pcDNA5/FRT/TO was used as a negative control. When these cells were treated with doxycycline (Dox) for 2 or 4 days, the synthesis of IE1 72, IE2 86, and pp65 proteins was induced (Fig. 3(B)). RT-PCR assay at 2 or 4 days after the addition of Dox demonstrated the downregulation of *SLITRK6* mRNA expression by IE2 86 (Fig. 3(A–b)) but not by IE1 72 (Fig. 3(A–a)) and pp65 (Fig. 3(A–c)). As expected, the control Flp-In/TREx U373 MG-pcDNA5/FRT/TO cells showed similar levels of *SLITRK6* mRNA with or without Dox treatment (Fig. 3(A–d)). In accordance with these mRNA data, *SLITRK6* protein levels were clearly reduced by Dox treatment in Flp-In/TREx U373 MG-IE2 86 cells (Fig. 3(B), lanes 5–8). In contrast, *SLITRK6* protein levels were not significantly reduced in Flp-In/TREx U373 MG-IE1 72 (Fig. 3(B), lanes 1–4), Flp-In/TREx U373 MG-pp65 (Fig. 3(B), lanes 13–16), or Flp-In/TREx U373 MG-pcDNA5/FRT/TO cells (Fig. 3(B), lanes 9–12) following treatment with Dox. These results clearly indicate that IE2 86 is involved in the HCMV-induced downregulation of *SLITRK6* expression.

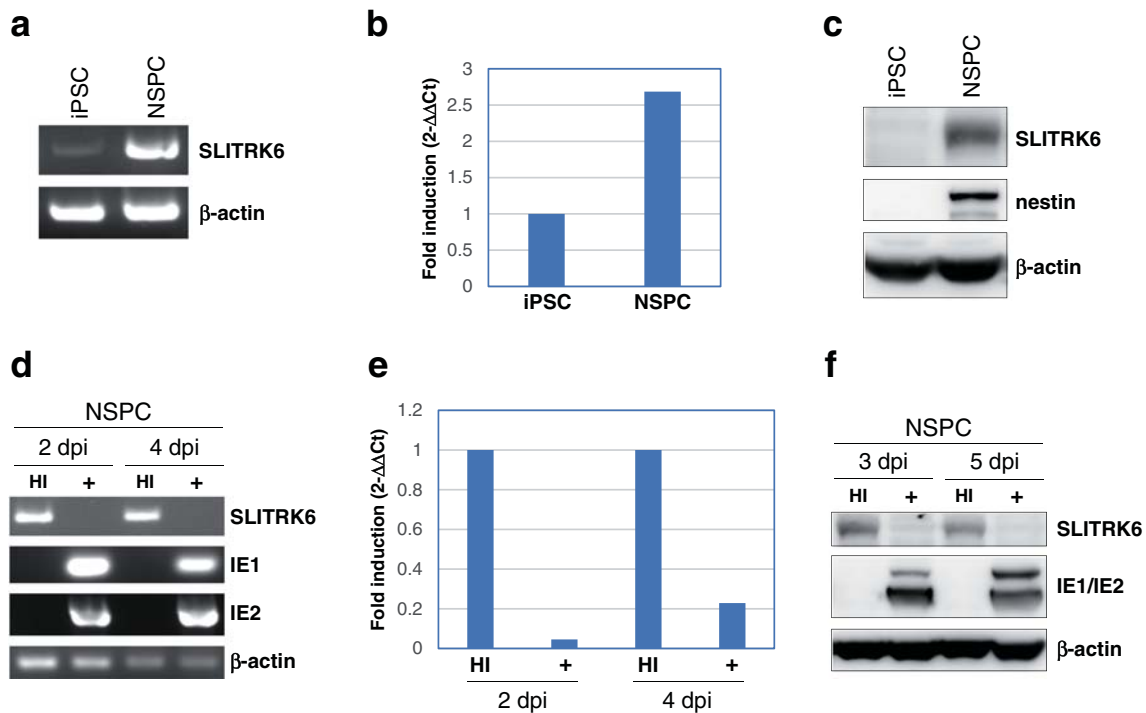


Fig. 2 SLITRK6 expression in iPSCs and iPSC-derived NSPCs. **(a)** Total RNAs extracted from iPSCs and iPSC-derived NSPCs were analyzed by RT-PCR for the expression of SLITRK6 and β -actin. **(b)** SLITRK6 mRNA expression in iPSCs and NSPCs was analyzed by RT-qPCR. RT-qPCR data was analyzed by the $2^{-\Delta\Delta$ Ct method. The mRNA expression was normalized to that of TBP. The fold induction was calculated as the ratio of mRNA levels. **(c)** Whole-cell lysates of iPSCs and NSPCs were analyzed by immunoblotting with antibodies against SLITRK6 or nestin. Equal protein loading was established with anti- β -actin antibody. **(d)** RT-PCR analysis of SLITRK6 mRNA expression in the HCMV-infected NSPCs. Total RNAs isolated from

NSPCs infected with AD169 HCMV (+) or heat-inactivated AD169 HCMV (HI) at indicated days post-infection (dpi) were subjected to RT-PCR assays for the expression of SLITRK6, IE1, and IE2. β -actin was used as an internal control. **(e)** RT-qPCR analysis of SLITRK6 mRNA expression in the HCMV-infected NSPCs. **(f)** Immunoblot analysis of SLITRK6 protein expression in the HCMV-infected NSPCs. Whole-cell lysates of cells infected with AD169 HCMV (+) or heat-inactivated AD169 HCMV (HI) were extracted at indicated dpi and separated by SDS-PAGE and analyzed by immunoblotting with antibodies against SLITRK6 and IE1/IE2. Equal protein loading was established with anti- β -actin antibody

Carboxy-terminal region of IE2 86 is required for the downregulation of SLITRK6 expression by HCMV

To address which region of IE2 86 is required for the SLITRK6 downregulation, we compared the wild-type IE2 86 (designated as IE2 (1–579)) and its several deletion mutants (Fig. 4(C)) in terms of the ability of the SLITRK6 downregulation. The deletion mutants IE2 (1–550), IE2 (1–547), and IE2 (1–543) were expressed in Flp-In/TREx U373 MG cells in a Dox-inducible manner as described above. RT-PCR analysis confirmed that IE2 (1–550) suppressed the SLITRK6 mRNA level markedly (Fig. 4(A-a)), whereas IE2 (1–547) (Fig. 4(A-b)) and IE2 (1–543) (Fig. 4(A-c)) had little or no effect. Immunoblot analyses demonstrated that individual deletion mutants were expressed at comparable levels, and immunofluorescence analysis showed that these deletion mutants localize in the nucleus. Immunoblot analyses demonstrate that the expression levels of the SLITRK6 protein was reduced by IE2 (1–550) (Fig. 4(A-g)), but not by IE2 (1–547) (Fig. 4(A-h)) or IE2 (1–543) (Fig. 4(A-i)). Collectively, these results

indicate that the carboxy-terminal region (548 to 550 a.a.) of IE2 86 is critically important for the downregulation of SLITRK6. Since these data suggested that the amino acid residues 548 to 550 of IE2 86 is involved in the downregulation of SLITRK6 expression, IE2 (Q548R), in which the glutamine residue at a.a. 548 was mutated to arginine, was expressed in U373 MG cells and SLITRK6 expression was analyzed. Remarkably, the downregulation of SLITRK6 was not seen with IE2 (Q548R) both by RT-PCR (Fig. 4(A-d)) and by immunoblotting (Fig. 4(A-j)). These results clearly show that glutamine residue at a.a. 548 has a critical role in the downregulation of SLITRK6 expression.

Internal methionine codons in the exon 5 of IE2 86 generates the IE2 isoforms IE2 60 and IE2 40 (Plachter et al. 1993; Puchtler and Stamminger 1991; Stenberg et al. 1989). To test whether these isoforms can induce the SLITRK6 downregulation, we established the Flp-In/TREx U373 MG-IE2 60 and Flp-In/TREx U373 MG-IE2 40 cells in which the individual isoforms are synthesized in a Dox-dependent manner. Both IE2 60 and IE2 40 proteins were detected in the nucleus in these cells by

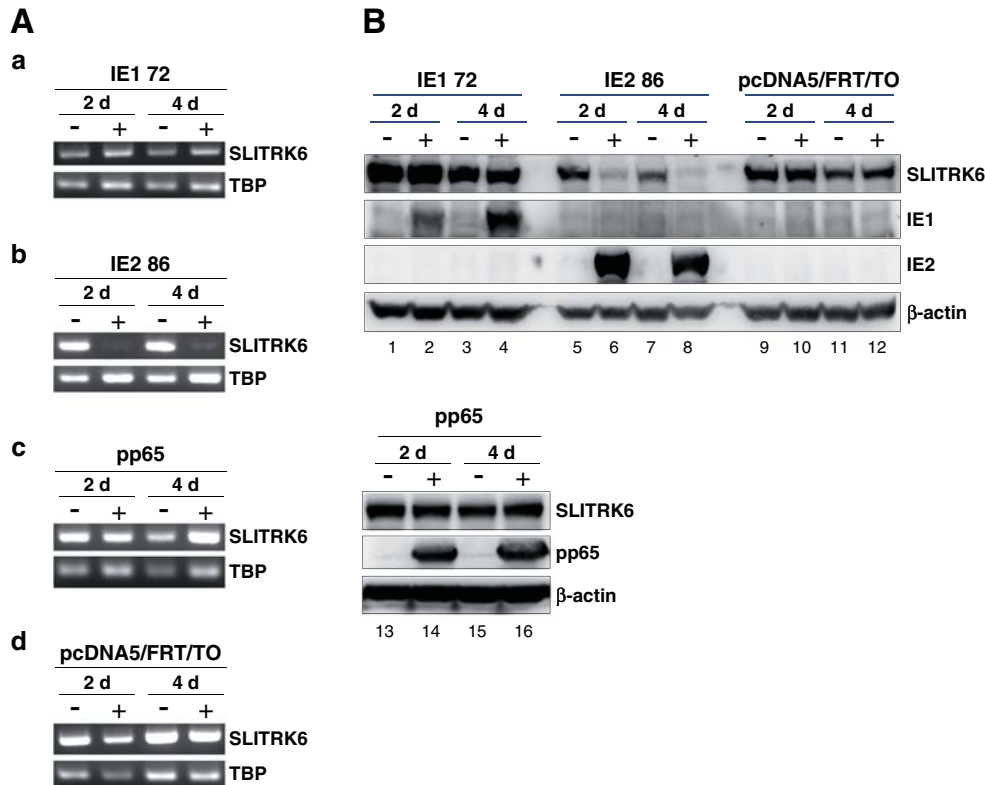


Fig. 3 Downregulation of *SLITRK6* expression by IE2. **A** Total RNAs extracted from Flp-In/TREx U373 MG-IE1 72 (*a*), Flp-In/TREx U373 MG-IE2 86 (*b*), Flp-In/TREx U373 MG-pp65 (*c*), and Flp-In/TREx U373 MG-pcDNA5/FRT/TO cells (*d*) were subjected to RT-PCR analysis. RNAs isolated from the cells harvested at the indicated time points were subjected to RT-PCR assays. TATA-binding protein (*TBP*) was used as an internal control. Total RNA was isolated from the cells treated with (+) or without (–) 3 µg/mL Dox and harvested after indicated

periods of Dox treatment. **B** Flp-In/TREx U373 MG-IE1 72 (lanes 1–4), Flp-In/TREx U373 MG-IE2 86 (lanes 5–8), Flp-In/TREx U373 MG-pp65 (lanes 13–16), and Flp-In/TREx U373 MG-pcDNA5/FRT/TO cells (lanes 9–12) were treated with (+) or without (–) 3 µg/mL doxycycline (Dox) and harvested after 2 days (2 *d*) and 4 days (4 *d*) post-induction by Dox treatment. Whole-cell lysates were prepared and used for immunoblot assays with the indicated antibodies. An anti-β-actin antibody was used to monitor general protein levels

immunofluorescence analysis (Fig. 4(B)). Both IE2 60 (Fig. 4(A-e)) and IE2 40 (Fig. 4(A-f)) clearly downregulated *SLITRK6* mRNA expression by RT-PCR assays. Immunoblot analyses also showed that IE2 60 (Fig. 4(A-k)) and IE2 40 (Fig. 4(A-l)) downregulate *SLITRK6* protein expression.

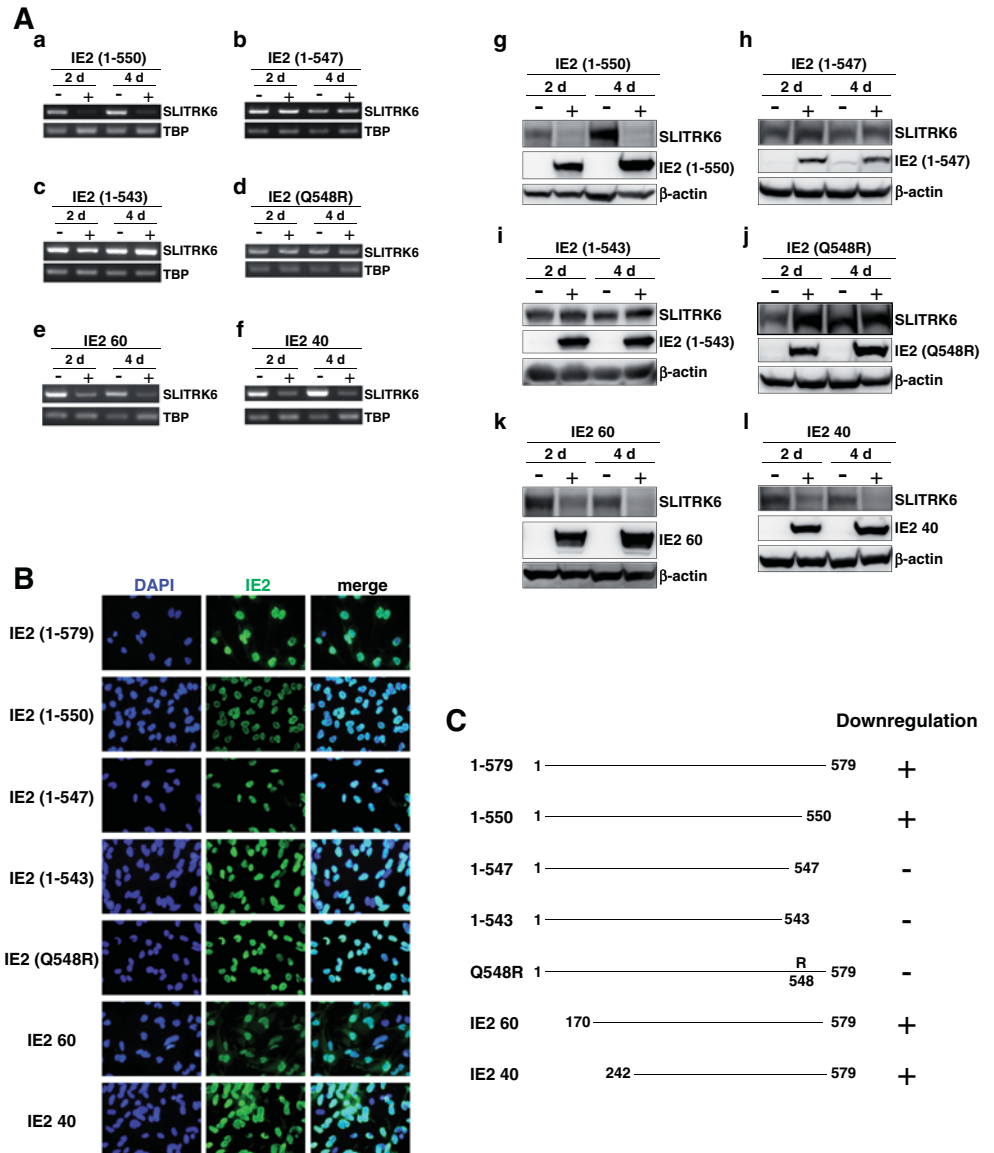
Discussion

In this study, we demonstrate that HCMV infection robustly downregulates the expression of *SLITRK6* in cultured neural cells such as SH-SY5Y, U373 MG, Hs 683, and NSPCs derived from iPSCs. HCMV-encoded IE2 86, IE2 60, and IE2 40 were shown responsible for this downregulation. Analyses of IE2 86 mutants showed that the carboxy-terminal region, especially Gln⁵⁴⁸, has a critical role in the *SLITRK6* downregulation. The Gln⁵⁴⁸ residue of IE2 has been shown to have a critical role in its association with p150, a component of chromatin assembly factor 1 (Lee et al. 2011). It is therefore speculated that similar association of IE2 with other cellular proteins via

Gln⁵⁴⁸ may be involved in the IE2-mediated *SLITRK6* downregulation.

Human *SLITRK6* encodes a type I transmembrane protein highly expressed in the brain of first-trimester human fetuses (Iruretagoyena et al. 2014). Homozygous nonsense mutations of *SLITRK6* were identified in Amish, Turkish, and Greek cases of familial myopia and SNHL (Tekin et al. 2013) and in nine cases of progressive auditory neuropathy in an endogamous Amish community (Morlet et al. 2014). In mice, *Slitrk6* expression is detected in the thalamus, lateral geniculate nucleus, and developing cochlear organs (Aruga 2003; Aruga and Mikoshiba 2003; Beaubien and Cloutier 2009; Katayama et al. 2009), and *Slitrk6* knock-out mice showed SNHL (Matsumoto et al. 2011). In *Slitrk6* knock-out mice, cell death in the spiral and vestibular ganglia was observed and innervation and survival of inner ear sensory neurons were disturbed (Katayama et al. 2009). *Slitrk6* is thus considered to play critical roles in auditory and vestibular functions, and suppression of its expression in the developing nervous system is expected to cause serious defects in the auditory and nervous systems.

Fig. 4 Carboxy-terminal region of IE2 86 is required for the *SLITRK6* downregulation. **A** RT-PCR analysis of the *SLITRK6* mRNA expression in Flp-In/TREx U373 MG cells expressing IE2 (1–550) (a), IE2 (1–547) (b), IE2 (1–543) (c), IE2 (Q548R) (d), IE2 60 (e), and IE2 40 (f). Immunoblot analysis of the *SLITRK6* protein expression in Flp-In/TREx U373 MG cells expressing IE2 (1–550) (g), IE2 (1–547) (h), IE2 (1–543) (i), IE2 (Q548R) (j), IE2 60 (k), and IE2 40 (l). Individual IE2 mutants were detected anti-IE2 antibody. **B** IE2 deletion mutant proteins induced by Dox in Flp-In/TREx U373 MG cells were detected by immunofluorescence analysis with anti-IE2 antibody. Nuclei were stained by DAPI. **C** Schematic diagram of IE2 86 and its deletion mutants, IE2 60, and IE2 40 and summary of the downregulation of *SLITRK6* expression by IE2 86 and its derivatives



The exact mechanism of HCMV neuropathogenesis including SNHL is not known. Although histological studies of patients with congenital HCMV infection have detected viral proteins in various parts of the nervous system, including the inner ear (Davis et al. 1981; Gabrielli et al. 2012, 2013; Stagno et al. 1977; Teissier et al. 2011), the exact nature and outcome of HCMV infection in the neural tissues remain largely unknown. The results obtained in this study imply that the downregulation of *SLITRK6* expression by HCMV-encoded IE2 may have some role in neurological dysfunctions, especially SNHL, induced by congenital HCMV infection. Abortive HCMV infection of neural cells at their critical period of development may result in the expression of a limited number of HCMV genes including *IE2* and eventually induce a serious dysfunction of the auditory system through downregulation of *SLITRK6*. It should be noted that children with homozygous *SLITRK6* mutation, *Slitrk6* knock-out mice,

and children with congenital HCMV infection exhibit not only SNHL but also other neurological problems in common, such as vestibular symptoms and behavioral problems, implying that the *SLITRK6* downregulation plays an important role in these conditions. Further investigation into the effect of the HCMV-induced downregulation of *SLITRK6* expression on the development of the nervous system may give a new insight into the neuropathogenesis of congenital HCMV infection.

Acknowledgments We thank M. Iikura for the excellent technical assistance. We also thank N. Inoue for providing the reagents.

This work was partly supported by Grants-in-Aid for Scientific Research from the Ministry of Education, Culture, Sports, Science and Technology of Japan (24591616) to H.N., the Ministry of Health, Labour and Welfare of Japan (H23-Jisedai-Ippan-001) to H.N., and the Grants of National Center for Child Health and Development (24-17 and 27-18 to H.N., 25-9 to S.F.).

Compliance with ethical standards

Conflict of interest The authors declare that they have no conflict of interest.

References

- Aruga J (2003) Slitrk6 expression profile in the mouse embryo and its relationship to that of Nlrr3. *Gene Expr Patterns* 3:727–733
- Aruga J, Mikoshiba K (2003) Identification and characterization of Slitrk, a novel neuronal transmembrane protein family controlling neurite outgrowth. *Mol Cell Neurosci* 24:117–129
- Beaubien F, Cloutier JF (2009) Differential expression of Slitrk family members in the mouse nervous system. *Dev Dyn* 238:3285–3296
- Bernard S, Wiener-Vacher S, Van Den Abbeele T, Teissier N (2015) Vestibular disorders in children with congenital cytomegalovirus infection. *Pediatrics* 136:e887–e895
- Cheeran MC, Lokensgard JR, Schleiss MR (2009) Neuropathogenesis of congenital cytomegalovirus infection: disease mechanisms and prospects for intervention. *Clin Microbiol Rev* 22:99–126 Table of Contents
- Davis LE, Johnsson LG, Kornfeld M (1981) Cytomegalovirus labyrinthitis in an infant: morphological, virological, and immunofluorescent studies. *J Neuropathol Exp Neurol* 40:9–19
- Fowler KB, Boppana SB (2006) Congenital cytomegalovirus (CMV) infection and hearing deficit. *J Clin Virol* 35:226–231
- Gabrielli L, Bonasoni MP, Santini D, Piccirilli G, Chiereghin A, Guerra B, Landini MP, Capretti MG, Lanari M, Lazzarotto T (2013) Human fetal inner ear involvement in congenital cytomegalovirus infection. *Acta Neuropathol Commun* 1:63
- Gabrielli L, Bonasoni MP, Santini D, Piccirilli G, Chiereghin A, Petrisli E, Dolcetti R, Guerra B, Piccioli M, Lanari M, Landini MP, Lazzarotto T (2012) Congenital cytomegalovirus infection: patterns of fetal brain damage. *Clin Microbiol Infect* 18:E419–E427
- Iruetagoiena JI, Davis W, Bird C, Olsen J, Radue R, Teo Broman A, Kendziorski C, Splinter BonDurant S, Golos T, Bird I, Shah D (2014) Differential changes in gene expression in human brain during late first trimester and early second trimester of pregnancy. *Prenat Diagn* 34:431–437
- Karlton E, Lofkvist U, Lewensohn-Fuchs I, Lindstrom K, Westblad ME, Fahnehjelm KT, Verrecchia L, Engman ML (2014) Impaired balance and neurodevelopmental disabilities among children with congenital cytomegalovirus infection. *Acta Paediatr* 103:1165–1173
- Katayama K, Zine A, Ota M, Matsumoto Y, Inoue T, Fritsch B, Aruga J (2009) Disorganized innervation and neuronal loss in the inner ear of Slitrk6-deficient mice. *PLoS One* 4:e7786
- Koyano S, Inoue N, Oka A, Moriuchi H, Asano K, Ito Y, Yamada H, Yoshikawa T, Suzutani T (2011) Screening for congenital cytomegalovirus infection using newborn urine samples collected on filter paper: feasibility and outcomes from a multicentre study. *BMJ Open* 1:e000118
- Lee SB, Lee CF, Ou DS, Dulal K, Chang LH, Ma CH, Huang CF, Zhu H, Lin YS, Juan LJ (2011) Host-viral effects of chromatin assembly factor 1 interaction with HCMV IE2. *Cell Res* 21:1230–1247
- Matsumoto Y, Katayama K, Okamoto T, Yamada K, Takashima N, Nagao S, Aruga J (2011) Impaired auditory-vestibular functions and behavioral abnormalities of Slitrk6-deficient mice. *PLoS One* 6:e16497
- Mitchell KJ (2011) The genetics of neurodevelopmental disease. *Curr Opin Neurobiol* 21:197–203
- Morlet T, Rabinowitz MR, Looney LR, Riegner T, Greenwood LA, Sherman EA, Achilly N, Zhu A, Yoo E, O'Reilly RC, Jinks RN, Puffenberger EG, Heaps A, Morton H, Strauss KA (2014) A homozygous SLITRK6 nonsense mutation is associated with progressive auditory neuropathy in humans. *Laryngoscope* 124:E95–103
- Morton CC, Nance WE (2006) Newborn hearing screening—a silent revolution. *N Engl J Med* 354:2151–2164
- Nakamura H, Liao H, Minami K, Toyoda M, Akutsu H, Miyagawa Y, Okita H, Kiyokawa N, Umezawa A, Imadome K, Inoue N, Fujiwara S (2013) Human cytomegalovirus induces apoptosis in neural stem/progenitor cells derived from induced pluripotent stem cells by generating mitochondrial dysfunction and endoplasmic reticulum stress. *Herpesviridae* 4:2
- Nakamura H, Lu M, Gwack Y, Souvlis J, Zeichner SL, Jung JU (2003) Global changes in Kaposi's sarcoma-associated virus gene expression patterns following expression of a tetracycline-inducible Rta transactivator. *J Virol* 77:4205–4220
- Omoy A, Diav-Citrin O (2006) Fetal effects of primary and secondary cytomegalovirus infection in pregnancy. *Reprod Toxicol* 21:399–409
- Petrik DT, Schmitt KP, Stinski MF (2006) Inhibition of cellular DNA synthesis by the human cytomegalovirus IE86 protein is necessary for efficient virus replication. *J Virol* 80:3872–3883
- Plachter B, Britt W, Vornhagen R, Stamminger T, Jahn G (1993) Analysis of proteins encoded by IE regions 1 and 2 of human cytomegalovirus using monoclonal antibodies generated against recombinant antigens. *Virology* 193:642–652
- Puchtler E, Stamminger T (1991) An inducible promoter mediates abundant expression from the immediate-early 2 gene region of human cytomegalovirus at late times after infection. *J Virol* 65:6301–6306
- Stagno S, Reynolds DW, Amos CS, Dahle AJ, McCollister FP, Mohindra I, Ermocilla R, Alford CA (1977) Auditory and visual defects resulting from symptomatic and subclinical congenital cytomegaloviral and toxoplasma infections. *Pediatrics* 59:669–678
- Stenberg RM, Depto AS, Fortney J, Nelson JA (1989) Regulated expression of early and late RNAs and proteins from the human cytomegalovirus immediate-early gene region. *J Virol* 63:2699–2708
- Teissier N, Delezoide AL, Mas AE, Chung-Savatovsky S, Bessieres B, Nardelli J, Vauloup-Fellous C, Picone O, Houhou N, Oury JF, Van Den Abbeele T, Gressens P, Adle-Biassette H (2011) Inner ear lesions in congenital cytomegalovirus infection of human fetuses. *Acta Neuropathol* 122:763–774
- Tekin M, Chioza BA, Matsumoto Y, Diaz-Horta O, Cross HE, Duman D, Kokotas H, Moore-Barton HL, Sakoori K, Ota M, Odaka YS, Foster J 2nd, Cengiz FB, Tokgoz-Yilmaz S, Tekeli O, Grigoriadou M, Petersen MB, Sreekantan-Nair A, Gurtz K, Xia XJ, Pandya A, Patton MA, Young JI, Aruga J, Crosby AH (2013) SLITRK6 mutations cause myopia and deafness in humans and mice. *J Clin Invest* 123:2094–2102

Novel Nonsense Mutation in the *NLRP7* Gene Associated with Recurrent Hydatidiform Mole

Yuki Ito^{a,c} Kayoko Maehara^a Eisuke Kaneki^d Kentaro Matsuoka^b
Naoko Sugahara^a Tomoko Miyata^a Hiromi Kamura^a Yuko Yamaguchi^a
Ayako Kono^a Kazuhiko Nakabayashi^a Ohsuke Migita^a Ken Higashimoto^e
Hidenobu Soejima^e Aikou Okamoto^c Hitomi Nakamura^f Tadashi Kimura^f
Norio Wake^d Takeshi Taniguchi^g Kenichiro Hata^a

^aDepartment of Maternal-Fetal Biology, National Research Institute for Child Health and Development, ^bDepartment of Pathology, National Center for Child Health and Development, and ^cDepartment of Obstetrics and Gynecology, The Jikei University School of Medicine, Tokyo, ^dDepartment of Obstetrics and Gynecology, Graduate School of Medical Science, Kyushu University, Fukuoka, ^eDivision of Molecular Genetics and Epigenetics, Department of Biomolecular Sciences, Faculty of Medicine, Saga University, Saga, ^fDepartment of Obstetrics and Gynecology, Osaka University Graduate School of Medicine, and ^gTaniguchi Hospital, Osaka, Japan

Key Words

Recurrent hydatidiform mole · DNA methylation · *NLRP7* · Genomic imprinting

Abstract

Aim: This study aimed to clarify the genetic and epigenetic features of recurrent hydatidiform mole (RHM) in Japanese patients. **Methods:** Four Japanese isolated RHM cases were analyzed using whole-exome sequencing. Villi from RHMs were collected by laser microdissection for genotyping and DNA methylation assay of differentially methylated regions (DMRs). Single nucleotide polymorphisms of *PEG3* and *H19* DMRs were used to confirm the parental origin of the variants. **Results:** A novel homozygous nonsense mutation in *NLRP7* (c.584G>A; p.W195X) was identified in 1 patient. Ge-

notyping of one of her molar tissue revealed that it was biparental but not androgenetic in origin. Despite the fact that the RHM is biparental, maternally methylated DMRs of *PEG3*, *SNRPN* and *PEG10* showed complete loss of DNA methylation. A paternally methylated DMR of *H19* retained normal methylation. **Conclusions:** This is the first Japanese case of RHM with a novel homozygous nonsense *NLRP7* mutation and a specific loss of maternal DNA methylation of DMRs. Notably, the mutation was identified in an isolated case of an ethnic background that has not previously been studied in this context. Our data underscore the involvement of *NLRP7* in RHM pathophysiology and confirm that DNA methylation of specific regions is critical. © 2015 S. Karger AG, Basel

Y. Ito and K. Maehara contributed equally to this work.

KARGER 125

© 2015 S. Karger AG, Basel
0378-7346/15/0000-0000\$39.50/0

E-Mail karger@karger.com
www.karger.com/goi

Kenichiro Hata, MD, PhD
Director, Department of Maternal-Fetal Biology
National Research Institute for Child Health and Development
2-10-1 Setagaya-ku, Tokyo 157-8535 (Japan)
E-Mail hata-k@ncchd.go.jp

Introduction

Complete hydatidiform mole (CHM) is an abnormal pregnancy that typically arises from an androgenote (diploid conception without maternal chromosomes) and predominantly gives rise to the development of only trophoblastic tissues [1, 2]. Recent studies of rare familial cases with recurrent molar pregnancies have shown that mutations of *NLRP7* and *KHDC3L* (*C6orf221*) are associated with recurrent hydatidiform moles (RHMs) [3, 4]. However, more than 20% of RHM cases have no mutations in these genes [5], and the mechanism underlying the occurrence of molar pregnancy associated with *NLRP7* and *KHDC3L* (*C6orf221*) mutation remains unknown. To clarify the genetic etiology of RHMs, further comprehensive genetic screening in various ethnic backgrounds is important.

In Japan, the incidence of CHM has become as low as that in western countries. The incidence of CHM per 1,000 live births was 0.49 in 2,000, with a recurrence rate of 1.3% [6, 7]. Nonetheless, a genetic and epigenetic analysis of RHM in Japan has not been performed previously.

CHM conceptions exhibit abnormal genomic imprinting. Although some villi of RHM possess normal biparental alleles, they exhibit loss of maternal DNA methylation of differentially methylated regions (DMRs) within imprinted loci, and thus have aberrant genomic imprinting [8, 9]. Because the histopathological findings of diploid biparental RHM are identical to those of diploid androgenetic CHM, diploid biparental RHM cannot be distinguished from typical CHM without a genetic and epigenetic diagnosis. To clarify the molecular mechanisms of RHM, we performed comprehensive genetic and epigenetic analyses of isolated Japanese RHM cases and in doing so, we identified a novel nonsense *NLRP7* mutation. The RHM tissue contained biparental alleles and showed a loss of maternal DNA methylation of imprinted genes. This evidence strongly supports the role for *NLRP7* in maternal DNA methylation of imprinted genes and the involvement of *NLRP7* in RHM.

Materials and Methods

Study Participants and Samples

Patients with RHM (n = 5) and CHM (n = 9) were included in this study. The profiles of the 5 RHM patients are shown in table 1. Each sample was histopathologically diagnosed as CHM or partial hydatidiform mole and previously genetically diagnosed as an androgenote or a triploid, with the exception of Patients 1, 2, 4 and 5 [10]. All the villi of the 9 CHM conceptions were androgenote. None of the CHM patients had a family history of the condition. Genomic DNA was extracted from peripheral blood cells and mo-

Table 1. Profiles of 5 patients with RHM

Patient ID	Pathological diagnosis	Genetic diagnosis	Familial history
1	5 CHM	This study	No
2	2 CHM	No samples	No
3	PHM, NP, SA, CHM	Triploid ¹	No
4	CHM, PHM	No samples	No
5	SA, PHM, NP, PHM	No samples	No

PHM = Partial hydatidiform mole; NP = normal pregnancy; SA = spontaneous abortion.

¹ Genetic diagnosis of the first molar pregnancy (PHM).

lar tissues. This study was approved by the Institutional Review Board Committee at the National Center for Child Health and Development, Tokyo, Japan (approval number 234), and written informed consent was obtained from all patients.

Whole-Exome Sequencing

The whole-exome library was prepared from the peripheral blood cells of 4 RHM patients (Patients 1–4 in table 1) by using Agilent SureSelect Human All Exon V3 capture reagent (Agilent Technologies, Inc., Santa Clara, Calif., USA), and sequenced using the Illumina HiSeq1000 platform. Data analysis procedures are described in the online supplementary materials and methods (for all online suppl. material, see www.karger.com/doi/10.1159/000441780).

NLRP7 Mutation Analysis

The mutations were confirmed by direct sequencing [11]. Ten coding exons and 1 non-coding exon of *NLRP7* were amplified using primers and PCR conditions that were previously described [12].

Genotyping of Molar Tissue

The molar tissue of Patient 1 was genotyped. The villi were selectively laser microdissected using an LMD7000 (Leica Microsystems GmbH, Wetzlar, Germany), and genomic DNA was extracted using the QIAamp DNA FFPE Tissue Kit (Qiagen, Hilden, Germany). The refSNP(rs) numbers of the 8 genotyped loci are shown in online supplementary table S1.

DNA Methylation Assay

The villi of a CHM from a patient with RHM (Patient 1), an androgenetic CHM and normal placenta were examined for *PEG3*, *SNRPN*, *PEG10* and *H19* gene methylation by bisulfite sequencing [13]. Bisulfite conversion was performed using the EpiTect Bisulfite kit (Qiagen, Hilden, Germany) with primers listed in online supplementary table S2.

Results

RHM is most likely caused by genetic factors, and 2 candidate genes have been previously reported [3, 4]. To search for additional mutations in genes that have not

Table 2. SNVs detected by whole-exome sequencing

Chromosome ¹	Position	Gene	Location	SNV	Protein alteration	RefSNP	Allele frequency in HGVB	Patient 1	Patient 2	Patient 3	Patient 4
1	52828383	<i>CC2D1B</i> ¹	Exon 3	c.G105A	p.M35I	rs183845075	0.02	G/G	G/G	G/G	A/A
3	10452493	<i>ATP2B2</i> ¹	Exon 3	c.C206T	p.P69L	N/A	N/A	T/T	C/C	C/C	C/C
3	16254129	<i>GALNT15</i> ¹	Exon 6	c.C1251A	p.H417Q	rs185944497	0.008	A/A	C/C	C/C	C/C
9	140007466	<i>DPP7</i> ¹	Exon 7	c.C809T	p.A270V	rs181036640	0.013	T/T	C/C	C/C	C/C
11	69063476	<i>MYEOV</i> ¹	Exon 3	c.C559T	p.R187W	rs116926312	0.044	C/C	C/C	C/C	T/T
13	41835028	<i>MTRF1</i> ¹	Exon 2	c.T16C	p.C6R	N/A	0.009	T/T	C/C	T/T	T/T
16	30735148	<i>SRCAP</i> ¹	Exon 25	c.C4403T	p.S1468L	rs75035256	0.019	T/T	C/T	C/C	C/C
17	27030713	<i>PROCA1</i> ¹	Exon 4	c.G874A	p.E292K	rs3744637	0.043	C/C	C/C	C/C	A/A
19	55451603	<i>NLRP7</i>	Exon 4	c.G584A	p.W195X	N/A	N/A	A/A	G/G	G/G	G/G
21	38439597	<i>PIGP</i> ¹	Exon 4	c.G239A	p.S80N	rs114319840	0.004	A/A	G/G	G/G	G/G

HGVB = Human Genetic Variation Browser; N/A = not available.

¹ Except for *NLRP7*, the 10 SNVs detected have no particular reported/predicted pathogenic features in the reproduction system.

Table 3. Summary of the SNVs found in *ZFP57*, *NLRP7* and *NLRP2* in 4 patients with RHM by whole-exome sequencing

Chromosome	Position	Gene	Location	SNV	Protein	RefSNP	Patient 1	Patient 2	Patient 3	Patient 4
6	29644668	<i>ZFP57</i>	Exon 14	c.G113>A	p.R38Q	rs142917604	G/G	G/G	G/A	A/A
19	55441902	<i>NLRP7</i>	Exon 9	c.A2775>G	p.A925A	rs269950	G/G	G/G	G/G	A/G
19	55441995	<i>NLRP7</i>	Exon 9	c.T2682>C	p.Y894Y	rs269951	G/G	G/G	G/G	A/G
19	55451050	<i>NLRP7</i>	Exon 4	c.G1137>A	p.K379K	rs10418277	A/A	G/G	G/G	G/G
19	55451232	<i>NLRP7</i>	Exon 4	c.G955>A	p.V319I	rs775882	A/A	G/G	G/G	G/G
19	55451603	<i>NLRP7</i>	Exon 4	c.G584>A	p.W195X	N/A	A/A	G/G	G/G	G/G
19	55451797	<i>NLRP7</i>	Exon 4	c.G390>A	p.Q130Q	rs775883	A/A	G/G	G/G	G/G
19	55485899	<i>NLRP2</i>	Exon 4	c.G312>A	p.K104K	rs2217659	G/G	A/A	G/G	A/A
19	55494881	<i>NLRP2</i>	Exon 7	c.C1815>G	p.L605L	rs11672113	G/G	C/C	G/G	C/C
19	55512137	<i>NLRP2</i>	Exon 14	c.C3060>A	p.I1020I	rs12768	A/A	C/A	A/A	A/A
19	55512232	<i>NLRP2</i>	Exon 14	c.C3155>A	p.A1052E	rs1043673	C/C	C/C	A/A	C/C

N/A = Not available.

¹ A novel homozygous nonsense mutation of *NLRP7* (c.584G>A; p.W195X) was found in Patient 1. Other SNVs are all commonly known SNPs with RefSNP(rs) numbers.

been previously associated with RHM, we performed whole-exome sequencing using peripheral blood cells from 4 RHM patients (Patients 1–4 in table 1). Quality filtering in the patients resulted in a set of 176,663 single nucleotide variations (SNVs) in coding regions. We excluded all non-coding SNVs and SNVs with more than 5% frequency in the 1000 Genomes database (<http://www.1000genomes.org/>, May 5, 2013) or the Human Genetic Variation Browser (<http://www.genome.med.kyoto-u.ac.jp/SnpDB/>). The remaining 10 SNVs (table 2) contained no particular potential pathogenic genes involved in the reproduction process except for an *NLRP7* mutation, as described later.

Next, we focused on *NLRP7*, *NLRP2*, *ZFP57* and *KHDC3L* (*C6orf221*), which were previously reported as candidate genes for RHM or were associated with DNA methylation defects [3, 4, 14, 15]. Based on the minor allele frequency information of the 1000 Genomes database and other reports [3, 5, 9, 12, 16], the homozygous nonsense mutation of *NLRP7* (c.584G>A; p.W195X) identified in Patient 1 is considered a mutation, which was not previously reported (table 3). Other SNVs found in *ZFP57*, *NLRP7* and *NLRP2* are common variants. Sanger sequencing of genomic DNA from 5 RHM patients (Patients 1–5 in table 1), 9 patients with typical androgenetic CHM and 86 controls confirmed that the *NLRP7* muta-

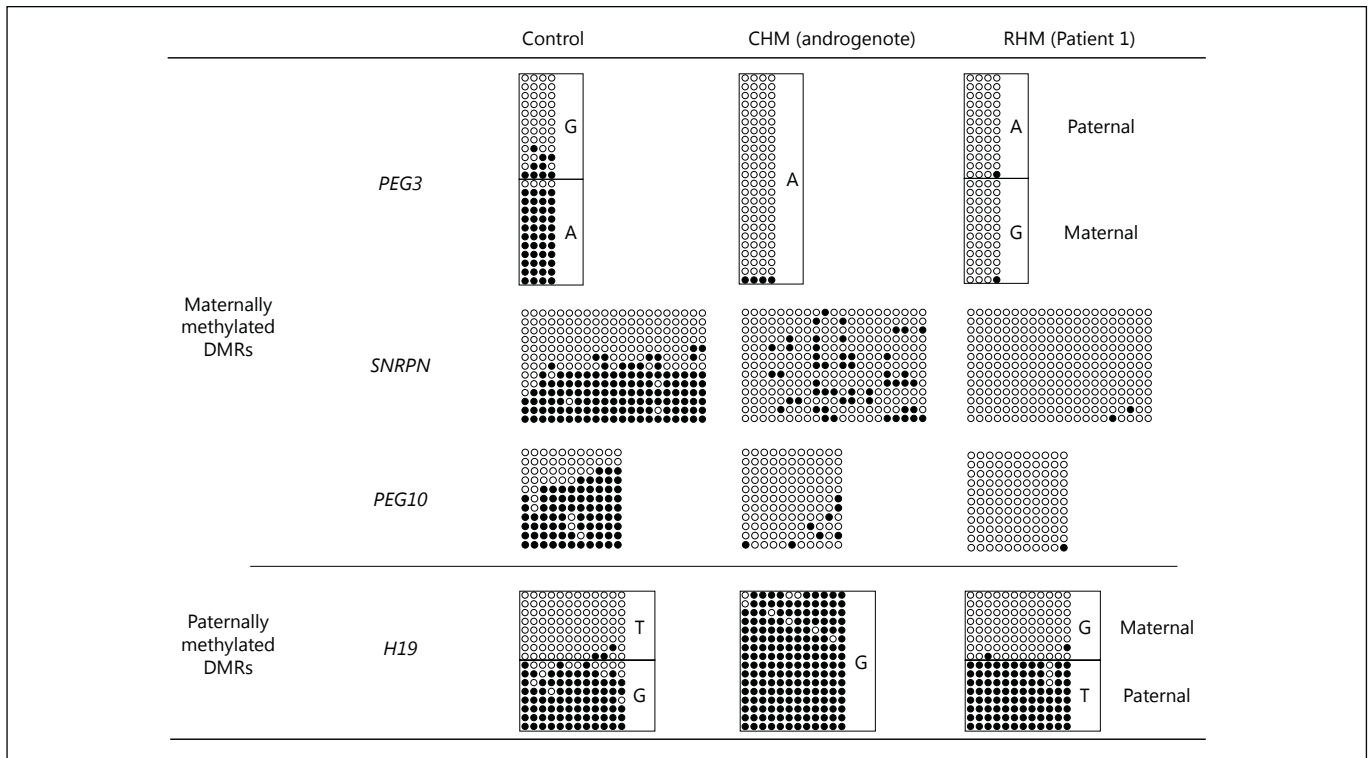


Fig. 1. DNA methylation assay of DMRs. Bisulfite sequencing was performed for 3 maternal DMRs (*PEG3*, *SNRPN* and *PEG10*) and 1 paternal DMR (*H19*). Each line indicates a single clone, and each circle denotes a CpG; filled and open circles represent methylated and unmethylated cytosine residues, respectively. Allele-specific methylation was definitively diagnosed by SNPs in *PEG3*

and *H19* DMRs. All maternally methylated DMRs (*PEG3*, *SNRPN* and *PEG10*) showed loss of DNA methylation in the villi of RHM (Patient 1). In contrast, paternal methylation of the *H19* DMR was maintained normally, even in the villi of RHM. Methylation defects were observed only in maternally methylated DMRs.

tion (c.584G>A; p.W195X) was observed only in 1 RHM (Patient 1; online suppl. table S3, fig. S1).

Previous reports have shown that the origin of a subset of RHM is not androgenic but biparental [12–14]. To precisely confirm the genotype of the villi of RHM Patient 1, the villi were selectively collected by laser microdissection, and a small amount of genomic DNA was obtained. Since the extracted DNA was fragmented and of low quality, analysis of polymorphic DNA markers was inconclusive. We then performed a comprehensive SNP analysis of the biological parents to confirm the origin of the villi of RHM Patient 1. Eight loci in which each parent (Patient 1 and her husband) possesses the opposite major or minor homozygous allele were genotyped, and all showed heterozygous genotypes in the villi (online suppl. table S1). These results clearly show that the villi of RHM Patient 1 contain both parental alleles and thus it is not androgenic, but biparental.

To clarify epigenetic abnormalities in the villi of Patient 1 RHM, DNA methylation analysis of DMRs of imprinted genes was performed using bisulfite sequencing

(fig. 1). Three maternally methylated DMRs in *PEG3*, *SNRPN* and *PEG10* and a paternally methylated DMR in *H19* were analyzed. SNPs of *PEG3* and *H19* were used to distinguish between paternal and maternal alleles, enabling specific estimations of allele-specific DNA methylation defects of DMRs. The villi of RHM Patient 1 showed a loss of methylation in all the analyzed maternal DMRs and retained completely normal methylation in the paternal DMR.

Discussion

It is currently not possible to distinguish diploid biparental RHM from typical diploid androgenetic CHM with conventional pathological criteria. In fact, the RHM of Patient 1 and control CHM are histopathologically identical and were both p57KIP2-negative upon immunohistochemical analysis (online suppl. fig. S2). Though striking features of RHM are being revealed with genetic and epi-

genetic analyses [3, 8, 17–19], there is no clear mechanistic understanding as to why certain candidate genes are associated with the condition. Furthermore, no candidate genes have been identified in approximately 20% of all cases [5]. Thus, there is a clear need to explore genetic mutations and epigenetic aberrations in different genetic backgrounds. Additionally, whole-exome sequencing is a potentially promising approach to identifying unknown genetic factors [20]; however, to our knowledge, this is the first report of whole-exome sequencing in RHM patients.

To clarify the features of these Japanese isolated RHM cases, we performed comprehensive genetic and epigenetic analyses. We successfully detected a novel pathogenic homozygous nonsense *NLRP7* mutation (c.584G>A; p.W195X). Since we could not obtain genomic DNA to confirm the mutation in the parents of Patient 1, the parental origin of the mutation is unknown. The approximate 1-Mb region around the *NLRP7* mutation (c.584G>A) shows copy neutral loss of heterozygosity (data not shown). Although the parents of the Patient 1 do not appear to be consanguineous, we speculate that the *NLRP7* region of Patient 1 most likely has alleles identical by descent.

The examination of DNA methylation abnormalities is indispensable for a definitive diagnosis of epigenetic mutations specifically observed in diploid biparental RHMs. In this study, the parental origin of the *PEG3* and *H19* DMRs were definitively confirmed by SNP analysis. The villi of RHM Patient 1 clearly showed complete loss of DNA methylation of maternally methylated DMRs (*PEG3*, *SNRPN* and *PEG10*) but retained methylation of a paternally methylated DMR (*H19*). Although the villi of the RHM were genetically normal, they showed abnormal DNA methylation and their DNA methylation profile was quite similar to that in a typical androgenetic CHM. This is in contrast to previous studies, in which patterns including hypermethylation of *H19* DMR [21] and retention of methylation at *PEG10* DMR were observed [12]. These differences are likely due to the multifactorial nature in which the DNA methylation machinery is regulated; this would account for the variable methylation changes within DMRs, as we previously reported in our study of *Dnmt3L* knockout mice [22].

RHM patients with *NLRP7* mutations are most likely to have failed in the establishment of methylation of maternal DMRs during oogenesis. The p.W195X mutation in Patient 1 is located upstream of the known nonsense mutations in RHM patients [5]. It is, therefore, expected that RHM from Patient 1 would exhibit the typical phenotype, and indeed this patient had 5 molar pregnancies. Some reported missense mutations could be hypomorph-

ic and show stochastic effects on the methylation of DMRs [9, 12]. If DMR methylation defects are partial, they may cause ordinary abortion or may be sufficiently mild so as to allow normal pregnancy rather than cause molar pregnancy [21]. In fact, patients with *NLRP7* missense mutations have a mixed reproductive history of molar pregnancy and abortion or normal pregnancy [23]. Thus, some unexplained cases of infertility might be attributed to such stochastic epigenetic aberrations.

The NLR family proteins have roles in inflammation and apoptosis [24]. *NLRP7* is involved in the secretion of IL-1 β [25–27], but there is no direct evidence that perturbations to the *NLRP7*-IL-1 β axis cause loss of DNA methylation and molar pregnancy. Since *NLRP7* is present in oocytes [16] and preimplantation embryos [28], it could be involved in the hypomethylation of DMRs observed in the villi of RHMs. However, because *NLRP7* has no ortholog in mice [24], evaluation of its function in oogenesis and early embryogenesis is challenging. Therefore, identification of genetic and/or epigenetic mutations in isolated cases and in different genetic backgrounds remains an important aspect of studies designed to unravel the mechanisms underlying RHM pathogenesis.

In conclusion, we have, for the first time, identified a novel nonsense homozygous mutation of *NLRP7* in a Japanese RHM patient. Our study is the first to report an isolated RHM case in a previously unreported ethnic background. This comprehensive genetic and epigenetic analysis approach can facilitate the definitive molecular diagnosis of diploid biparental RHM in isolated cases and can be performed using fragmented DNA extracted from formaldehyde-fixed and paraffin-embedded tissue samples. *NLRP7* mutations cause abnormal DNA methylation in DMRs [21]. However, the mechanisms underlying region-specific DNA methylation remain unknown. Further analysis of RHM will shed light on the unknown etiology of infertility and the mechanisms that control region-specific DNA methylation.

Acknowledgments

This research has been conducted using the National Central Biobank Network (NCBN), Japan.

Funding Sources

This study was supported by a grant from the Ministry of Health, Labor and Welfare, Japan (H26-082, H26-001, H25-001), the CREST Program of the Japan Science and Technology Agency (JST), a grant from the Ministry of Education, Culture, Sports, Sci-

ence and Technology (MEXT), Japan (grant numbers: 26670734, 26293365), and a grant from the National Center for Child Health and Development (NCCHD), Japan (26-13). The study sponsors had no involvement in study design, in the collection, analysis and interpretation of data, in the writing of the report and in the decision to submit the report for publication.

Disclosure Statement

None to declare.

References

- Kajii T, Ohama K: Androgenetic origin of hydatidiform mole. *Nature* 1977;268:633–634.
- Sánchez-Ferrer ML, Hernández-Martínez F, Machado-Linde F, Ferri B, Carbonel P, Nieto-Díaz A: Uterine rupture in twin pregnancy with normal fetus and complete hydatidiform mole. *Gynecol Obstet Invest* 2014;77:127–133.
- Murdoch S, Djuric U, Mazhar B, Seoud M, Khan R, Kuick R, Bagga R, Kircheisen R, Ao A, Ratti B, Hanash S, Rouleau GA, Slim R: Mutations in NALP7 cause recurrent hydatidiform moles and reproductive wastage in humans. *Nat Genet* 2006;38:300–302.
- Parry DA, Logan CV, Hayward BE, Shires M, Landolsi H, Diggle C, Carr I, Rittore C, Touitou I, Philibert L, Fisher RA, Fallahian M, Huntriss JD, Picton HM, Malik S, Taylor GR, Johnson CA, Bonthron DT, Sheridan EG: Mutations causing familial biparental hydatidiform mole implicate c6orf221 as a possible regulator of genomic imprinting in the human oocyte. *Am J Hum Genet* 2011;89:451–458.
- Nguyen NM, Slim R: Genetics and epigenetics of recurrent hydatidiform moles: basic science and genetic counselling. *Curr Obstet Gynecol Rep* 2014;3:55–64.
- Matsui H, Iitsuka Y, Suzuka K, Seki K, Sekiya S: Subsequent pregnancy outcome in patients with spontaneous resolution of HCG after evacuation of hydatidiform mole: comparison between complete and partial mole. *Hum Reprod* 2001;16:1274–1277.
- Matsui H, Iitsuka Y, Yamazawa K, Tanaka N, Seki K, Sekiya S: Changes in the incidence of molar pregnancies. A population-based study in Chiba prefecture and Japan between 1974 and 2000. *Hum Reprod* 2003;18:172–175.
- Judson H, Hayward BE, Sheridan E, Bonthron DT: A global disorder of imprinting in the human female germ line. *Nature* 2002;416:539–542.
- Kou YC, Shao L, Peng HH, Rosetta R, del Gaudio D, Wagner AF, Al-Hussaini TK, Van den Veyver IB: A recurrent intragenic genomic duplication, other novel mutations in NLRP7 and imprinting defects in recurrent biparental hydatidiform moles. *Mol Hum Reprod* 2008;14:33–40.
- Kaneki E, Kobayashi H, Hirakawa T, Matsuda T, Kato H, Wake N: Incidence of postmolar gestational trophoblastic disease in androgenetic moles and the morphological features associated with low risk postmolar gestational trophoblastic disease. *Cancer Sci* 2010;101:1717–1721.
- Li C, Qiao B, Zhan Y, Peng W, Chen ZJ, Sun L, Zhang J, Zhao L, Gao Q: Association between genetic variations in MTNR1A and MTNR1B genes and gestational diabetes mellitus in Han Chinese women. *Gynecol Obstet Invest* 2013;76:221–227.
- Hayward BE, De Vos M, Talati N, Abdollahi MR, Taylor GR, Meyer E, Williams D, Maher ER, Setna F, Nazir K, Hussaini S, Jafri H, Rashid Y, Sheridan E, Bonthron DT: Genetic and epigenetic analysis of recurrent hydatidiform mole. *Hum Mutat* 2009;30:E629–E639.
- Clark SJ, Harrison J, Paul CL, Frommer M: High sensitivity mapping of methylated cytosines. *Nucleic Acids Res* 1994;22:2990–2997.
- Meyer E, Lim D, Pasha S, Tee LJ, Rahman F, Yates JR, Woods CG, Reik W, Maher ER: Germline mutation in NLRP2 (NALP2) in a familial imprinting disorder (Beckwith-Wiedemann Syndrome). *PLoS Genet* 2009;5:e1000423.
- Li X, Ito M, Zhou F, Youngson N, Zuo X, Leder P, Ferguson-Smith AC: A maternal-zygotic effect gene, *zfp57*, maintains both maternal and paternal imprints. *Dev Cell* 2008;15:547–557.
- Wang CM, Dixon PH, Decordova S, Hodges MD, Sebire NJ, Ozalp S, Fallahian M, Sensi A, Ashrafi F, Repiska V, Zhao J, Xiang Y, Savage PM, Seckl MJ, Fisher RA: Identification of 13 novel NLRP7 mutations in 20 families with recurrent hydatidiform mole; missense mutations cluster in the leucine-rich region. *J Med Genet* 2009;46:569–575.
- Moglabey YB, Kircheisen R, Seoud M, El Mogharbel N, Van den Veyver I, Slim R: Genetic mapping of a maternal locus responsible for familial hydatidiform moles. *Hum Mol Genet* 1999;8:667–671.
- Helwani MN, Seoud M, Zahed L, Zaatari G, Khalil A, Slim R: A familial case of recurrent hydatidiform molar pregnancies with biparental genomic contribution. *Hum Genet* 1999;105:112–115.
- Fisher RA, Khatoon R, Paradinas FJ, Roberts AP, Newlands ES: Repetitive complete hydatidiform mole can be biparental in origin and either male or female. *Hum Reprod* 2000;15:594–598.
- Rabbani B, Tekin M, Mahdieh N: The promise of whole-exome sequencing in medical genetics. *J Hum Genet* 2014;59:5–15.
- El-Maarri O, Seoud M, Coullin P, Herbiniaux U, Oldenburg J, Rouleau G, Slim R: Maternal alleles acquiring paternal methylation patterns in biparental complete hydatidiform moles. *Hum Mol Genet* 2003;12:1405–1413.
- Henckel A, Nakabayashi K, Sanz LA, Feil R, Hata K, Arnaud P: Histone methylation is mechanistically linked to DNA methylation at imprinting control regions in mammals. *Hum Mol Genet* 2009;18:3375–3383.
- Deveault C, Qian JH, Chebaro W, Ao A, Gilbert L, Mehio A, Khan R, Tan SL, Wischmeijer A, Coullin P, Xie X, Slim R: NLRP7 mutations in women with diploid androgenetic and triploid moles: a proposed mechanism for mole formation. *Hum Mol Genet* 2009;18:888–897.
- Tian X, Pascal G, Monget P: Evolution and functional divergence of NLRP genes in mammalian reproductive systems. *BMC Evol Biol* 2009;9:202.
- Kinoshita T, Wang Y, Hasegawa M, Imamura R, Suda T: PYPAF3, a PYRIN-containing APAF-1-like protein, is a feedback regulator of caspase-1-dependent interleukin-1beta secretion. *J Biol Chem* 2005;280:21720–21725.
- Messaed C, Akoury E, Djuric U, Zeng J, Saleh M, Gilbert L, Seoud M, Qureshi S, Slim R: NLRP7, a nucleotide oligomerization domain-like receptor protein, is required for normal cytokine secretion and co-localizes with Golgi and the microtubule-organizing center. *J Biol Chem* 2011;286:43313–43323.
- Khare S, Dorfleutner A, Bryan NB, Yun C, Radian AD, de Almeida L, Rojanasakul Y, Stehlik C: An NLRP7-containing inflammasome mediates recognition of microbial lipopeptides in human macrophages. *Immunity* 2012;36:464–476.
- Zhang P, Dixon M, Zucchelli M, Hambiliki F, Levkov L, Hovatta O, Kere J: Expression analysis of the NLRP gene family suggests a role in human preimplantation development. *PLoS One* 2008;3:e2755.

Augmenting effects of gestational arsenite exposure of C3H mice on the hepatic tumors of the F₂ male offspring via the F₁ male offspring

Keiko Nohara^{a*}, Kazuyuki Okamura^a, Takehiro Suzuki^a, Hikari Murai^a, Takaaki Ito^b, Keiko Shinjo^c, Shota Takumi^d, Takehiro Michikawa^a, Yutaka Kondo^c and Kenichiro Hata^e

ABSTRACT: Gestational exposure can affect the F₂ generation through exposure of F₁ germline cells. Previous studies reported that arsenite exposure of only F₀ females during their pregnancy increases hepatic tumors in the F₁ males in C3H mice, whose males are predisposed spontaneously to develop hepatic tumors later in life. The present study addressed the effects of gestational arsenite exposure on tumorigenesis of the F₂ males in C3H mice. Expression analysis of several genes in the normal livers at 53 and 80 weeks of age clearly showed significant changes in the F₂ males obtained by crossing gestational arsenite-exposed F₁ (arsenite-F₁) males and females compared to the control F₂ males. Some of the changes were shown to occur in a late-onset manner. Then the tumor incidence was assessed at 75–82 weeks of age in the F₂ males obtained by reciprocal crossing between the control and arsenite-F₁ males and females. The results demonstrated that the F₂ males born to arsenite-F₁ males developed tumors at a significantly higher rate than the F₂ males born to the control F₁ males, irrespective of exposure of F₁ females. Gene expressions of hepatocellular carcinoma markers β -catenin (CTNNB1) and interleukin-1 receptor antagonist in the tumors were significantly upregulated in the F₂ males born to arsenite-F₁ males compared to those born to the control F₁ males. These results show that arsenite exposure of only F₀ pregnant mice causes late-onset changes and augments tumors in the livers of the F₂ males by affecting the F₁ male offspring. Copyright © 2015 John Wiley & Sons, Ltd.

Keywords: arsenic; gestational exposure; hepatic tumor; transgenerational; gene expression

Introduction

Gestation is known to be vulnerable to a variety of environmental conditions, including chemical exposure and nutritional imbalances, and the adverse effects of environmental conditions in this period can lead to a number of adult-onset diseases in the F₁ offspring and in subsequent multiple generations (Aiken and Ozanne, 2014; Guerrero-Bosagna and Skinner, 2012; Perera and Herbstman, 2011). A possible causative route of the effects on the F₂ and subsequent generations by gestational chemical exposure is through direct exposure of germline cells in the F₁ fetuses and the responsible germ cells can be those of male, female, or both (Aiken and Ozanne, 2014; Guerrero-Bosagna and Skinner, 2012; Perera and Herbstman, 2011).

Naturally occurring inorganic arsenic, which is known as a human carcinogen, is causing serious health problems, including cancer, in many areas in the world (Hughes *et al.*, 2011). Although animal models are pivotal to elucidate the mechanism of arsenic toxicity, it has been difficult to verify the carcinogenicity of arsenic in rodents (Rossman *et al.*, 2002). Pioneering studies by Waalkes and colleagues showed that exposure of pregnant C3H mice (F₀) from gestational day (GD) 8–18 to inorganic arsenite results in an increase in tumors in the liver and adrenal gland of their F₁ male offspring at 74 weeks of age (Waalkes *et al.*, 2003). As male C3H mice are predisposed to spontaneously develop hepatic tumors in adulthood (Köhle *et al.*, 2008; Maronpot *et al.*, 1995), the finding by Waalkes and colleagues supports the notion that arsenic acts in combination with other tumor promoting factors or dispositions

(Klein *et al.*, 2007). The results obtained by Waalkes *et al.* (2003) also indicate that gestation is a vulnerable period for arsenic carcinogenicity. Epidemiological studies have reported that gestational exposure to arsenite is associated with increased cancers in adulthood (Smith *et al.*, 2006; Yuan *et al.*, 2010). These findings on the sensitivity of gestational period against arsenic imply the possibility that gestational arsenic exposure may also affect F₁ germline cells and have an impact on late-onset tumorigenesis in the F₂ and subsequent generations, while those issues have not been addressed.

*Correspondence to: Keiko Nohara, Center for Environmental Health Sciences, National Institute for Environmental Studies, Tsukuba 305-8506, Japan.
E-mail: keikon@nies.go.jp

^aCenter for Environmental Health Sciences, National Institute for Environmental Studies, Tsukuba, Japan

^bDepartment of Pathology and Experimental Medicine, Kumamoto University Graduate School of Medical Sciences, Kumamoto, Japan

^cDepartment of Epigenomics, Nagoya City University Graduate School of Medical Sciences, Nagoya, Japan

^dDepartment of Public Health and Environmental Medicine, The Jikei University School of Medicine, Tokyo, Japan

^eDepartment of Maternal-Fetal Biology, National Research Institute for Child Health and Development, Tokyo, Japan

We previously investigated the causal factors of hepatic tumor augmentation in the F₁ male offspring by gestational arsenite exposure in the experimental model reported by Waalkes *et al.* (2003) Nohara *et al.*, 2012). The results showed several characteristic changes, such as late-onset gene expression changes in the normal livers and an increase in hepatic tumors, particularly those having a C to A somatic mutation at codon 61 in oncogene *Ha-ras*, in the F₁ offspring by gestational arsenite exposure (Nohara *et al.*, 2012). In the present study, we addressed the effects of gestational arsenite exposure on the F₂ males of C3H mice by investigating gene expression changes in the normal livers, the hepatic tumor incidence, and the incidence of *Ha-ras* mutation at codon 61 in the tumors. In the assessment of tumor incidence, we performed a reciprocal crossing experiment between the control and arsenite-F₁ males and females to clarify the F₁ sex responsible for the tumor augmentation in the F₂ males. We also measured gene expression of several human hepatocellular carcinoma markers in the tumors of the F₂ males for confirmation of the tumor augmenting effects of gestational arsenite exposure.

The results of the present study made the novel findings on the tumor augmenting effects of gestational arsenite exposure on the F₂ generation.

Materials and methods

Design of Animal Experiments

Pregnant C3H/HeN mice (F₀) were purchased from CLEA Japan (Tokyo, Japan) and given free access to a standard diet (CA-1; CLEA Japan) and tap water (control mice) or tap water containing 85 ppm sodium arsenite (Sigma, St. Louis, MO, USA) from day 8 to 18 of gestation as described previously (Nohara *et al.*, 2012). Throughout the experiments, arsenite was only given to F₀ pregnant mice and not to F₁ or F₂ mice. To assess the tumor incidence and the F₁ sex responsible for the F₂ tumor augmentation, we did a reciprocal crossing experiment among the control F₁ males and females and arsenite-F₁ males and females, which originated from 22 control F₀ females and 29 arsenite-F₀ females. Male and female mice were mated at 10 weeks of age. The resulting F₂ males were reared until 75–82 weeks (17.5–19 months) of age and used for the assessment. Hepatic tumors were examined macroscopically (Nohara *et al.*, 2012) and some were subjected to histological analysis as described below.

The animals were handled in accordance with the National Institute for Environmental Studies guidelines for animal experiments.

Histological Analysis

Sections prepared from paraffin-embedded liver tissues were stained with hematoxylin and eosin as previously described (Nohara *et al.*, 2012). The histology of the liver neoplasms was classified as hepatocellular adenoma or hepatocellular carcinoma. Briefly, hepatocellular adenoma is characterized by a well-circumscribed lesion composed of well-differentiated hepatocytes, and hepatocellular carcinoma is characterized by an abnormal growth pattern and both cytological and nuclear atypia (Harada *et al.*, 1999).

cDNA Preparation and Real-Time Polymerase Chain Reaction

Total RNA of individual livers was prepared with an RNeasy Mini Kit (Qiagen, Valencia, CA, USA). After checking the quality of the RNA by electrophoresis, reverse transcription reactions were performed with an AMV Reverse Transcriptase XL (TaKaRa Bio, Shiga, Japan) using 100 ng of total RNA. Quantitative real-time polymerase chain reaction (PCR) analysis was performed on a LightCycler 480 instrument, version 1.5 (Roche Diagnostics, Basel, Switzerland) as described previously (Nohara *et al.*, 2006). The primer sequences and annealing temperatures used for real-time PCR are shown in Table 1.

Ha-ras Mutation

Ha-ras mutations at codon 61 were analyzed by the pyrosequencing method (Ogino *et al.*, 2005). The DNA region containing the sequence coding codon 61 in the *Ha-ras* gene was amplified by PCR using the biotinylated primers (5'-cggaacaggtggtcattgat-3' and biotin-5'-tgatggcaatacacagaggaag-3') and a PyroMark PCR kit (Qiagen). Amplification was achieved by heating at 95 °C for 5 min, cycling at 95 °C for 30 s, 55 °C for 30 s and 72 °C for 45 s, and was followed by extension at 72 °C for 10 min after the final cycle. The biotinylated PCR product was captured on streptavidin-coated beads (GE Healthcare Bio-Science, Little Chalfont, UK), denatured and washed. The sequence primer for codon 61 (5'-ggacatcttagacacagca-3') was annealed to the biotinylated PCR product and pyrosequencing analysis was performed by using a

Table 1. Primers for real-time polymerase chain reaction analysis

Gene	Forward primer 5'-3'	Reverse primer 5'-3'	Annealing temp. (°C)
<i>Crel2</i>	gcagacagcagaaggcaaa	tgcccgtcacaatcctc	60
<i>Slc25a30</i>	gaacgcccagaagatgaaac	ctgttctgtgcttgattcg	60
<i>Eil3</i>	ccagaaacgcctggacaa	cttgaggctagaggcagagc	64
<i>Fabp4</i>	cagcctttctcacctggaag	ttgtggcaaagcccactc	60
<i>Gpat-1</i>	agcaagtctctgcgtatcat	ctcgtgtgggtgattgtgac	64
<i>Afp</i>	cccaaccttctgtctcagt	tggctctctgatgtgttt	64
<i>Il-1m</i>	tgcaacaactagaggctga	agtgatcaggcagttggtga	64
<i>Ctnnb1</i>	ccctgagacgctagatgagg	tgctcagctcaggaattgcac	64
<i>Cpb</i>	agactgttccaaaacagtgga	gatgctcttctcctgtgac	64
rRNA	tgccaatggctcattaatcagtt	ccgtcggcagctattagctctag	64

PyroMark Q96 ID system (Qiagen) and PyroMark Q96 ID Software 2.5 (Qiagen) according to the manufacturer's instructions.

Western Blotting

Tissues were homogenized in ice-cold lysis buffer (1% Triton X-100, 0.1% sodium dodecyl sulfate [SDS], 0.5% deoxycholic acid, 1 mM EDTA, 1 mM EGTA, 2.5 mM sodium pyrophosphate, 1 mM β -glycerophosphate, 1 mM sodium orthovanadate, 1 mM phenylmethylsulfonyl fluoride, 50 mM Tris-HCl [pH 7.5] and 150 mM NaCl) with a pellet mixer and then with a Bioruptor UCD-200TM (Cosmo Bio, Tokyo, Japan). The supernatant was boiled with the same volume of $\times 2$ SDS sample buffer (100 mM Tris-HCl [pH 6.8], 4% SDS, 20% glycerol, 200 mM DTT, 0.002% bromophenol blue), and subjected to SDS-polyacrylamide gel electrophoresis. The first antibodies used were anti-p44/42 MAPK (Cell Signaling Technology, Danvers, MA, USA; 9102), anti-phospho-p44/42 MAPK (Cell Signaling Technology; 9101) and anti- β -actin (Sigma; A5441). The second antibodies were horseradish peroxidase-conjugated anti-rabbit IgG (Sigma) and antimouse IgG (Sigma). The membranes were developed using the ECL Prime Western Blotting Detection System (GE Healthcare) and the images were captured using a VersaDoc imaging system (Bio Rad, Hercules, CA, USA).

Statistical Analysis

The difference in the tumor incidence between the two groups was analyzed by a chi-squared test. The difference in gene expression between the two groups was analyzed by Student's *t*-test.

Those analyses were conducted with Stata11 (Stata Corporation, College Station, TX, USA).

Results

Late-Onset Gene Expression Changes Detected in the Normal Liver of the F₂ Generation

Analyses of mouse livers with Affymetrix GeneChips in our previous study showed that expression of two genes, *Crel2* and *Slc25a30*, was upregulated more than twofold and expression of another two genes, *Fabp4* and *Ell3*, was downregulated more than twofold in the normal livers of arsenite-F₁ males in comparison with those of the control males at 74 weeks of age (Nohara *et al.*, 2012). The expression changes of these genes were found to occur in an adult-onset manner (Nohara *et al.*, 2012). To examine whether arsenite exposure of F₀ pregnant mice has any effect on the F₂ offspring, we measured the expression of these four genes in the normal livers of the control F₂ males and the F₂ males obtained by crossing arsenite-F₁ males and females (arsenite-F₂) at 53 weeks and 80 weeks of age.

The results of the measurements showed significant downregulation of *Crel2* from 53 weeks of age and late-onset downregulation of *Slc25a30* at 80 weeks of age in arsenite-F₂ males in comparison with the control F₂ males. On the other hand, those genes were upregulated in arsenite-F₁ males in comparison with the control F₁ males at 49 and/or 74 weeks of age. Thus, direction of the changes by gestational arsenite exposure in the arsenite-F₁ and arsenite-F₂ males was the opposite (Fig. 1). Expression of *Ell3* was significantly upregulated in arsenite-F₂ males in comparison

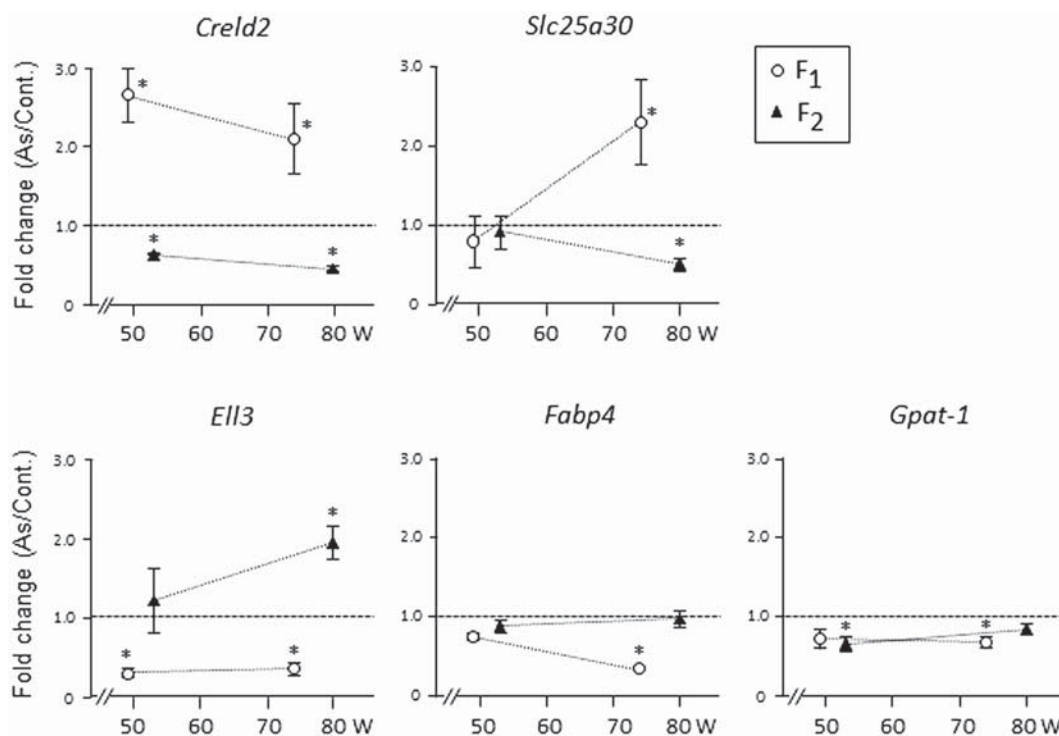


Figure 1. The changes in hepatic gene expression in the arsenite-F₁ males and arsenite-F₂ males in comparison with their control males. The expressions of five genes in the livers of the control F₂ males and arsenite-F₂ males were measured by real-time polymerase chain reaction at 53 weeks of age ($n = 4$ in each group) and 80 weeks of age ($n = 6$ in each group) and normalized to expression of *Cpb*. For the gene expressions in the F₁ generation, data obtained at 49 weeks of age ($n = 4$ in each group) and 74 weeks of age ($n = 8$ in each group) in our previous study (Nohara *et al.*, 2012) were used. The graphs show the ratios of the expression in the arsenite-exposed group normalized to the expression in the control group. The error bar shows the standard error. *Significant difference ($P < 0.05$) between the offspring of the control females and the offspring of the arsenite-exposed females.

with the control F₂ males also in a late-onset manner. The effect of gestational arsenite exposure on *Elb3* expression in the F₂ males was again the opposite of its effect in the F₁ males. Downregulation of *Fabp4*, which was detected in the arsenite-F₁ males, was not detected in the F₂ generation (Fig. 1).

In our previous study, we also observed downregulation of a lipid metabolism-related gene *Gpat-1* at 74 weeks of age in the normal livers of arsenite-F₁ males in comparison with the control males (Nohara *et al.*, 2012). This gene was downregulated in arsenite-F₂ males in comparison with the control F₂ males at 53 weeks of age (Fig. 1).

These changes in gene expression clearly showed significant effects of gestational arsenite exposure on the F₂ males, and the effects on the F₁ and the F₂ were varied.

Increased Hepatic Tumors in the F₂ Males Born to the Arsenite-F₁ Males

We performed the reciprocal crossing experiment with the control and arsenite-F₁ males and females as shown in Fig. 2 to assess the effects of gestational arsenite exposure on tumorigenesis in the F₂ males and determine the F₁ sex responsible for the F₂ tumor augmentation.

The tumor incidences in each F₂ group were 33.8% in CC, 34.3% in CA, 49.2% in AC and 43.6% in AA (Fig. 2A). Comparison of the tumor incidence between the F₂ male offspring of arsenite-F₁ males (AC and AA) and the control F₁ males (CC and CA) showed a significantly higher tumor incidence in the F₂ offspring of arsenite-F₁ males (45.9% in AC and AA vs 34.1% in CC and CA) (Fig. 2B). On the other hand, the tumor incidence of the F₂ male offspring of arsenite-F₁ females (39.9% in CA and AA) and the control F₁ females (41.1% in CC and AC) were not different (Fig. 2B). These results showed that the tumor-augmenting effect of gestational arsenite exposure is transmitted to the F₂ males via the F₁ male offspring, but not via the F₁ female offspring.

Pathological examination of tumor tissues from the control F₂ and arsenite-F₂ males (10 samples from each group) showed that hepatocellular adenoma was the predominant histological tumor type (Fig. 3). This finding was consistent with the observation of the hepatic tumors of the control mice and arsenite-F₁ mice in our previous study (Nohara *et al.*, 2012).

Ha-ras Mutation in the Tumors of the F₂ Generation

Our previous study showed that gestational arsenite exposure particularly increased the percentage of hepatic tumors containing

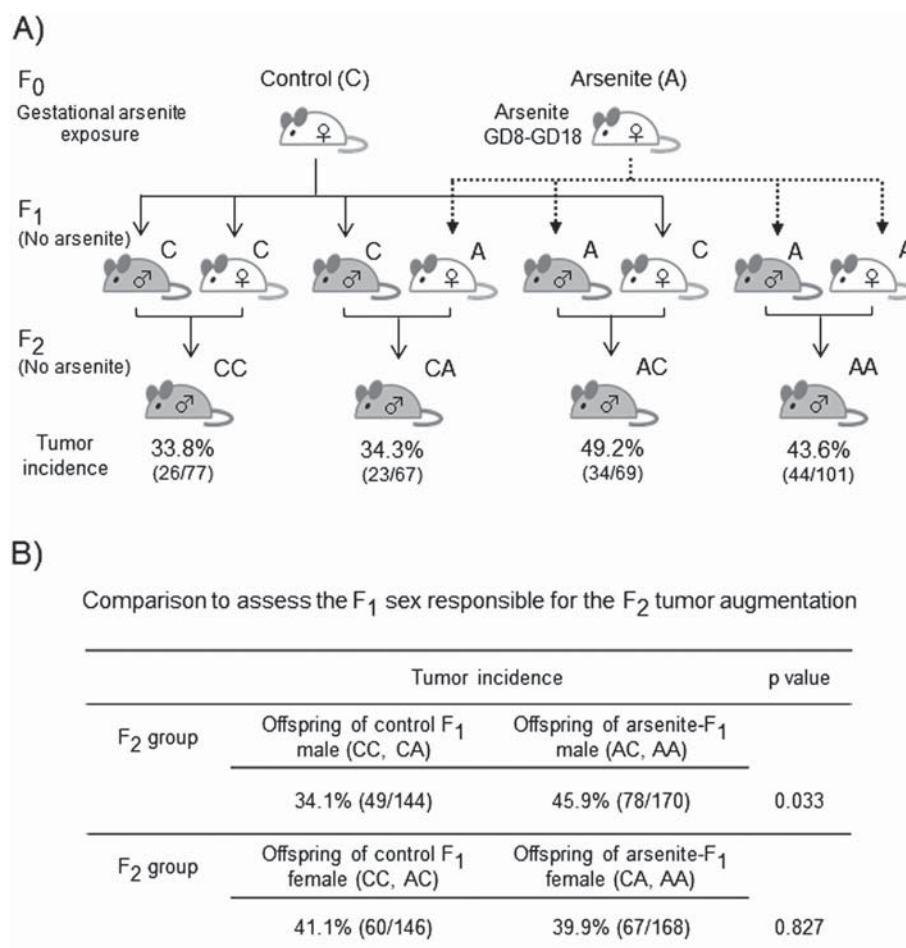


Figure 2. Increase in the tumor incidence in the F₂ male offspring born to arsenite-F₁ males but not to arsenite-F₁ females. (A) The F₂ males were obtained by reciprocally crossing the control and arsenite-F₁ males and females as shown in the figure. The F₂ mice were macroscopically examined for hepatic tumors at 75–82 weeks of age in an age-matched manner. Small lesions (≤ 1 mm in diameter) were omitted. The number in parenthesis is that of mice bearing hepatic tumors/the number of mice investigated. (B) The difference between the tumor incidences in the two groups was analyzed by chi-squared test. GD, gestational day.

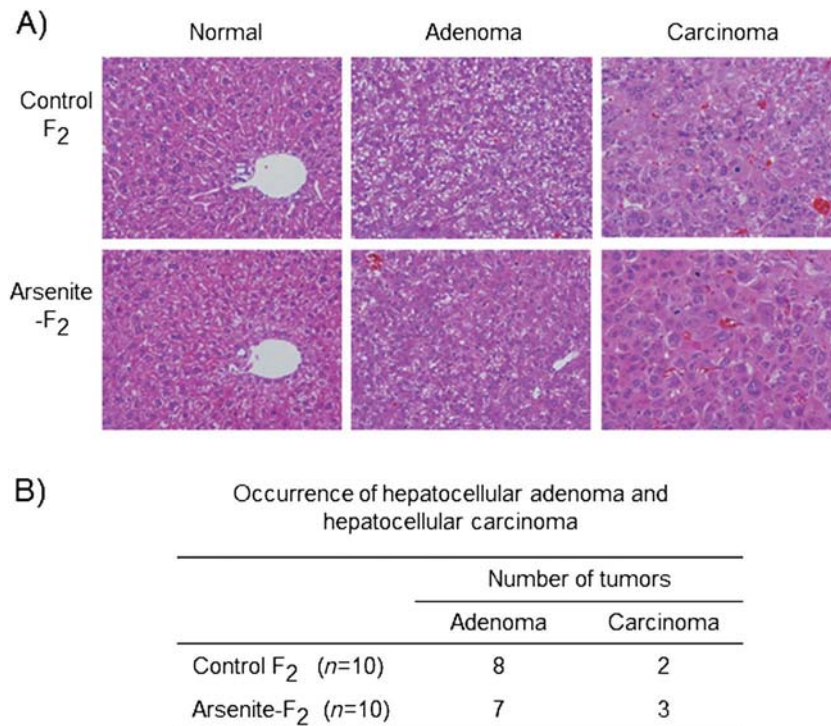


Figure 3. Histological analysis of the hepatic tumors of the control and arsenite-F₂ males. (A) Representative sections of hepatocellular adenoma and hepatocellular carcinoma of the control F₂ males and arsenite-F₂ males. (B) Occurrence of hepatocellular adenoma and hepatocellular carcinoma.

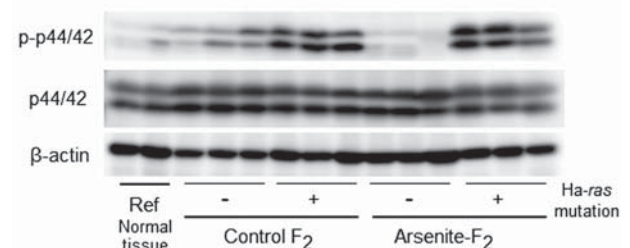
the *Ha-ras* C61A somatic mutation in the F₁ males (Nohara *et al.*, 2012). *Ha-ras* mutation is thought to be involved in carcinogenesis by activating several signaling pathways, including the RAF/MEK/ERK cascade (Pylayeva-Gupta *et al.*, 2011). The investigation in the present study confirmed that the *Ha-ras* mutations increase the activating phosphorylated forms of ERKs, ERK1 (p44 MAPK) and ERK2 (p42 MAPK) in the tumor tissues harboring codon 61 *Ha-ras* mutations in both the control F₂ males and arsenite-F₂ males (Fig. 4A). p44/p42 MAPK was shown to be hypophosphorylated in the non-tumor tissues of tumor-bearing livers, which do not contain mutated *Ha-ras* (Fig. 4B).

On the other hand, *Ha-ras* C61A mutation or the total *Ha-ras* mutations in codon 61 in the tumor tissues was shown not to be increased in the F₂ males born to arsenite-F₁ males (AC and AA) in comparison with the F₂ males born to the control males (CC and CA) (Table 2). Thus, the existence of *Ha-ras* mutations seems not to be the major causation of the increased hepatic tumor incidence in the F₂ males born to arsenite-F₁ males.

Upregulation of Cancer Related Genes in the Tumor Tissues of F₂ Males Born to the Arsenite-F₁ Males

In an effort to establish early diagnostic markers for detecting human hepatocellular carcinoma, increases in several serum proteins, including α -fetoprotein, β -catenin (CTNNB1) and interleukin-1 receptor antagonist (IL1-RN), were shown to be closely associated with hepatocellular carcinoma (Sun *et al.*, 2008). The expression of those genes was shown to be higher in the tumor tissues compared to the normal tissues or the non-tumor tissues of tumor-bearing livers, while the expression of *Afp* is varied widely among samples (Fig. 5). The expressions of *Cttnb1* and *Il1rn* genes were significantly higher in the F₂ males born to arsenite-F₁ males (AC and AA) than those born to the control males (CC and CA) (Fig. 5).

A) Tumor tissues



B) Non-tumor tissues

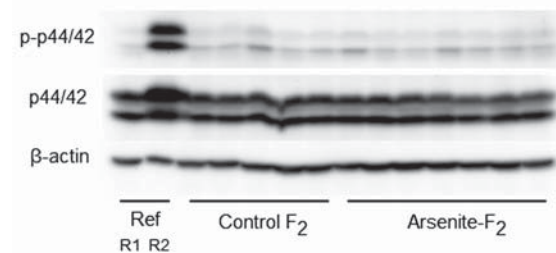


Figure 4. p44/42 MAP kinases activation as a result of *Ha-ras* mutation in the hepatic tumors of C3H males. Western blots of hepatic tumor tissues (A) and non-tumor tissues in the tumor-bearing livers (B) of the control F₂ and arsenite-F₂ males were prepared as described in the Materials and methods section. Labels in (B) are R1, normal tissue and R2, tumor tissue with a *Ha-ras* mutation.

Interestingly, when the gene expression was assessed separately in tumor tissues with and without *Ha-ras* mutation, the expression of *Il-1rn* seemed to be upregulated by *Ha-ras* mutation (Fig. 5).

Table 2. Spectra of Ha-ras codon 61 mutations in the hepatic tumors of the F₂ males

F ₂ group (n)	Ha-ras codon 61 type (%)			
	CAA wild-type	AAA	CTA	CGA
CC (29)	31	41	7	7
CA (33)	61	18	3	3
AC (34)	38	35	3	3
AA (49)	39	45	6	6

The hepatic tumor tissues were obtained in the reciprocal crossing experiment (Fig. 2) and analyzed for mutations in Ha-ras codon 61 by a pyrosequencing method.

Discussion

The earliest studies carried out primarily in the middle 1900s reported that maternal exposure or germ cell exposure to radiation and some carcinogenic chemicals transgenerationally affect the susceptibility of the progeny to cancer (Tomatis, 1994). The transgenerational effects of radiation, chemicals and nutritional imbalances on cancers and other disorders have been reported to be transmitted paternally, maternally, or both paternally and maternally (Aiken and Ozanne, 2014; Anway *et al.*, 2005; Barber *et al.*, 2002; Mohamed *et al.*, 2010; Tomatis, 1994). The individual molecular mechanisms of the transmission are yet to be clarified.

The present study showed that gestational arsenite exposure of pregnant C3H mice from GD8 to GD18 increases the incidence of hepatic tumors in the F₂ males born to arsenite-F₁ males (AC and AA in Fig. 2) compared to the F₂ males born to the control males (CC and CA in Fig. 2), irrespective of exposure of the F₁ females. These results showed that tumor augmenting effects by gestational arsenite exposure is transmitted to the F₂ males through the F₁ males. We also detected significant late-onset changes in gene expression in the normal livers of arsenite-F₂ (AA F₂) males compared to those of the control F₂ males (Fig. 1), indicating that transient gestational arsenite exposure of pregnant females causes a significant impact on the F₂ generation. Furthermore, the cancer-related genes *Ctnnb1* and *Il1m* were shown to be upregulated in the hepatic tumors of the F₂ males born to arsenite-F₁ males (AC and AA) compared to those born to the control males (CC and CA) (Fig. 5). These results show the augmenting effects of gestational arsenite exposure on the hepatic tumors of the F₂ male offspring.

The F₁ male fetuses in the present study were exposed from GD8 to GD18, when the primordial germ cells appear and differentiate into the sperm precursor cells (Sasaki and Matsui, 2008). The epigenetic profile of the primordial germ cells undergoes dynamic alterations, including imprint erasure, during the development stage, and disruption of the epigenetic profile during this stage has been implicated in transgenerational effects of F₀ gestational exposure (Aiken and Ozanne, 2014; Guerrero-Bosagna and Skinner, 2012; Perera and Herbstman, 2011). A previous study (Devesa *et al.*, 2006) reported the concentrations of inorganic arsenic and methylated arsenic at GD18 in the fetus organs, including

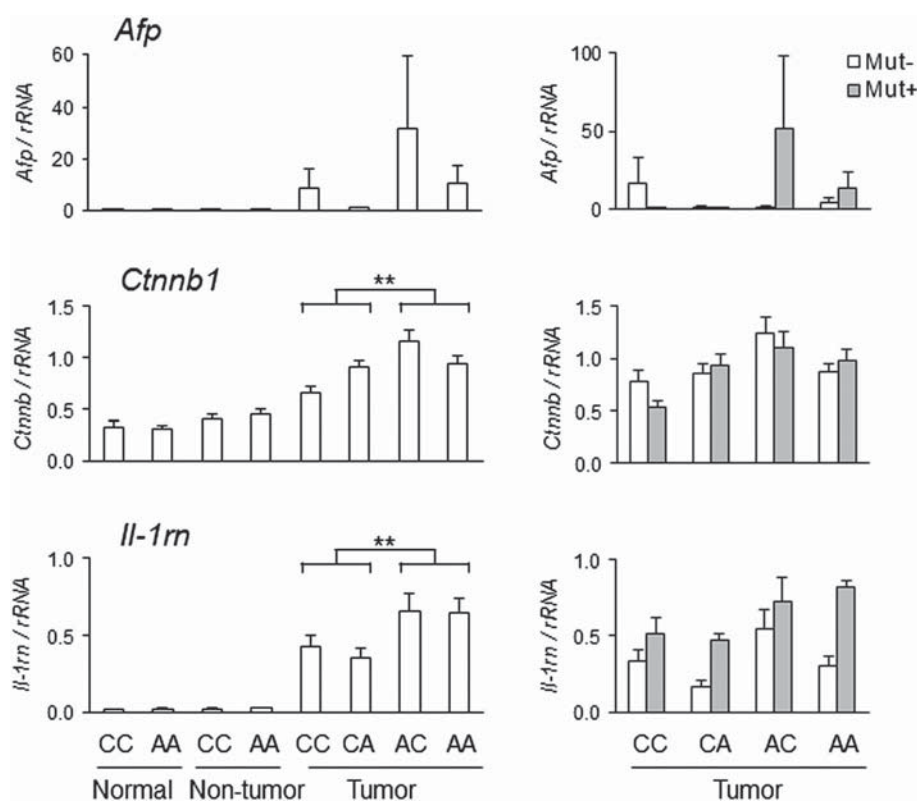


Figure 5. Expression of cancer-related genes in the hepatic tissues in the F₂ mice. The expressions of *Afp*, *Ctnnb1* and *Il-1m* were measured by real-time PCR for the normal livers ($n = 6$), non-tumor tissues from tumor-bearing livers ($n = 6$) and tumor tissues ($n = 9-11$) from the F₂ males and normalized to the expression of rRNA. The difference in the gene expressions in the tumor tissues between the F₂ males born to the control F₁ males (CC and CA) and those born to arsenite-F₁ males (CA and AA) was analyzed by Student's *t*-test. *** $P < 0.01$.

the liver and blood in the same gestational arsenite exposure model of C3H mice we used. The study showed that fetus organs are directly exposed upon gestational arsenite exposure. As arsenic has been reported to induce epigenetic changes, particularly DNA methylation changes (Reichard and Puga, 2010; Ren *et al.*, 2011; Suzuki *et al.*, 2013), the gestational arsenite exposure may alter the phenotype of the F₂ generation by affecting the epigenetic profile of genes, possibly including imprinted genes, in the F₁ male germ cells.

Arsenic has been thought to be a weak mutagen or not a mutagen based on the results of assays using bacteria and mammalian cells *in vitro* (reviewed by Rossman, 2003). Our recent study using *gpt* delta transgenic mice clarified that arsenite exposure greatly increases the incidence of G:C to T:A transversion *in vivo* (Takumi *et al.*, 2014). Thus, mutation in the proliferating and differentiating primordial germ cells might be another possible causation of the F₂ effect by arsenite exposure of F₀ pregnant mice.

In the present study, we found that gestational arsenite exposure significantly affects hepatic expression of *Crel2*, *Slc25a30* and *Ell3* even in the F₂ generation, but the effect of the exposure was the opposite of its effect on the F₁ generation (Fig. 1). The difference seems to be attributable to the fact that exposure of the F₁ and F₂ mice occurred in a different manner, e.g., the fetal liver is directly exposed in the F₁ and F₂ is exposed at the germ cell stage. On the other hand, *Gpat-1* was significantly downregulated in the liver of the F₂ generation, as was also observed in the F₁ generation (Nohara *et al.*, 2012) (Fig. 1). *Gpat-1* is one of the target genes of sterol regulatory element-binding protein 1, a member of the central transcription factors that control intracellular cholesterol and fatty acid levels (Raghow *et al.*, 2008; Wendel *et al.*, 2010). Lipid accumulation in the liver has been implicated in hepatic carcinogenesis through an increase in oxidative stress (Ziech *et al.*, 2011). The change in *Gpat-1* expression in the liver of the F₁ and F₂ mice may indicate involvement of lipid metabolism changes in the increase in hepatic tumors.

We previously found a higher proportion of C61A Ha-*ras* mutation in the hepatic tumors of arsenite-F₁ males (Nohara *et al.*, 2012). In the present study, we confirmed that Ha-*ras* mutation increases activated forms of ERKs in the hepatic tumors of C3H mice (Fig. 4). However, the percentage of Ha-*ras* mutation in the tumors was not increased in the F₂ males born to arsenite-F₁ males (Table 2), which indicated that the tumor increase in the exposed F₂ males could not be attributed to the increase in Ha-*ras* codon 61 mutation 1.

In summary, we demonstrated the novel finding that gestational arsenite exposure of F₀ pregnant mice increases hepatic tumor incidence in the F₂ male offspring through the impact on the F₁ males. Further studies will be required to identify the factors that cause tumor augmentation in the liver of the F₂ generation by arsenite exposure of F₀ pregnant mice and to explore changes in the F₁ male germ cells that induce such tumor-augmenting factors in the liver of the F₂ generation.

Acknowledgments

We wish to thank Dr. A. Furuyama, Dr. Y. Aoki, Dr. H. Nitta (National Institute for Environmental Studies) and Dr. Kayo Ueda (Kyoto University) for their useful discussions, M. Owada and F. Ishitsuka for their excellent technical assistance and S. Itaki, Y. Yamazaki and S. Umehara for their helpful secretarial assistance. The authors also wish to thank the staff of the Animal Care Company (Tokyo, Japan) for their excellent assistance in the maintenance of mice. This study was partly supported by the National Institute for Environmental Studies (1115AA082; 1315AT001 KN), and Grant-in-Aid

for Scientific Research (B) (no. 23390166, 26293154, KN) from the Ministry of Education, Culture, Sports, Science and Technology of Japan.

References

- Aiken CE, Ozanne SE. 2014. Transgenerational developmental programming. *Hum. Reprod. Update* **20**: 63–75.
- Anway MD, Cupp AS, Uzumcu M, Skinner MK. 2005. Epigenetic transgenerational actions of endocrine disruptors and male fertility. *Science* **308**: 1466–1469.
- Barber R, Plumb MA, Boulton E, Roux I, Dubrova Y. 2002. Elevated mutation rates in the germ line of first- and second-generation offspring of irradiated male mice. *Proc. Natl. Acad. Sci. U. S. A.* **99**: 6877–6882.
- Devesa V, Adair BM, Liu J, Waalkes MP, Diwan BA, Styblo M, Thomas DJ. 2006. Arsenicals in maternal and fetal mouse tissues after gestational exposure to arsenite. *Toxicology* **224**: 147–155.
- Guerrero-Bosagna C, Skinner MK. 2012. Environmentally induced epigenetic transgenerational inheritance of phenotype and disease. *Mol. Cell. Endocrinol.* **354**: 3–8.
- Harada T, Enomoto A, Boorman GA, Maronpot RR. 1999. Liver and gallbladder. In *Pathology of the Mouse*, Maronpot RR, Boorman GA, Gaul BW (eds). Cache River Express: St. Louis, MO; 119–183.
- Hughes MF, Beck BD, Chen Y, Lewis AS, Thomas DJ. 2011. Arsenic exposure and toxicology: a historical perspective. *Toxicol. Sci.* **123**: 305–332.
- Klein CB, Leszczynska J, Hickey C, Rossman TG. 2007. Further evidence against a direct genotoxic mode of action for arsenic-induced cancer. *Toxicol. Appl. Pharmacol.* **222**: 289–297.
- Köhle C, Schwarz M, Bock KW. 2008. Promotion of hepatocarcinogenesis in humans and animal models. *Arch. Toxicol.* **82**: 623–631.
- Maronpot RR, Fox T, Malarkey DE, Goldsworthy TL. 1995. Mutations in the *ras* proto-oncogene: clues to etiology and molecular pathogenesis of mouse liver tumors. *Toxicology* **101**: 125–156.
- Mohamed el-SA, Song WH, Oh SA, Park YJ, You YA, Lee S, Choi JY, Kim YJ, Jo I, Pang MG. 2010. The transgenerational impact of benzo(a)pyrene on murine male fertility. *Hum. Reprod.* **25**: 2427–2433.
- Nohara K, Ao K, Miyamoto Y, Ito T, Suzuki T, Toyoshiba H, Tohyama C. 2006. Comparison of the 2,3,7,8-tetrachlorodibenzo-p-dioxin (TCDD)-induced CYP1A1 gene expression profile in lymphocytes from mice, rats, and humans: most potent induction in humans. *Toxicology* **225**: 204–213.
- Nohara K, Tateishi Y, Suzuki T, Okamura K, Murai H, Takumi S, Maekawa F, Nishimura N, Kobori M, Ito T. 2012. Late-onset increases in oxidative stress and other tumorigenic activities and tumors with a Ha-*ras* mutation in the liver of adult male C3H mice gestationally exposed to arsenic. *Toxicol. Sci.* **129**: 293–304.
- Ogino S, Kawasaki T, Brahmandam M, Yan L, Cantor M, Namgyal C, Mino-Kenudson M, Lauwers GY, Loda M, Fuchs CS. 2005. Sensitive sequencing method for KRAS mutation detection by pyrosequencing. *J. Mol. Diagn.* **7**: 413–421.
- Perera F, Herbstman J. 2011. Prenatal environmental exposures, epigenetics, and disease. *Reprod. Toxicol.* **31**: 363–373.
- Pylayeva-Gupta Y, Grabocka E, Bar-Sagi D. 2011. RAS oncogenes: weaving a tumorigenic web. *Nat. Rev. Cancer* **11**: 761–774.
- Raghow R, Yellaturu C, Deng X, Park EA, Elam MB. 2008. SREBPs: the crossroads of physiological and pathological lipid homeostasis. *Trends Endocrinol. Metab.* **19**: 65–73.
- Reichard JF, Puga A. 2010. Effects of arsenic exposure on DNA methylation and epigenetic gene regulation. *Epigenomics* **2**: 87–104.
- Ren X, McHale CM, Skibola CF, Smith AH, Smith MT, Zhang L. 2011. An emerging role for epigenetic dysregulation in arsenic toxicity and carcinogenesis. *Environ. Health Perspect.* **119**: 11–19.
- Rossman TG. 2003. Mechanism of arsenic carcinogenesis: an integrated approach. *Mutat. Res.* **533**: 37–65.
- Rossman TG, Uddin AN, Burns FJ, Bosland MC. 2002. Arsenite cocarcinogenesis: An animal model derived from genetic toxicology studies. *Environ. Health Perspect.* **110**: S749–S752.
- Sasaki H, Matsui Y. 2008. Epigenetic events in mammalian germ-cell development: reprogramming and beyond. *Nat. Rev.* **9**: 129–140.
- Smith AH, Marshall G, Yuan Y, Ferreccio C, Steinmaus C. 2006. Increased mortality from lung cancer and bronchiectasis in young adults after exposure to arsenic in utero and in early childhood. *Environ. Health Perspect.* **114**: 1293–1296.
- Sun H, Chua MS, Yang D, Tsalenko A, Peter BJ, So S. 2008. Antibody arrays identify potential diagnostic markers of hepatocellular carcinoma. *Biomark. Insights* **3**: 1–18.

- Suzuki T, Yamashita S, Ushijima T, Takumi S, Sano T, Michikawa T, Nohara K. 2013. Genome-wide analysis of DNA methylation changes induced by gestational arsenic exposure in liver tumors. *Cancer Sci.* **104**: 1575–1585.
- Takumi S, Aoki Y, Sano T, Suzuki T, Nohmi T, Nohara K. 2014. *In vivo* mutagenicity of arsenite in the livers of *gpt* delta transgenic mice. *Mutation Res.* **760**: 42–47.
- Tomatis L. 1994. Transgenerational carcinogenesis: A review of the experimental and epidemiological evidence. *Jpn. J. Cancer Res.* **85**: 443–454.
- Waalkes MP, Ward JM, Liu J, Diwan BA. 2003. Transplacental carcinogenicity of inorganic arsenic in the drinking water: induction of hepatic, ovarian, pulmonary, and adrenal tumors in mice. *Toxicol. Appl. Pharmacol.* **186**: 7–17.
- Wendel AA, Li LO, Li Y, Cline GW, Shulman GI, Coleman RA. 2010. Glycerol-3-phosphate acyltransferase 1 deficiency in ob/ob mice diminishes hepatic steatosis but does not protect against insulin resistance or obesity. *Diabetes* **59**: 1321–1329.
- Yuan Y, Marshall G, Ferreccio C, Steinmaus C, Liaw J, Bates M, Smith AH. 2010. Kidney cancer mortality: fifty-year latency patterns related to arsenic exposure. *Epidemiology* **21**: 103–108.
- Ziech D, Franco R, Pappa A, Panayiotidis MI. 2011. Reactive oxygen species (ROS)-induced genetic and epigenetic alterations in human carcinogenesis. *Mutat. Res.* **711**: 167–173.